Application of a 2-Dimensional Hydrodynamic Model for the Assessment and Design of Instream Channel Restoration Works

by

R.W.J. Lacey[1] and R.G. Millar[1]

[1]Department of Civil Engineering, University of British Columbia, 2324 Main Mall, Vancouver, British Columbia, Canada, V6T 1Z4

Watershed Restoration Management Report No. 9

2001

ABSTRACT

Lacey, R.W.J., and R.G. Millar. 2001. Application of a 2-dimensional hydrodynamic model for the assessment and design of instream channel restoration works. Province of British Columbia, Ministry of Water, Land and Air Protection, and Ministry of Forests. Watershed Restoration Management Report No. 9: 70p.

Currently, stream restoration activities in British Columbia emphasise the use of large woody debris, boulder, and other habitat structures (Slaney and Zaldokas 1997). The purpose of these works is to create locally varied hydraulic conditions; promote scour and pool formation; and create low velocity refuges. Little work, however, has been done to characterize the changes to local flow hydraulics, morphology and in stream habitat that results from these efforts.

This study provides a methodology, through the use of field surveys and 2-dimensional hydrodynamic modelling, to assess morphological and hydraulic effects of instream LWD and boulder structures. Changes in available fish habitat were quantified through the use of Bovee (1978) probability-of-use curves. The selected field study site is a side channel of the Chilliwack River. Instream structures, installed in the summer of 1999, were subjected to a bankfull flow event that caused significant scour and bed morphology change. Results indicate that pool area increased by 50% due to the hydraulic effects of the instream structures. Two-dimensional flow model velocity and depth predictions compare favourably to recorded field values, while the predicted shear stresses, derived from the model's output, coincide reasonably with the newly formed pool locations. Pre- and post-restoration differences in fish habitat were quantified for a range of discharges using the weighted usable area method. This analysis determined that the greatest benefit offered by the instream restoration structures was in supplying low velocity refuge areas during high flow events.

PREFACE

This project was undertaken because many restoration specialists who provide prescriptions for channel and fish habitat rehabilitation projects may have an incomplete appreciation of hydraulic effects of various instream and streambank structures such a lateral log jams and groynes. The ultimate hydraulic effects of stream works are only evident well after the prescriptions are implemented because they must be subjected to significant floods. Hydraulic results are often inspiring, and more predictive tools should limit those that may also be unexpected or even surprising. The procedure described in this report facilitates improved understanding and judgement in predicting scour points and magnitudes, which was the primary intent of this study, enhanced by use of applied hydraulic modelling. The latter can be taken a step further, and if desired, more quantitative predictions can be generated if sufficient channel data was available or collected, although it is recognized that is unlikely for most rehabilitation projects.

ACKNOWLEDGEMENTS

Funding for this study has been provided by Forest Renewal BC for the Watershed Restoration Program through the Ministry of Environment, Lands and Parks. The authors are particularly grateful to Pat Slaney, Technical Coordination Manager, Watershed Restoration Program, who provided the opportunity to undertake this project and guidance. The authors would also like to thank the field assistants: Colin Rennie, Dan Walker, Wayne Jenkinson, Martin McKay, Tim Fisher, and Lillian Zaremba for their valuable aid.

TABLE OF CONTENTS

ABSTRACT i

PREFACE i

ACKNOWLEDGEMENTS i

TABLE OF CONTENTS ii

INTRODUCTION 1

BACKGROUND 3

Channel Hydraulics 3

Flow modelling 4

Natural LWD 6

Sedimentation 6

Orientation 7

Pool type, spacing and formation 7

Hydraulics of LWD 8

Flow resistance 8

Scour 9

LWD Structures 13

Durability 14

Fish Habitat 15

Cover 15

Coho salmon habitat 15

Steelhead trout habitat 16

Pool use 16

Logging 17

Habitat Requirements 17

TAMIHI SIDE CHANNEL FIELD SITE 19

Site History 19

Watershed History 21

Flood Events 22

Flood frequency analysis of the Chilliwack River 22

November 1999 flood event 23

105-03627/

RESULTS AND DISCUSSION 24
Field Surveys 24
Structures 24
Pebble counts 24
Site bathymetry 27
Measured scour 27
Two-Dimensional Flow Model – River2D 35
Data manipulation 35
Model verification 35
Discharge scenarios 38
Pool distributions 38
Shear predictions 48
Fish habitat 52
SUMMARY AND RECOMMENDATIONS 56
REFERENCES 59
APPENDIX A: GRAIN SIZE DISTRIBUTION CURVES 63

INTRODUCTION

There has been a long history of large woody debris (LWD) removal from the world's river systems. Removal has been undertaken for a variety of purposes including navigation, flood control, and agriculture. In the Pacific Northwest, it was common practice up until the mid-1970's to remove all merchantable timber and LWD from riparian zones and channels (Ralph *et al* 1994). During this time, many fisheries managers believed that LWD impaired fish production by creating impassable jams which blocked anadromous fish migration (Cherry and Beschta 1989) or scouring channels (Slaney and Martin 1997). Furthermore from the 1960's to 1970's a previous section of the Canadian Fisheries Act promoted the removal of LWD from streams. Most streams in coastal British Columbia were logged to the stream banks up until 1988 (Slaney and Zaldokas 1997) when the Government of British Columbia introduced the Coastal Fisheries-Forestry Guidelines (superseded by the Forest Practices Code in 1995) that included instream and riparian zone protection. The long history of disturbance in the Pacific Northwest has left many natural streams and rivers severely impacted and unstable (resulting from increased sediment loads and bank destabilization).

Past forest practices have played an important role in river disturbance where the impacts are not solely restricted to the streams, but are indicative of basin wide problems (Frissell and Nawa 1992). Studies have focused on old logging methods (including riparian vegetation removal, cross-stream felling and instream yarding) that, for the most part, have been replaced by less disruptive methods. Yet recently, declines in coho (*Oncorhynchus kisutch*) and steelhead (*O. mykiss*) stocks in British Columbia have been related to logging activities (Slaney *et al* 1996).

The dominant channel impacts due to logging are caused by increases in sediment loads (not peak flow) (Beschta 1984). Excess loads of coarse material promote bed aggradation leading to expanded bars and riffles, infilled pools (particularly where gradients start to decrease (Allan and Lowe 1997) and bank erosion (Hogan *et al* 1998). Logging roads have been shown to increase coarse and suspended sediment supply to streams through accelerated landslide activity and improper drainage systems. When the bedload transport capacity is insufficient to carry the increased sediment supply (coarse fraction), sediment storage bars become more prominent. Bank destabilization and subsequent channel widening is caused by lateral or medial bars that redirect and concentrate flow towards the banks causing erosion (Madej 1978). Hartman and Scrivener (1990) and Millar (2000) observed significant channel width increases in study reaches where stream banks had been logged. Bank stability declines with riparian vegetation removal (Millar 2000) and the dominance of sand and gravel in alluvial valley streambanks renders them highly susceptible to erosion – particularly when riparian vegetation has been removed by logging (Frissell and Nawa 1992). Intensive timber harvesting, including riparian removal, significantly decreases pool area (Beschta 1984) and depth (Ralph *et al* 1994). Main channel sections are straightened and pool-riffle diversity is reduced causing a loss of fish habitat (Keller and Tally 1979; Hartman and Scrivener 1990).

LWD in forest streams has been found to influence channel morphology [and stability], the movement of sediment, the retention of organic mater, and the composition of the biological community (Bilby and Ward 1989). While the number of small woody debris (less than 3 m in length) increases after logging, the amount, size, and stability of LWD decreases resulting in reduced cover and complexity of stream habitat (Hartman and Scrivener 1990). The trend of increasing LWD size with increasing stream order (Bilby and Ward 1989; Ralph *et al* 1994) is not apparent in logged basins. As well, the interaction of LWD with the low-flow channel decreases in logged systems (Ralph *et al* 1994). Rehabilitation of damaged streams for the purpose of fish habitat restoration has gained much interest in recent years. Fish habitat is directly improved by the addition of instream structures through the creation of locally varied hydraulic condition and low velocity refuges; and the promotion of scour and pool formation.

Slaney and Zaldokas (1997) emphasise the use of cabled-LWD structures, boulder complexes, and other structures as intermediate means of preserving structural diversity as streams and their riparian zones recover from past logging disturbance. Between 1983 through 1998, U.S.A. federal agencies have reintroduced thousands of instream structures to mitigate the effects of timber harvesting (Roper *et al* 1998).

Little work has been done to characterize the hydraulic, morphological and habitat changes imparted by instream restoration efforts. Many instream restoration activities are performed assuming the problem is a lack of wood, and the simple addition of LWD structures will create incremental fish habitat improvement. Large and costly projects continue to be planned and implemented by federal and state agencies with little or no analysis of their effectiveness (Frissell and Nawa 1992). Instream LWD structures are assumed to act similarly to natural LWD, yet specific knowledge of local flow hydraulics in relation to optimizing fish habitat is unavailable. Engineering interest in fluvial morphology is relatively new and has come about with the realization that design practices are much improved with the understanding and interpretation of morphological features (Kellerhals and Church 1989). Methods of determining structure locations have included determining areas of instability and bank erosion, determining pre-disturbance pool-riffle spacing and investigating existing pool locations. The selected design is usually left to the discretion of the engineer or field biologist and may vary from site to site. As well restoration approaches should consider the interconnectiveness of the physical and biological processes within a watershed (Slaney and Martin 1997). The instream habitat structure design process may be improved through the use of advancements in computational flow modeling programmes.

The ability to perform complex river analysis using either one- or two-dimensional flow models has increased along with the computational ability of desktop computers. One-dimensional (1D) models are generally used to determine flood stage, while two-dimensional (2D) models can be used to determine local hydraulic conditions in terms of local depth (y), and depth-averaged velocity ($\overline{u}$). Knowledge of local hydraulics prior to instream construction would allow for adjustments and potential optimization of design. The hydraulic outputs from 2D models can be used to assess changes in habitat characteristics for a system – thus allowing both physical and biological contributions of the designed restoration works.

The purpose of this study is to provide a methodology, using a 2D flow model, to assess the morphological and hydraulic effects of instream habitat structures (including LWD). The study investigated the use of a 2D hydraulic model, River2D, to determine local values of y and $\overline{u}$ at a side channel of the Chilliwack River, British Columbia. The future application of this work is to provide a means of assessing and optimizing planned instream habitat structures. Chapter 2 contains a review of previous literature on channel hydraulics, flow modelling, natural LWD, instream structures, fish habitat and habitat assessment procedures. In Chapter 3 the history, morphology, hydrology and fish biology of the selected field site, the Tamihi side channel, are discussed. Chapter 4 contains the field bathymetric survey results, the model verification results, and the hydraulic and habitat results calculated by the River2D model. Chapter 5 contains a summary of the study results and the methodology for the studies generalized application.

BACKGROUND

Channel Hydraulics

Channel hydraulics can be simplified by investigating only one or two dimensions (instead of three dimensions). In one-dimensional (1D) analysis cross-sectional parameters are averaged producing representative values in the longitudinal direction. The Manning equation is a widely used 1D empirical resistance equation. The equation relates the cross-sectional average depth ($\overline{y}$), cross-sectional area (A), flow (Q), and bed slope (S_o) in the following relationship (wide channel form) (SI units):

$$Q = \frac{1}{n} A \overline{y}^{\frac{2}{3}} S_o^{\frac{1}{2}} \tag{1}$$

where n is the Manning roughness value.

The Manning equation, like other 1D equations, is used to give simple parameter approximations, which include flow, velocity, flow depth and flow resistance. Equation 1 was simplified by assuming the channel is wide enough that flow can be considered the same as a rectangular channel of infinite width. The wide channel approximation can be used when the bankfull width (w_b) exceeds $10\,\overline{y}$ (Chow 1959:p.27).

While the information obtained through 1D analysis is restricted to average cross-sectional values, two-dimensional (2D) analysis allows for the estimation of local flow parameters across the channel. Local hydraulics such as bed shear stress (τ_o) and depth-averaged velocity ($\overline{u}$) play important rolls in determining channel morphology. The following equations allow for the determination of local hydraulics and were used in this study for determining local τ_o. Shear velocity (u^*) can be calculated from the Keulegan equation (SI units):

$$\frac{\overline{u}}{u^*} = 5.75 \log\left[\frac{12.2y}{k_s}\right] \tag{2}$$

where k_s is equivalent roughness height, ρ is the density of water (1000 kg/m^3) and

$$u^* = \sqrt{\frac{\tau_o}{\rho}} \tag{3}$$

Bray (1980) derived the following empirical relationship between the equivalent roughness height and the mean grain size (D_{50}):

$$k_s = 6.8 D_{50} \tag{4}$$

Substituting Equation 3 and Equation 4 into Equation 2 results in a definition of τ_o in terms of y and $\overline{u}$ (SI units):

$$\tau_o = \frac{\rho\,\overline{u}^2}{\left\{5.75 \log\left[\frac{12.2y}{6.5D_{50}}\right]\right\}^2} \tag{5}$$

In the 1930's, Shields investigated the threshold of motion through the application of shear stress. Shields experimental works developed values of critical shear stress (τ_{cr}) in relation to the particle Reynolds number (Re*). When Re* values are in the turbulent flow range, as is the case in most gravel

bed rivers (Carling 1996), Shields found that dimensionless critical shear stress (τ_{*crit}) values were constant at 0.056. The value of τ_{*crit} can be dimensionalised by the following equation (SI units):

$$\tau_{crit} = \tau_{*crit}\gamma \cdot D_{50}(S_s - 1) \tag{6}$$

where γ is the specific weight of water (9800 N/m^3) and S_s is the specific gravity of particle (2.65).

Some studies on gravel bed rivers have indicated that the value of Shields τ_{*crit}, which was based on uniform grain experiments, can be greater than 0.1 due to cluster formation and imbrication between stones which would resist entrainment (Church *et al* 1998). In non-uniform bed material τ_{*crit} is also dependent on: local hydraulic conditions, grain size, grain shape and relative protrusion. The mean value reported by Church *et al* (1998) is τ_{*crit} = 0.079 (for widely graded surfaces). A study by Shvidchenko and Pender (2000) indicated the relative depth of flow also influences τ_{*crit}. Reorganization of bed material takes place after a fully mobile bed event has occurred. Experiments indicated that stone clusters and stone lines form during periods lower than τ_{crit} and add greatly to bed stability during periods of higher than τ_{crit} (Church *et al* 1998). Once the τ_{crit} threshold has been exceeded, scour occurs and increases with applied stress (Carling 1996). A shear stress intensity (τ_{*int}), defined as the ratio of τ_o/τ_{crit}, greater than 1.0 indicates the threshold for entrainment has been exceeded.

Flow modelling

Shear stress and scour processes can be determined at varying degrees of complexity through the use of numerical models. In general, one-dimensional (1D) models are appropriate for use in calculating general aggradation or degradation using available scour equations (Melville and Coleman 2000), while two-dimensional (2D) models can be used to address localised scour and morphological issues. Melville and Coleman (2000) investigated previous work on 1D and 2D models and found that the models used, were heavily data dependent – where data was essential for each of the model development, calibration, verification, and implementation stages.

1D models simulate flow conditions in one direction (generally longitudinally) while averaging velocity and depth values over the entire cross-section (producing $\bar{y}$ and $\bar{u}_c$). These models are generally used for determining flood stage at various reach locations and can only be applied when changes in cross-sectional area and hydraulic roughness are gradual. 1D models are effective for large-scale flow variation calculations (Melville and Coleman 2000) but do not offer the resolution required for detailed, localised applications.

Two-dimensional models are much more useful for characterizing river hydraulic behaviour. The majority of 2D models are depth-averaged and compute lateral variations in depth and velocity. While 2D models have become relatively sophisticated, the models have not been extensively generalised to the case of an erodible bed (Melville and Coleman 2000). Depth-averaged models assume uniform vertical velocity distribution and thus are unable to simulate spiralling flow and flow curvature. All 2D models are based on solving the mass (continuity) and momentum equations (Steffler 1999). The governing differential equations can be solved using finite difference, finite element or finite volume methods: finite element methods offer the best geometric flexibility and finite volume methods offer the best stability and efficiency (Steffler 1999). The finite element method offers the flexibility of allowing complex boundaries to be traced by changing element shape and size.

Jia and Alonso (1994) used a case study investigated the difference between 1D and 2D models. The 2D model used in their study was CCHE-2D, a finite element model based on the Saint-Venant continuity and momentum equations. Jia and Alonso (1994) noticed that the qualitative aspects of stream flow were similar in the 1D and 2D model results, yet significant quantitative differences existed. The 2D model was able to calculate lateral flow currents and local hydraulics around every grid point and was

therefore more applicable for simulation of intense cross flows, scour and deposition around structures.

Enggrob and von Lany (1994) investigated the use of a 2D curvilinear model to describe scour around river bends and at river confluences. The 2D model used was System21 developed by the Danish Hydraulic Institute. The model solves vertically integrated (depth-averaged) Saint-Venant equations of continuity and conservation of momentum. Comparison of bend and confluence scour with field data showed a great deal of scatter, yet the mean scour depth simulated in the model corresponded closely to the mean maximum scour depth measured in the field. Sensitivity analysis indicated significant sensitivity to lateral distribution of discharge, grain size distribution, eddy viscosity, and upstream boundary conditions.

A quasi-3D model was used by Lisle *et al* (2000) to examine the relationship between modeled shear stress and measured sediment size. The flow model calculated depth-average velocities (as a 2D model) and used a subsequent subroutine to calculate the vertical structure. While local values of τ_o and D_{50} were poorly correlated, the approach lends credibility to the use of 2D or 3D flow models to predict local hydraulics.

River2D is a two-dimensional, depth-averaged, finite element model intended for use on natural streams due to its accommodation of supercritical/subcritical flow transitions and variable wetted area. Input data for River2D is channel bed bathymetry, roughness and transverse eddy viscosity distributions, boundary conditions and initial flow conditions. The model creates a finite element mesh composed of triangular polygons (of varying shapes and sizes) for the hydrodynamic component input. River2D is based on the Saint-Venant equations for conservation of mass and momentum, which are used along with the Petrov-Galerkin implicit method to solve depth and discharge intensities in the lateral (x) and longitudinal (y) directions. The conservation of mass formula is:

$$\frac{\partial H}{\partial t}+\frac{\partial q_x}{\partial x}+\frac{\partial q_y}{\partial y}=0 \tag{7}$$

where H is the flow depth, t is time, q_x is the x-discharge intensity and q_y is the y-discharge intensity. The conservation of momentum in the x-direction is:

$$\frac{\partial q_x}{\partial t}+\frac{\partial}{\partial x}(Uq_x)+\frac{\partial}{\partial y}(Vq_x)+\frac{g}{2}\frac{\partial}{\partial x}H^2 = gH(S_{ox}-S_{fx})+\frac{1}{\rho}\left(\frac{\partial}{\partial x}(H\tau_{xx})\right)+\frac{1}{\rho}\left(\frac{\partial}{\partial y}(H\tau_{xy})\right) \tag{8}$$

The conservation of momentum in the y-direction is:

$$\frac{\partial q_y}{\partial t}+\frac{\partial}{\partial x}(Uq_y)+\frac{\partial}{\partial y}(Vq_y)+\frac{g}{2}\frac{\partial}{\partial y}H^2 = gH(S_{oy}-S_{fy})+\frac{1}{\rho}\left(\frac{\partial}{\partial x}(H\tau_{yx})\right)+\frac{1}{\rho}\left(\frac{\partial}{\partial y}(H\tau_{yy})\right) \tag{9}$$

where g is the gravitational acceleration (9.81 m^2/s), U & V are the x- and y-depth averaged velocities, S_{ox} & S_{oy} are the x- and y-bed slopes, S_{fx} & S_{fy} are the x- and y-friction slopes, and τ_{xx}, τ_{xy}, τ_{xx} & τ_{xx} are the horizontal turbulent stress tensors.

River2D has 3 basic assumptions: the pressure distribution in the vertical direction is hydrostatic; the distribution of horizontal velocities over the depth is constant; and coriolis and wind forces are neglected. Momentum dispersion closure is made by weighted eddy viscosity coefficient. The habitat

component of the River2D uses modelled velocity, and depth values to determine the weighted usable area (WUA) for a specific fish species. Species preference is determined using the Bovee (1978) preference curves.

Natural LWD

LWD hydraulically controls the downstream movement of debris, sediments and organic nutrients causing local scour and deposition. The definition of LWD varies between studies, but generally pieces are < 0.10 m – 0.15 m and < 1.0 – 3.0 m, in diameter and length, respectively (Keller and Tally 1979; Bilby and Ward 1989; Cherry and Beschta 1989; Ralph *et al* 1994; Montgomery *et al* 1995). Specifying a minimum diameter proves problematic, as the significance of LWD is dependent on stream size (Gippel *et al* 1992). Small LWD becomes less important as river size increases (Gippel *et al* 1992). LWD size increases with increasing stream order (Bilby and Ward 1989; Ralph *et al* 1994) while the frequency of LWD decreases due to increased river transport capacity (Keller and Tally 1979; Bilby and Ward 1989; Montgomery *et al* 1995)(contrary to Robison and Beschta (1990)).

The interactions of LWD with the stream channel vary significantly with stream order. LWD supplied to 1st and 2nd order streams is suspended above the channel and only through breakage does interaction with the stream take place (Nakamura and Swanson 1993). LWD either forms effective cross-channel structures (depending on length) or are swung to the side by flow and offer bank protection. LWD in higher order systems mainly deflects the thalweg, which results in lateral scouring and deposition of sediments (Nakamura and Swanson 1993). Higher order streams conglomerate LWD pieces together and form jams (Keller and Tally 1979) that are unevenly distributed (Gippel *et al* 1992). LWD is predominantly delivered to low-order stream via debris slides, debris flows and windthrow, and deposits in unevenly distributed clumps (Gippel *et al* 1992) rather than alone. LWD is supplied to 3rd order and higher streams mainly through treefall and occasionally pieces floating down from upstream.

Sedimentation

Investigations of sediment storage by LWD indicate an inverse relationship to stream size (Bilby and Ward 1989) and a direct relationship with LWD loading (Montgomery *et al* 1995). In headward systems, coarse sediments remain in storage for long periods of time behind LWD and are remobilized only during extreme events (after degradation or collapse of LWD pieces) (Mosley 1981; Nakamura and Swanson 1993). Remobilized sediments travel only short distances before being re-deposited behind downstream LWD (Mosley 1981; Nakamura and Swanson 1993). Rates of transport were found to be entirely dependent on sediment availability. LWD offers important storage sites for bed sediments, which help regulate bed material load transport (Keller and Tally 1979). Keller and Tally (1979) found debris-stored sediment accounted for 40% of total channel area in higher order streams. Sediment accumulations in 3rd and 4th order streams by individual LWD are small relative to LWD-jams (Nakamura and Swanson 1993). LWD-jams in these systems cause widening (upstream) and steepening (downstream); yet at higher stream orders LWD-jams (and subsequent sediment storage) are rare due to increased stream competence. Klein (1984) investigated the effects of removing road fill from stream crossings and found where sufficient LWD was not present downstream degradation and a paved bed occurred. The paved bed was not observed in streams that had sufficient LWD. Structural LWD steps developed early after initial disturbance and remained relatively stable throughout the study period (Klein 1984).

The field investigations conducted by Lisle (1986) found that stream obstructions caused the deposition of bars 3 w_b to 4 w_b downstream and 1 w_b upstream. The bars formed on the obstruction side of the channel or in the case of bends – on the outside bank of the bend. Upstream deposition of material occurred due to backwater reductions in stream power, while downstream deposition was caused by flow

expansion. Heede (1972) observed the average spacing in headward systems between bars and LWD to be 1 w_b to 4 w_b (results were not given as ratios to bankfull width: estimations were made using the data provided). Heede (1972) suggests that when frequency of LWD recruitment is insufficient for the required energy reduction, gravel bars form instead.

Orientation

Perpendicularly oriented (or channel spanning) LWD are more frequent in smaller streams, while orientation in larger streams is more commonly in the downstream direction (Bilby and Ward 1989; Robison and Beschta 1990). Gippel *et al* (1992), as well, found LWD orientation was downstream resulting in small projected cross-sectional area. Bilby and Ward (1989) observed orientation parallel to flow to be similar in all stream orders, while upstream oriented LWD was thought to be unstable and was found infrequently in all stream orders. LWD oriented either oblique or perpendicular to flow has the greatest influence on pool formation (Montgomery *et al* 1995), while Bilby and Ward (1989) did not find orientation to have much effect on sediment entrapment.

Gippel *et al* (1992) observed the median LWD angle of tilt from horizontal to be 5° in higher order streams. Blockage ratios were low with the average LWD occupying only 0.4% of the channel while the largest pieces occupied 10% of the channel. As with Nakamura and Swanson (1993), Gippel *et al* (1992) observed only large accumulations consisting of multiple-LWD caused significant backwater effects. Furthermore, most LWD at angles of less than 40° (with the downstream bank) were hydraulically benign.

Cherry and Beschta (1989) conducted flume experiments investigating how the orientation of LWD affects scour. Wooden dowels were used as scale representations of LWD. When dowels were positioned flat on the bed, scour usually occurred along the full length of the dowels with maximum scour depth occurring near the middle. Upstream oriented dowels were found to induce large scour holes and conduct water towards the stream bank, while the scour holes produced by downstream oriented dowels were less extensive and projected water away from the bank. When one end of the dowel was elevated off the bed (assuming it rested on a bank) the maximum scour areas moved out towards the tip. Extrapolation of the flume study indicates that partial elevation of the LWD produces more localised scour than positioning the LWD on the channel bed. Upstream orientations caused major flow disturbances; produced relatively large scour holes; and appeared to increase the potential for stream bank erosion, while perpendicular and downstream orientations produced lesser disturbances and were thought to be more stable (Cherry and Beschta 1989).

The flow depths in the Cherry and Beschta (1989) experiments were only slightly greater than the diameter of the dowels; and therefore, flow patterns that develop as a result of significant structure burial were not investigated (and may differ considerably). Upstream oriented dowels can be likened to one-sided upstream V-weirs, which are used in restoration practices to scour out holes in the middle of the channel (Allan and Lowe 1997). Flow under the design conditions (high stage) is not directed towards the bank, but towards the middle of the channel instead. By this comparison, LWD oriented upstream in a river may serve to protect banks at higher flow rather than erode them.

Pool type, spacing and formation

Pool types were investigated and classified by Bisson *et al* (1981). Backwater pools are formed by eddies of large obstructions such as rootwads or boulders (they characteristically have low velocities and accumulate fine-grained sediments). Plunge pools occur when flow passes over a complete or nearly complete channel obstruction (water is plunged vertically into the streambed below, scouring out a depression that often results in a large deep pool with variable substrate size). Lateral scour pools occur when flow is directed to one side of the steam by a partial channel obstruction and often result in eroded

banks. Trench pools are characteristically U-shaped scour holes with bedrock controls. Dammed pools consist of impounded water upstream of complete or nearly complete channel obstructions (accumulations of fine gravels and sand occur in the pools with characteristically low water velocities).

Free-formed pool-riffle channels are rare in forested environments as LWD forced pools dominate (Montgomery *et al* 1995). LWD loading is directly proportional to pool frequency (Keller and Tally 1979; Robison and Beschta 1990; Montgomery *et al* 1995) and LWD size is proportional to scour pool surface area (Bilby and Ward 1989). In forest environments, in contrast to free-formed pools in alluvial reaches, local scour caused by LWD can form more than one pool in a single cross-section (Montgomery *et al* 1995). Montgomery *et al* (1995) found that LWD forced the creation of 73% of channel pools (n = 471), while Keller and Tally (1979) found 50% of pools were associated with LWD. Typically, up to 40% of the in-channel debris exerts a dominant influence on pool formation (Montgomery *et al* 1995). Mosley's (1981) investigations of headward streams indicate LWD is responsible for the location of riffles, pools and gravel bars in 40% of the sample reach.

Robison and Beschta (1990) observed pool types to vary with stream size: deflector and under-scour pools comprised 10% and 17%, respectively, in smaller streams; and increased to 22% and 27%, respectively, in the largest stream investigated. As stream size increases pool morphology becomes more complex (Robison and Beschta 1990). LWD in smaller streams is more likely to span the entire channel and cause plunge pools (also local widening). In medium to larger streams (although cross channel spanning is still possible) LWD is more easily moved by flow and is therefore pushed diagonally or jammed up against other pieces forming more complex structures and lateral scour pools (Bilby and Ward 1989; Robison and Beschta 1990). Abbe and Montgomery (1996) observed that LWD-jams strongly influence the formation of scour pools and bars in large alluvial channels and were associated with 70% of all pools.

Pool frequency is also directly related to w_b (Robison and Beschta 1990; Montgomery *et al* 1995). Pool frequency in 1st and 2nd order channels are characteristically 2 w_b to 4 w_b while lengths in 3rd and 4th order channels are often 4 w_b to 7 w_b (Church 1992; Keller and Tally 1979). Robison and Beschta (1990) found the percentage channel length comprised of pools increased from 45% to 65% from small to larger streams (n = 5). Heede (1972) observed the average spacing between individual LWD to be 2 w_b to 10 w_b (results were not given as ratios to bankfull width, estimations were made using the data provided). Pool-riffle sequences in intermediate streams decreased from greater than 13 w_b to less than 1.0 w_b with increasing LWD supply (Montgomery *et al* 1995). Montgomery *et al* (1995) suggest that the 4 w_b to 7 w_b spacing suggested in the literature may represent a morphology without obstructions such as LWD. They found that even low debris loadings (< 0.03 pieces/m^2) resulted in pool spacing of 2 w_b to 4 w_b.

Hydraulics of LWD

Obstructions such as LWD are of interest to geomorphologists because they are commonly formed or introduced by non-fluvial processes and can independently affect stream behaviour. LWD removal eliminates or reduces zones of near zero velocity and causes zones of highest velocity to shift towards the centre of the channel. This reduces the capacity of the channel to dissipate the hydraulic energy (Hartman and Scrivener 1990) and causes bank erosion and headward-progressing degradation (Shields and Gippel 1995).

Flow resistance

Shields and Gippel (1995) investigated the effects of LWD on flow resistance by analyzing streams before and after LWD removal. The method used by the study split the Darcy-Weisbach friction factor into four roughness components: grain; bar and bed form; meander bend; and LWD. In their

procedure, the cumulative effects of LWD were distributed evenly throughout the reach (a gross simplification of local hydraulic characteristics). At high flows, friction factors for cleared and uncleared reaches converged (indicating the effects of LWD are drowned out (or buried) with increasing stage). Energy dissipation through flow-contraction and pool-formation processes was gradually eliminated as flows increased in LWD streams (Shields and Gippel 1995). The removal of LWD caused and overall friction factor decreased of 20% to 30%, while flow capacity increased by 5% to 20%. Gippel *et al* (1992) suggested that increased channel capacity due to LWD removal may not be due to decreased roughness, but rather enlargement of the channel due to bed scour.

Gippel *et al* (1992) conducted laboratory experiments on horizontal cylinders (representing LWD) and found that blockage ratio, orientation to flow and shielding effect were the most important factors affecting flow resistance. Flow resistance caused by the objects was determined by calculating the drag coefficient (C_D) from the measured drag force (F_D) given the following equation (SI units):

$$C_D = \frac{F_D}{\frac{1}{2}\rho \bar{u}_c^{\,2} \phi_o \cdot l_o} \tag{10}$$

where l_o is the object projected length and ϕ_o is the object diameter.

The calculated C_D value was high when oriented parallel to flow due to the flow disturbance caused by the blunt end of the cylinder. As the cylinder was rotated from parallel to perpendicular an initial sharp decrease followed by a subsequent increase in C_D was calculated. Less variation with rotation was calculated when branches were attached to the cylinder. An empirical relationship (SI units) for calculating C_D for a single cylinder of known length was presented:

$$C_D = 0.81\left(\frac{l_o}{\phi_o}\right)^{0.062} \tag{11}$$

When a cylinder was placed close to the bed surface it created the highest C_D values, which decreased as the cylinder was raised towards the water surface. This variation occurred since, close to the bed, a zone of low velocity develops upstream of the cylinder disturbing the turbulent wake. Gippel *et al* (1992) found that the blockage ratio (defined as the cross-sectional area obstructed over the total cross-sectional area) was the most important parameter affecting C_D. Blockage ratios were related to C_D by an exponential relationship and measurable effects were observed when blockage ratios were above 0.1.

Scour

Often hydraulic studies conducted on other types of structures like piers or rock groynes offer useful incite into the potential effects of LWD (Cherry and Beschta 1989), but with respect to bridge piers results have to be extrapolated to the case of complex horizontal cylinders (Gippel *et al* 1992). General scour occurs as a result of upstream conditions such as increased flow or decreased sediment load, whereas local scour occurs below the equilibrium bed elevation due to some localised obstruction. Local scour in rivers is generally the result of flow concentration and secondary currents or vortices that occur as a result of river features such as bends, impingements, constrictions, confluences and local obstructions (Galay *et al* 1987). The extent of the local scour hole formed is dependent on the strength of the secondary currents developed due to the upstream obstruction or impingement.

Bend scour occurs as flow curves around the outside of a bend. Secondary currents are formed which are forced down towards the bed accelerating flow and causing higher shear stresses. Flow is in the form of a spiral or corkscrew and decelerates as it approaches the inside bank where deposition

occurs. Contraction scour occurs when the channel is restricted either through width or depth and flow is concentrated and forced through a smaller area. Confluence scour occurs at the junction of two converging channels where flow is directed towards the channel bed and returns to the water surface along the sides of the confluence (Melville and Coleman 2000). The resulting helicoidal secondary currents create a deep scour hole.

Bridge pier scour has been extensively studied over the past few decades (Laursen 1963; Galay *et al* 1987; Melville and Coleman 2000) for the purpose of preventing bridge failures. Flow patterns undergo significant changes as a result of piers (Melville and Coleman 2000). Upstream flow undergoes separation and rolls down to form a vortex system in front of the pier caused by flow deceleration and pressure gradients. The sides of the vortex are swept downstream by flow giving the system a horseshoe appearance. The depth of scour has been found to be strongly dependent on the width of the pier (Melville and Coleman 2000).

Abutments, spurs and rock groynes have similar scour processes as piers. The principal features comprised of surface roller, downflow, principal vortex and wake vortices are similarly present (Melville and Coleman 2000). In addition there is a large reversed eddy generated in front of the obstruction near the bank (Melville and Coleman 2000). Figure 1 and Figure 2 developed by Kwan (1984) and reproduced in Melville and Coleman (2000) illustrate the local hydraulic effects of an abutment. The deepest scour hole seen in Figure 2 is located at the apex of the abutment. This is consistent with Galay *et al* (1987) who observed the deepest scour hole to be associated with strong secondary currents located at the nose or apex of the obstruction.

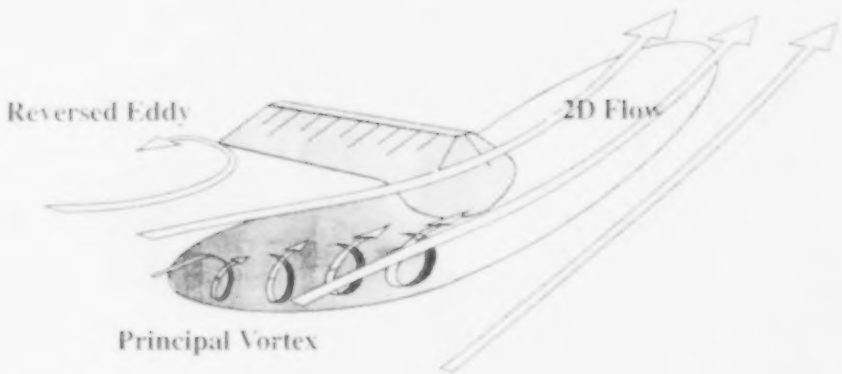

Figure 1: Illustration of the flow and scour patterns at an abutment (Kwan 1984 cited by Melville and Coleman 2000).

Figure 2: Photograph of flow around an abutment (Kwan 1984 cited by Melville and Coleman 2000).

Garde *et al* (1961) conducted sand flume experiments of scour around spur-dikes perpendicular to flow for a range of opening ratios. Spur-dikes restrict channel width, thereby altering flow patterns and inducing scour. Maximum scour was significantly affected by sediment size. Scour tended to extend downstream from the tip of the dike toward the opposite bank. Maximum d_s occurred at the outer tip (or apex) of the dike. Garde *et al* (1961) developed an empirical equation to predict d_s given $\overline{y}$, $\overline{u}_c$, w_b and spur-dike length. The equation, developed for sand, is very sensitive to small grain size differences (0.00029 m to 0.00245 m) and is most likely not applicable to gravel bed rivers.

Melville and Coleman (2000) present a mean scour depth equation (SI units) for large gravel rivers ($D_{50} > 0.002$ m) originally developed by Blench (1969):

$$d_s = 1.23\left[\frac{q^{\frac{2}{3}}}{D_{50}^{\frac{1}{12}}}\right] \tag{12}$$

where q is the discharge intensity.

The above equation was based on general regime theory and was originally presented by Blench (1969) as two separate equations: a general regime equation, and a "bed-factor" equation. The Blench (1969) equations were not meant to predict local scour, but were instead intended to be "crude tentative formula" for general regime depth calculations.

The empirical scour equations developed for bridge piers, groins and abutments, are based on average depth ($\overline{y}$) and cross-sectional average velocity ($\overline{u}_c$) and are therefore not generally applicable for local scour predictions. These equations give maximum scour for the purpose of determining the design depths of pier footings or buried pipes. Local scour, for which predictive equations are not found in the literature, is dependent on local velocity and depth values.

Field investigations conducted by Gippel *et al* (1992) indicate that LWD exerts considerable influence on local hydraulics: creating a wide variety of channel velocities. Erosional zones are

associated with large turbulent eddies rather than high velocities. Similarly to abutment flow patterns stated above, flow against the upstream face of an obstruction produces high velocities near the base forming a large persistent vortex that scours the bed and deflects bedload particles across the channel away from the obstruction (Melville 1975 cited by Lisle 1986). The vortex and associated secondary currents are thereby capable of radically altering sediment transport patterns and completely changing downstream channel morphology (Lisle 1986).

In a summary study of previous lab and field work, Smith and Beschta (1994) investigating the hydraulics responsible for LWD pool formation and maintenance. In their flume experiments with cylinders, they found average pool velocities within 0.05 m of the bed were only half the average velocities outside the pool. The time derivative of velocity (used as an index of turbulence) was 1.4 to 1.8 times greater inside the pools than outside. Gravel particles (D_{50} = 0.0054 m) were observed to lift vertically and subsequently saltate downstream. Field results indicated near-bed velocity increased linearly with discharge, and velocities measured in the deepest parts of the pool did not exceed the pool head or tail velocities. Pool cross-sectional area remained relatively constant over the range of subjected flows. Obstruction related pools anchor the location of scouring vortices and turbulent velocity fluctuations, creating more stable pool morphology than in non-obstruction related pools (Smith and Beschta 1994). Smith and Beschta (1994) found that scour and deposition in their study pool occurred in pulses at discharges well below bankfull on both the rising and falling hydrograph limbs. Although mean shear stress in the pool was lower than in the surrounding areas, bedload rate, competence, and grain-size distribution were not significantly different from those at the pool head or tail. Smith and Beschta (1994) believe that turbulent lift and drag forces may be supplementing the mid-pool shear stress. Velocity reversal theory (where velocities in pools are lower than riffles at low flows and become greater than in riffles at high flows – scouring out any deposited sediment) does not account for pool formation or maintenance in obstruction-related pools (Smith and Beschta 1994).

Lisle (1986) observed scour holes with steep upstream slip-faces located adjacent to all obstructions (the deepest scour was located just downstream of the farthest obstruction projection). Scour holes gradually shoaled and widened downstream. The total volume of material mobilized from the bars accounted for a large proportion of the total bedload transported during storm events. Although sediment transport rates were determined to be sufficient enough to cause major bar changes, observed changes were solely associated with movement of LWD and flow approach angel. The bars therefore appeared to be in dynamic equilibrium with bedload transport and the obstructions that formed them. Results indicate that obstructions wider than 1/3 w_b formed channel-spanning pools while smaller obstructions formed scour holes within a single bar. When obstructions were spaced too close (less than 2 w_b) pools were less likely to form. When spacing between obstructions was greater than 5 w_b, diagonal bars formed downstream with their location and length determined by the obstruction. Obstructions that occur at a minimum frequency ensure channel stability and arrest migrating bar movement (Lisle 1986).

Lisle (1986) observed water surface superelevation against some of the obstructions with transverse water surface gradients increasing with discharge. These gradients in some cases were greater than the channel slope and generated strong secondary currents. Scour was associated with these large-scale circulation patterns. Approach angles appeared to be less important than the blockage ratio in establishing pools and scour holes. Lisle (1986) developed a series of empirical (dimensionless) equations predicting scour hole width, length and angle:

$$\frac{w_{scr}}{w_b} = 0.616\left(\frac{w_{str}}{w_b}\right)^{0.606} \tag{13}$$

$$\frac{l_{scr}}{w_b} = 1.41\left(\frac{w_{str}}{w_b}\right)^{0.548} \tag{14}$$

$$\frac{\sin\beta}{\sin\alpha} = 1.05\left(\frac{w_{str}}{w_b}\right) - 0.0279 \tag{15}$$

where w_{str} is the structure or bend width, w_{scr} is the scour hole width (perpendicular axis at widest structure point), l_{scr} is the scour hole length (widest point of structure to downstream terminus), β is the deflection angle of scour hole from parallel with banks, and α is the angle of upstream side of structure with upstream flow lines.

Christner and Custer (1998) investigated the Lisle (1986) scour prediction equations and found them site dependent. For the most part, Christner and Custer (1998) found poor correlations between the Lisle (1986) relationships.

Abbe and Montgomery (1996) investigated flow around bar apex jams (BAJ) (which are essentially the same as single-LWD structures with rootwads (where the rootwad faces upstream) with additional LWD members caught up on the upstream side). Several alluvial bedforms were associated with these structures: a crescentric pool (directly upstream the LWD) due to vortex development; a semi-parabolic bar (upstream of the vortex) formed by flow deceleration; and an elliptical depositional zone (around the LWD trunk) formed by flow separation and re-circulation. The upstream vortex (which is similar to pier vortices) is downward circulating and develops as a result of the translation of predominantly horizontal flow to downward directed vertical flow. Accumulation of static pressure directly upstream of the LWD leads to flow reversal near the bed and formation of a point of zero velocity some distance directly upstream from the LWD. Flow is constricted adjacent to the LWD rootwad causing flow to accelerate around the sides which results in flow separation along the sides. Downstream drag occurs accounting for energy losses due to pressure gradients, skin friction and flow separation.

Abbe and Montgomery (1996) investigated an empirical constriction scour equation (Imperial units) developed by Laursen (1963) and found total predicted scour was within 3% and 17% of observed pool depth for two structures investigated. The Laursen (1963) equation is as follows:

$$d_s = \overline{y}\left[\left(\frac{\tau_o}{\tau_{crt}}\right)^{0.429}\left(\frac{w_b}{w_{con}}\right)^{0.857} - 1\right] \tag{16}$$

where w_{con} is the constricted width of channel.

As with the empirical equations devised for bridge piers and abutments, the scour equations developed by Laursen (1963) and Abbe and Montgomery (1996) are based on $\overline{u}_c$ and $\overline{y}$ conditions upstream and/or downstream of the obstruction and do not adequately represent local hydraulic effects.

LWD Structures

Deep-water habitat can be simply created by excavating holes in the streambed, but these pools would fill in over time (Allan and Lowe 1997). Instream structures attempt to duplicate the natural process of hydraulically controlled pool formation by promoting and maintaining scour (Allan and Lowe 1997). Allan and Lowe (1997) recommend opposing rock deflectors (double rock groynes) as the most suitable alternative to create deep-water runs and pools. Paired opposing deflectors have the advantage of directing flow to the centre of the channel and reducing erosion risk to the adjacent banks (Allan and Lowe 1997).

Tripp (1986) investigated the morphological effect of introducing 13 LWD structures (primarily cross-stream placements) to a debris torrented stream and found the structures greatly increased morphological variability in the channel. Within the first year, many different types of pools were created including under scour pools and backwater pools. After the second year, most of the pool types were either lateral scour or plunge (which would be predicted by cross-stream placements). The change in pool types occurred as sediments and debris deposited upstream of the structures. Total pools area increased from 2.5% to 15.4% two years after the installation.

Durability

Durability is an important criterion in assessing the effectiveness of LWD structures. Instream restoration structures that fail (moved, buried or broken apart such that they no longer influence flow) within 5 years of their installation may have minimal stream benefits (Roper *et al* 1998). Keeping structures in place and useful after high flows has proven to be difficult (even in stable reaches). Often the hydraulic stability and function of these structures cannot be ascertained until they have undergone one or more periods of high flow (Cherry and Beschta 1989). In general, success rates have been found to decreased with increasing return periods and stream order (Roper et al 1998; Frissell and Nawa 1992).

Roper *et al* (1998) analyzed the durability of almost 4000 structures in 94 streams located in the Pacific Northwest. All structures had undergone floods with return periods exceeding 5 years. The overall success rate was over 80%, yet this included structures that had shifted but remained on site. Specific types of structures were not discussed. If shifted structures are not included as successes, the rate reduces to 63%. Roper *et al* (1998) found that structures in large streams were up to 20 times more likely to fail than structures in small streams. Furthermore 63% of structures in 6th order streams failed, while only 3% failed in 1st order streams.

Frissell and Nawa (1992) investigated 161 structures from 16 streams (mostly low order) from the Pacific Northwest. Overall success rate was 68%, which included damaged (or impaired) structures. Success rate was reduced to 38% if damaged structures were discounted. The Frissell and Nawa (1992) study found much lower success rates than Roper *et al* (1998). This may be a result of definitional and flood return period differences, which makes strict comparisons between the two studies difficult. The Roper *et al* (1998) study investigated a much broader range of flows; and the rivers investigated by Frissell and Nawa (1992) were highly unstable. The highest rates of structure failure observed by Frissell and Nawa (1992) occurred in watersheds severely damaged by roads, logging, and landslides that delivered very high sediment loads to the channel. Structure failure was found to occur due to cables and anchoring device failures, bank erosion, lateral channel movement, and burial (especially in low gradient reaches). Lateral LWD deflectors and cross-stream LWD weirs had high rates of failure (>50%). Structural failure (cabling or ballasting failure) appears to be far less prevalent than failures resulting from watershed driven channel changes. Frissell and Nawa (1992) believe it is unrealistic to expect LWD structures to stabilize channels with basin wide instabilities.

An extreme event during the first year of the Tripp (1986) study resulted in the partial or entire filling of many of the pools with sediments. Most of the pools were re-scoured, but LWD structures at some locations were isolated by channel shift. Three years after the study was initiated, a debris torrent occurred which destroyed all but three of the LWD structures – bringing into question the effectiveness of restoration under such unstable conditions. Yet Tripp (1986) suggests that waiting until the channel settles before initiating restoration measures increases the risk of losing fish populations altogether.

Only 3 out of the 13 structures installed by Tripp (1986) had some amount of cabling, and these were the only structures left after the last debris torrent. Anchored structures were found to be more durable (Tripp 1986; Roper *et al* 1998). Roper *et al* (1998) found that structures not connected to the

channel edge were 50% more likely to fail. In low order streams, structures that spanned the entire channel (perpendicular to flow) were found to be more effective (Roper *et al* 1998, Tripp 1986) as they were less likely to become isolated through channel meanderings.

Guidelines for ballasting LWD structures, using hydrodynamic force balances, were developed by D'Aoust and Millar (1999). Two types of structures were investigated: single-LWD structures which consist of a LWD (with or without rootwad) ballasted at both ends by boulders using steel cables; and multiple-LWD structures which are triangular structures (V-shaped with the apex directed out into the channel) ballasted on the bank and at the apex with boulders and steel cables). The observed stability of the single-LWD structures (with and without rootwads) agreed well with predicted stability analysis where all structures predicted to not-move remained in place, while predicted movement occurred in 11 of the 13 unstable structures. The multiple-LWD structure results were less predictable. It was assumed that sliding would not occur as the structures were sufficiently braced; therefore stability of these structures was only dependent on buoyancy. Movement occurred in 6 of the 21 triangular structures predicted to be stable, while predicted movement occurred in 8 of the 13 unstable triangular structures.

Fish Habitat

Numerous factors influence site productivity – these include: pool depth, local velocity, food availability, structural complexity, riparian vegetation, and substrate size (Blackwell *et al* 1999). LWD provides important habitat for direct use by aquatic and terrestrial organisms. Uses include shelter form fast flows, shade, feeding sites, spawning sites, nursery areas for larvae and juvenile fish, territory markers and refuge from predators (Rutherfurd *et al* 1999).

LWD influences pool frequency and type; and therefore has a large effect on fish habitat. Deep pools often form around these obstructions and the combination of deep, slow water and good cover offers important wintering areas, particularly for older salmonids (Bustard and Narver 1975). Direct relationships have been found between near-natural LWD structures and salmonid smolt production (Slaney and Martin 1997). Stable sediment sites between pools, created by LWD, represent desirable spawning areas for adult fish (Tripp 1986).

Cover

Cover refers to instream and overhead features that: protect fish from high current velocities, provide concealment for both predators and prey, and provide cold water refuges by interfering with incoming light (Bovee 1982). Bisson *et al* (1981) identified eight distinct types of cover. These included three types of woody debris: rootwads, large debris (tree trunks), and small debris (branches and twigs). Also included were: overhanging terrestrial vegetation, undercut banks, water turbulence (where bubbles prevented a clear view through the water column), rocks (which provided overhead ledges and crevices for hiding); and deep water zones (which provided cover from non-diving predators).

LWD is the most abundant and diverse cover type in pools (Bisson *et al* 1981) and provides complex cover and nutrient trapping (Abbe and Montgomery 1996). Bisson *et al* (1981) found it difficult to correlate fish preference with cover type, as there are many other factors that were not specifically investigated in their study such as: the presence of competitor and predator species, population densities, and food availability.

Coho salmon habitat

Coho fry migrate to off-channel areas such as side channels, beaver ponds, wetlands, protected alcoves and tributaries for summer and overwintering rearing. Migration into most off-channel habitats in

coastal streams and rivers occurs during the fall, winter, and spring when main-channel discharges are high (Swales and Levings 1989). Yet McMahon and Hartman's (1989) experiments indicate significantly more coho remain in the channel and use LWD when it is provided under simulated freshet conditions. Increased off-channel structural complexity such as woody debris has been shown to increase overwinter survival of coho (Nickelson *et al* 1991). In general overwintering coho abundance increased with increased cover complexity and overwintering fish are more dependent on cover than those during the summer (McMahon and Hartman 1989). Tripp (1986) showed that the installation of LWD structures in a debris torrented stream resulted in a four-fold increase in coho overwinter survival.

Coho fry seemed to prefer rootwads and LWD abundance in pools; while in riffles they prefer overhanging riparian vegetation and undercut banks (Bisson *et al* 1981). Coho use of structures increases significantly when overhead shade is provided (McMahon and Hartman 1989). The presence of deep pools maximises survival of spring smolt emigration since the smolts tend to conglomerate in deeper areas before migrating in groups downstream (Nickelson *et al* 1991).

Steelhead trout habitat

Juvenile steelhead are able to occupy a much wider variety of microhabitats while steelhead fry strongly prefer shallow water (less than 0.15 m) close to shore (Hartman 1965; Bustard and Narver 1975). Steelhead are more commonly found in mainstem and tributary streams where they have adapted to surface temperature regimes with relatively high water velocities such as riffles (Swales and Levings 1989). Off-channel habitats are important refuge areas during flood events, yet steelhead are reported to use them much less than coho (Swales and Levings 1989).

Yearling steelhead had a mild preference to bank cover in pools, and preferred LWD in riffles. With decreasing water temperatures juvenile steelhead, moved closer to objects providing cover preferring rootwads and LWD (Bisson *et al* 1981). Rocks and boulder were the principal source of cover for steelhead fry (Bustard and Narver 1975).

Pool use

Bisson *et al* (1981) found very few coho or steelhead occupied secondary channel pools during the summer. It was thought that these habitats, being isolated from the main channel, had high temperatures and dense algal growth. Coho fry utilized backwater, plunge, and dammed pools (Bisson *et al* 1981; Nickelson *et al* 1991). Side pools (which dried up in the summer) provided good coho refuge from severe winter freshets (Bustard and Narver 1975). Juvenile steelhead preferred riffles, rapids, cascades, plunge pools, lateral scour pools, and dammed pools (Bisson *et al* 1981).

A summary of the average habitat utilization coefficients for coho salmon and steelhead trout obtained by Bisson *et al* (1981) is presented in Table 1. From the table, it is apparent that coho prefer pools while steelhead fry prefer riffles. Steelhead juveniles appear to prefer all habitat types investigated.

Table 1: Average habitat utilization coefficients for coho salmon and steelhead trout. Negative values indicate avoidance, while positive values indicate preference.

Habitat type	Coho 0+	Steelhead 0+	Steelhead 1+
Pools	1.46	-0.23	0.70
Riffles	-0.90	0.60	0.29
Glides	-0.91	0.34	0.86

Logging

The removal of LWD within the low-flow active channel generally decreases habitat quantity and variability required to sustain aquatic species (Ralph *et al* 1994). Hartman and Scrivener (1990) study of Carnation Creek found survival to emergence of coho salmon decreased from 29% to 16% following logging. Survival declined due to bed aggradation, which prevented fry emergence. Steelhead numbers also declined following logging due to loss of main channel summer and winter habitats (Hartman and Scrivener 1990). Juvenile steelhead preference for main stem habitats makes them more vulnerable to logging impacts than coho (Hartman and Scrivener 1990).

Habitat Requirements

Methodologies have been developed to quantify instream fish habitat. One widely used method devised by Bovee (1982), is the weighted usable area (WUA) concept used in the development of the physical habitat simulation system (PHABSIM). The method quantifies physical habitat requirements on a unit area basis using habitat indices. Bovee (1978) developed preference curves (probability of use curves) to describe the habitat conditions (depth, velocity, substrate size and temperature) preferred by selected fish species. The Bovee (1978) preference curves for juvenile steelhead trout are presented in Figure 3. Preference curves are a simple way of representing very complex or discontinuous mathematical functions describing fish preference (Bovee 1982). Criticism of the preference curves has included inadequate representation of 'nose level' water velocities (0.2 m above the bed for a spawning salmon) and the validity of transferring habitat suitability from the rivers in which they were derived to other systems (Mosley 1982). However, the PHABSIM model is widely used in practice for assessing instream habitat.

The WUA is discharge and species dependent and is calculated as follows:

$$\mathrm{WUA}_{Q,s} = \sum_{i=1}^{n} (c_{i,s} \cdot A_i) \tag{17}$$

$$c_{i,s} = f_u \cdot f_y \cdot f_c \cdot f_{sb} \cdot f_t \tag{18}$$

where $c_{i,s}$ is the suitability index, A_i is the unit surface area, f_u is the velocity factor, f_y is the depth of flow factor, f_c is the cover factor, f_{sb} is the substrate factor, and f_t is the temperature factor.

The velocity, depth, cover, substrate and temperature factors range between 0.0 - 1.0 and are determined for each unit area. Velocity, depth, substrate and temperature factors are extrapolated from the Bovee (1978) preference curves; while the cover factor is determined subjectively for each given unit area investigated.

Hogan and Church (1989) used probability of use curves and the WUA method in a study of coho salmon habitat in the Queen Charlotte Islands. Different flow scenarios were determined through at-a-station hydraulic geometry. WUA increased initially and subsequently declined significantly as flows increased towards the $Q_{1.0}$ event. Channel characteristics changed from relatively deep, slow moving water at low flows, through to fast flowing water at high flows (unsuitable for fish). The initial rise in WUA was due to an increase in the total water surface area as stage increased. As the discharge increased still further, there was a drop in available habitat (since velocity increased at a faster rate than depth). Although substrate and temperature preference curves are available (Bovee 1978), for simplicity Hogan and Church (1989) used only velocity and depth curves to demonstrate their technique. They also chose not to include habitat cover. Even though the WUA method may not reflect actual use by fish it remains a useful measure of area potentially available under appropriate management (Hogan and Church 1989).

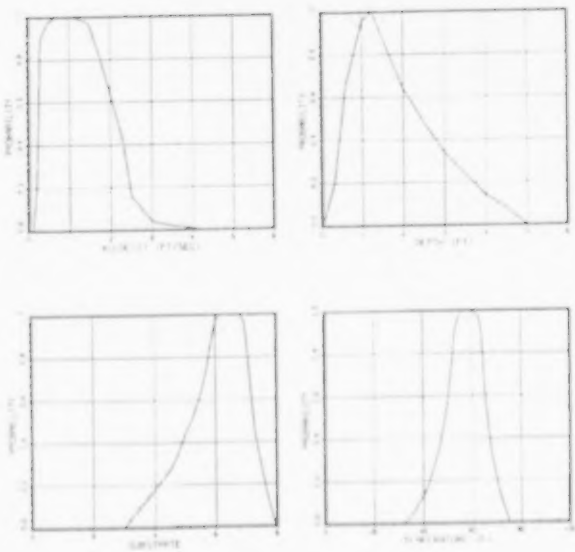

Figure 3: Juvenile steelhead preference curves (Bovee 1978). Velocity and depth refer to local (net cross-sectional average) values.

Mosley (1982) used velocity and depth measurements to investigate the WUA method for braided streams. In the analysis, water temperature, cover and sediment size were assumed to be optimum (as with the Hogan and Church (1989) study) so that habitat changes could be more accurately observed. Contrary to the Hogan and Church (1989) study, WUA remained relatively stable for discharges below $Q_{2.33}$. The apparent stability is due to the nature of braided systems. New-flow channels are created as the channel widens (with increasing discharge and stage) replacing the pre-existing channels, which are drowned out by the increased discharge (Mosley 1982). When discharges rose above $Q_{2.33}$ WUA decreased dramatically.

Both Mosley (1982) and Hogan and Church (1989) studies calculated WUA by extrapolating velocity and depth measurements (taken at a few distinct cross-sections) over the entire reach. This limits the accuracy of predicting WUA since many local reach irregularities, which cause velocity and depth changes, would not be taken into account. The use of local flow parameters with the Bovee (1978) preference curves should improve the accuracy of the calculated WUA, even though the original curves were designed for reach average values. For these reasons, 2D models are better suited for habitat assessment as they provide local $\overline{u}$ and y values throughout the channel.

TAMIHI SIDE CHANNEL FIELD SITE

Site History

Restoration activities within the Chilliwack watershed have been ongoing for the past 15 years (Blackwell *et al* 1999). Works have been completed by the Department of Fisheries (DFO) and through the Watershed Restoration Program (WRP). During the 1998-1999 budget period, seven WRP projects were in progress. Such projects included 'Bulbeard side channel and ponds' and 'Foley Creek side channel fish habitat restoration'. In the summer of 1999, instream structures were installed at the Tamihi side channel through the WRP. The purpose of the instream structures was to create channel diversity and to provide additional habitat for coho fry and steelhead fry and juveniles. Additional habitat for salmonid spawners was also desired.

The Tamihi side channel was selected as a field site based on its density and age of instream structures, as well as, its relative ease of access. The side channel is located (49°04'32" latitude and 121°46'25" longitude) on the Chilliwack River approximately 13.5 km east of Vedder Crossing, halfway between the confluences of Tamihi Creek and Slesse Creek. A site location map is presented on Figure 4. Figure 5a presents an aerial photograph, taken on May 23 1999, of a section of the Chilliwack River with the Tamihi side channel included at the top of the photo. The Tamihi Bridge located just above the confluence of Tamihi Creek with Chilliwack River can be seen at the bottom of Figure 5a. Large scale meanders and wandering braided stretches with frequent gravel bars and islands can be seen in Figure 5a. The Chilliwack River is approximately 45 m in width along this reach (Hay and Company Consultants Limited 1992).

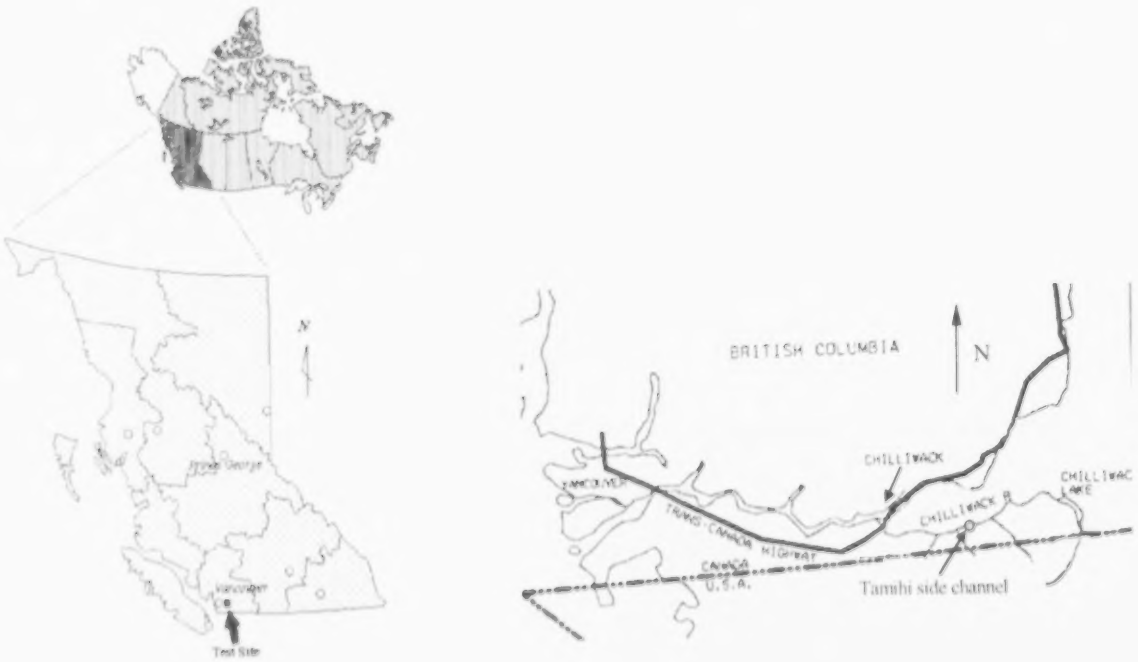

Figure 4: Site map and site location.

a)

b)

Figure 5: a) Aerial photograph of the Chilliwack River above Tamihi Bridge. Photo was taken on May 23, 1999 and is approximately 1:30 000. The Tamihi side channel is located adjacent to a large medial bar of approximately 400 m in length – seen in the upper portion of the photo. b) Aerial photograph of the Tamihi side channel (enlarged view – approximate scale 1:7000).

a)

b)

Figure 5: a) Aerial photograph of the Chilliwack River above Tamihi Bridge. Photo was taken on May 23, 1999 and is approximately 1:30 000. The Tamihi side channel is located adjacent to a large medial bar of approximately 400 m in length – seen in the upper portion of the photo. b) Aerial photograph of the Tamihi side channel (enlarged view – approximate scale 1:7000).

An enlarged view of the Tamihi side channel is presented in Figure 5b. The side channel has an average w_b of approximately 15 m and is located on the south side of a stable medial gravel bar, which is approximately 400 m in length. The gravel bar forms a sill at the side channel's inlet and thereby controls inflow to the channel. During low flow seasons (late winter and late summer) the water level in the Chilliwack River is below the inlet sill and the resulting flow in the channel is limited to groundwater seepage. The right bank (looking upstream) of the side channel is heavily rip rapped for the full length of the reach to protect the adjacent road from erosion. Historical aerial photos of the area were investigated for the years 1963, 1979, 1983 and 1993. The side channel and medial bar are not present prior to and including 1983, but are present in 1993 indicating that the side channel has only been in existence for 8 to 18 years.

Watershed History

The Chilliwack River is a 5th order system with a drainage area of approximately 1230 km^2. The headwaters are located in the Cascade Mountain Range in northwestern Washington and drain north across the border into Chilliwack Lake (southern British Columbia). At the outlet of the lake, the river makes an abrupt change in direction and flows west towards the City of Chilliwack. As it enters the outskirts of the city it passes under Vedder Crossing and is re-named the Vedder River, which joins the Sumas River and flows into the Fraser River approximately 10 km to the west of Vedder Crossing. The Chilliwack use to flow north at Vedder Crossing, but during a late 1800's flood, it avulsed and flowed down Vedder Creek instead. Pressures from urbanization and agriculture have resulted in the dyking of 84% of the Vedder River and the subsequent loss of most of the lower channel habitat (Blackwell *et al* 1999).

The Chilliwack watershed is a dry maritime Coastal Western Hemlock ecosystem. The mainstem of the river is narrow in the upstream reaches and widens downstream of Slesse Creek where it becomes well braided with channel bars and islands (Hay and Company Consultants Limited 1992). The Chilliwack River meanders along the valley floor degrading through glacial and glaciolacustrine sediments exposing bedrock locally (Hay and Company Consultants Limited 1992). Soils and bedrock types within the area are diverse ranging from plutonic to sedimentary and metamorphic rock. Soils within the watershed are composed of deposits of till, glaciofluvial and fluvial materials and colluvium (Zaldokas 1999). The Chilliwack watershed is prone to natural landslides due to glacial clay deposits and studies have indicated that landslide activity has increased as a result of logging roads. The bulk of the landslide materials are wash load sized silts and sands and as a result do not significantly effect channel morphology until downstream of Vedder Crossing (Hay and Company Consultants Limited 1992). Conversely, sediment inputs from tributary streams do have morphological significance (Hay and Company Consultants Limited 1992).

Logging in the Chilliwack River watershed began in the 1800's and by the late 1930's most of the easily accessible timber had been harvested (Hay and Company Consultants Limited 1992). Logging then shifted into the steeper sloped major tributaries where it continues to the present day. The upper Chilliwack River, as well as, the headwaters of Slesse Creek and Tamihi Creek are located in the United States in areas classified as either national parks or wilderness areas: where logging is not permitted (Hay and Company Consultants Limited 1992). The total cumulative percent of watershed area logged by 1992 was 20% (Hay and Company Consultants Limited 1992). Many of the side channels below Chilliwack Lake were formed as a result of redirected flow due to semi-permanent log-jams. Streamside logging eliminated most of the LWD recruitment, which maintained the log-jams and as a result many of the historical side channels only receive flow during extreme events (Zaldokas 1999). Roads and dyking have cut across off-channel habitats rendering them impassable to fish through poorly designed culverts.

The present populations of wild salmonids in the Chilliwack River are below historical levels due to urban development and logging related habitat changes (Zaldokas 1999). Natural instabilities such as

sediment input due to landslides are compounded by the disturbances associated with logging, dyking and roadways (Blackwell *et al* 1999).

Most species of anadromous salmonids are present in the Chilliwack watershed. These include coho, chum (*O. keta*), chinook (*O. tshawytscha*), and pink (*O. gorbuscha*) salmon, as well as, steelhead trout (Zaldokas 1999). Resident rainbow trout, anadromous and resident char and mountain whitefish are also present (Zaldokas 1999). The freshwater residency of coho is typically 1 year, while the majority of steelhead rear for 2 years and some may remain up to 3 years (Hartman 1965; Bustard and Narver 1975; Hay and Company Consultants Limited 1992). Coho salmon spawn in the main stem and tributaries of the Chilliwack River during November to January with the heaviest spawning occurring in the upper reaches near Chilliwack Lake (Hay and Company Consultants Limited 1992). Blackwell *et al* (1999) found coho outmigration on the Chilliwack River occurred in peaks between May 13 and June 10 while steelhead outmigrated in early May.

Flood Events

In most intermediate and large systems, channel forming events recur every 1.5 to 2.5 years (Church 1992). The mean annual flood ($Q_{2.33}$), which recurs every 2.33 years, is generally accepted and often used for river characterization. The bankfull flood (Q_b) is defined as the discharge at which the channel is completely full. In many cases the mean annual flood is equivalent to a bankfull event. In headward systems, channel forming events occur much more infrequently and the $Q_{2.33}$ is generally insufficient in size.

Flood frequency analysis of the Chilliwack River

Three gauging stations in the Chilliwack watershed were investigated. Station 08MH101 is located downstream of the site at the Vedder Bridge, station 08MH103 is located upstream of the site (above the confluence with Slesse Creek) and station 08MH056 is located on Slesse Creek just upstream of its confluence with the Chilliwack River. The drainage area of the Chilliwack River adjacent to the Tamihi side channel is 880 km^2. The area was determined using a 1:125 000 topographic map and recorded gauging station areas. Hydrologic maximum daily and instantaneous peak flows from all three gauging stations were downloaded from the Water Survey of Canada's HYDAT CD-ROM. The maximum monthly and yearly flows were extracted from each data set.

The downloaded maximum monthly flows produced a bimodal distribution (two distinct high flows periods): snowmelt events occurred between April and August (spring/summer), while rainfall events usually occurred between October and March (fall/winter). Log Pearson Type III frequency analysis was performed on the maximum monthly flow records from the lower and the combined upper gauging stations using the Consolidated Frequency Analysis (CFA) statistical package (originally distributed by the Surface Water and Sediment Data Atmospheric Environment Service). The Vedder Crossing predicted flows ($Q_{2.33}$, Q_{100}, and Q_{200}) were adjusted to the site's drainage area using the following equation presented by Coulson and Obedkoff (1998) (Vedder Crossing values were chosen since the records date back much further than those of the upper two gauging stations):

$$Q_u = Q_g \left[\frac{A_u}{A_g} \right]^{0.785} \tag{19}$$

where Q_u is the ungauged flow, Q_g is the gauged flow, A_u is the ungauged watershed area, and A_g is the gauged watershed area.

The exponent value 0.785 is a constant for the whole Province of British Columbia and was determined by plotting and comparing peak flow against drainage area for each hydrologic zone (Coulson and Obedkoff 1998). The daily maximum flood frequency analysis for the Chilliwack River adjacent to the site is presented in Table 2.

Table 2: CFA - Log Pearson Type III flood predictions.

Chilliwack River (adjacent to site)	$Q_{2.33}$ (m^3/s)	Q_{100} (m^3/s)	Q_{200} (m^3/s)
spring/summer	180	300	315
fall/winter	205	500	540

The predicted fall/winter period peak flows (Q_{100} and Q_{200}) were almost double the predicted values of the spring/summer period. The instantaneous daily discharges were evaluated and are related to the maximum daily flows by a peaking factor of 1.46. The instantaneous Q_{200} for the fall/winter period is 790 m^3/s. Rainfall events were flashy lasting only 1 to 5 days, while snowmelt events were greater in volume and duration (lasting for greater then two weeks). At lower return periods the difference between the two time periods shrunk (especially higher up in the watershed where $Q_{2.33}$ for the combined upper gauging stations showed little difference between fall/winter and spring/summer periods). Hay and Company Consultants Limited (1992) determined that most extreme floods in the Chilliwack basin occur during the fall/winter period with heavy rain and the subsequent melting of some or all of the early snow pack.

November 1999 flood event

On November 12, 1999, the Chilliwack River experienced an estimated 5 year return period flood (Q_5). The estimated peak discharge adjacent to the site (based on peak flows recorded at the Vedder Bridge gauging station 08MH103) for this event was approximately 290 m^3/s. As previously mentioned in Section 3.1, flow into the Tamihi side channel is restricted at its entrance by a sill formed by the adjacent medial gravel bar. As a result, only a portion of the predicted fall/winter mean annual flood or Q_5 would pass through the side channel. During this event, flows in the side channel were likely bankfull. The side channel is not gauged; therefore Q_b had to be predicted. The side channel's Q_b was calculated using two different methods: the Manning equation and the two-dimensional flow model – River2D. The Manning's roughness (n) was calculated using measured low-flow $\overline{u}_c$, $\overline{y}_c$, S, and A. The bankfull average cross-sectional depth ($\overline{y}_b$) was determined by examining the cross-sectional profile at-a-station and predicting the over bank flow depth. This value was compared to the observed high flow mark elevation (where flood-debris was caught up on the sides of the channel) (the two values were within 0.15 m of each other). The bankfull discharge was then calculated using Equation 1.

The second method of calculating Q_b modelled different discharge scenarios using River2D and compared output water surface elevations with the observed bankfull depths. Many different flow scenarios were attempted in order to predict a reasonable bankfull flow event. The high flow mark elevation was compared to the model output water surface values. Analysis of the two methods led to the acceptance of a bankfull discharge of approximately 40 m^3/s in the Tamihi side channel.

RESULTS AND DISCUSSION

Field Surveys

Structures

The current study investigated eleven structures (Str) installed at the Tamihi side channel in August 1999 (during minimum flow). The type of structures installed consisted of: 4 multiple-LWD triangular, 4 single-LWD rootwad, 2 double-rock groynes, and 1 single-rock groyne (an example of each type of structure is presented in Figure 6 through Figure 9). As previously discussed single-LWD structures consist of a LWD (with or without rootwad) ballasted at both ends by boulders; multiple-LWD triangular structures are V-shaped with the apex directed out into the channel, ballasted on the bank and at the apex with boulders; double- and single-rock groyne structures are V-shaped (apex directed into flow) and are constructed using stones of classes large enough to withstand the shear stress caused by the river.

Pebble counts

A Wolman (1954) pebble count was performed at upstream, middle, and downstream locations of the study channel. The methodology involved measuring the intermediate or "B" axis of 100 pebbles randomly picked off the channel bed. The pebble counts were completed prior to the November 1999 flood. The D_{50}, D_{90}, geometric mean (D_g), geometric standard deviation (σ_g), and equivalent roughness height (k_s) (from Equation 4) are presented in Table 3. Grain size distribution curves for all three pebble counts are presented in Appendix A.

Table 3: Tamihi side channel grain size analysis.

Sample Location	Coverage (m)	D_{50} (m)	D_{90} (m)	D_g (m)	σ_g (–)	k_s (m)
Upstream	-160 – -10	0.095	0.240	0.070	2.793	0.65
middle	-9 – -62	0.070	0.170	0.061	2.449	0.48
downstream	-63 – -160	0.060	0.170	0.059	2.366	0.41

The results indicate a trend towards downstream fining of bed sediments in the side channel. Observations of varying D_g and σ_g values indicate a progressive downstream sorting of the bed material. Field observations indicated large classed material at the toe of the adjacent gravel bar (at the entrance to the side channel).

Figure 6: Multiple-LWD triangular structure (Str11).

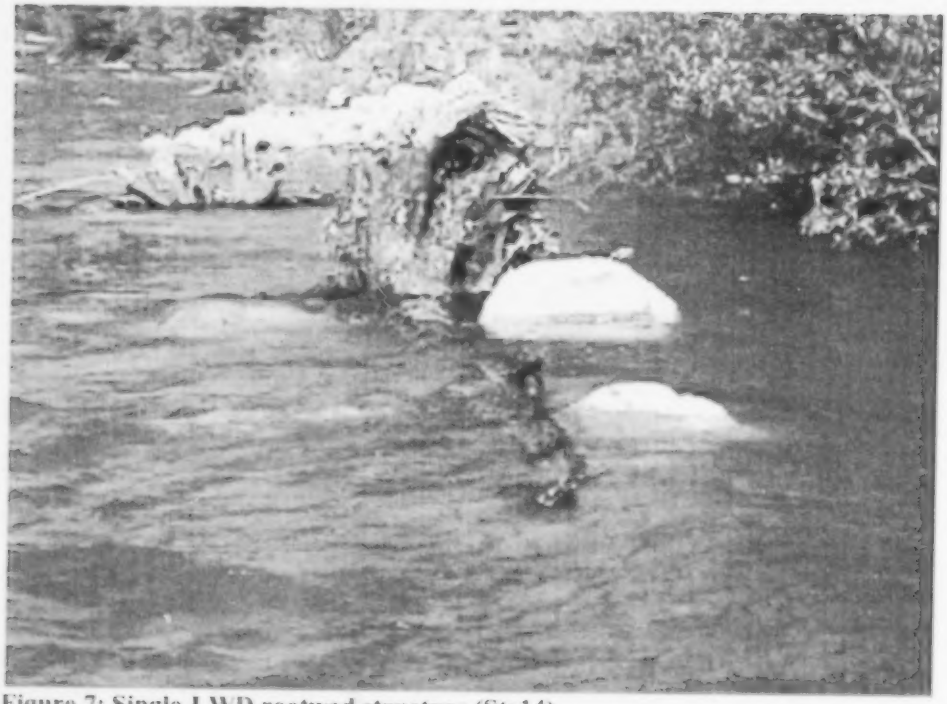

Figure 7: Single-LWD rootwad structure (Str14).

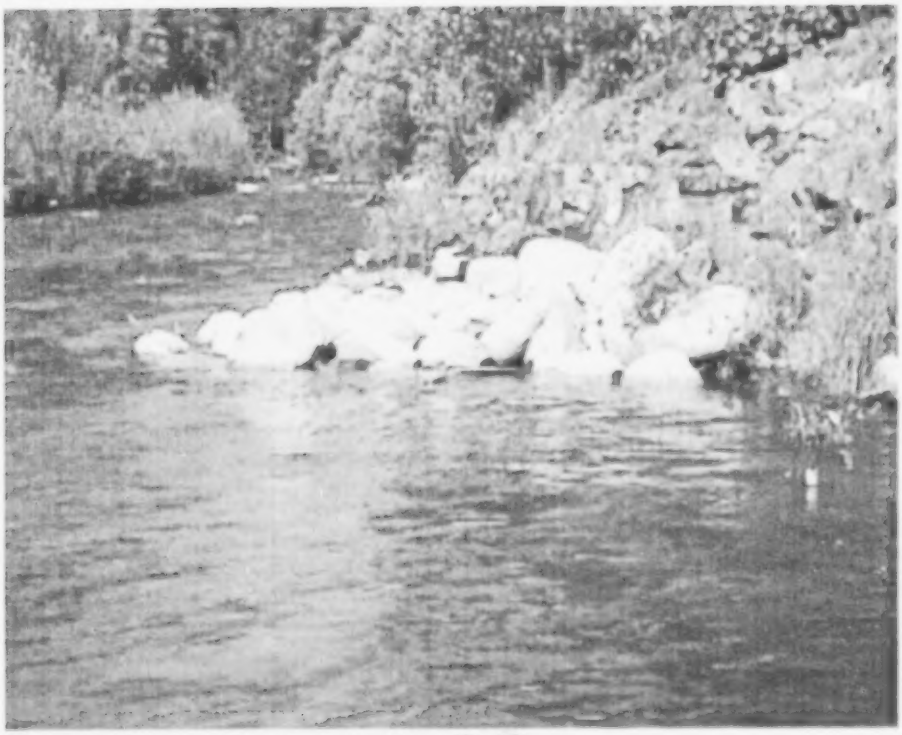

Figure 8: Single-rock groyne structure (Str12).

Figure 9: Double-rock groyne structure (Str9).

Site bathymetry

The November 12th 1999 bankfull flood was large enough to mobilize the bed of the Tamihi side channel. Bathymetric pre- and post-flood surveys were conducted in late-September 1999 and mid-February 2000, respectively, using Nikon 500 and Leika 700 series total station equipment. The channel was surveyed subjectively, with a high density of measurements (approximately 0.5 – 1.0 m apart) around and below LWD structures. The survey attempted to pick up any irregularities or inconsistencies in the bathymetry, which could cause local hydraulic changes. The survey data was downloaded to a desktop computer and a surface mapping programme (Surfer™) was used to create a digital elevation model (DEM) with a 0.5 m spacing for both the pre- and the post-flood surveys.

The side channels pre- and post-flood DEM bathymetries are presented on Figure 10a, Figure 10b, and Figure 10c. Instream structures are represented by square symbols. Greater bed variation around instream structures can be seen in the post-flood bathymetries. The variation is observed to be dependent on instream structure placement – with scour occurring at or around structure nick points (furthest points projected into flow). Figure 11 presents the longitudinal pre- and post-flood thalweg profile for the side channel. The local slope around instream structures in the post-flood profile has changed significantly, while the total slope has increased only slightly from 0.0041 m/m to 0.0050 m/m, pre- and post-flood, respectively. Aggradation, as seen in Figure 11, occurred at the top of the reach (upstream of Str6), while local degradation around individual structures was observed downstream. The upstream aggradation is most likely not a result of instream structure hydraulic effects, but rather a result of increased sediment load (due to the Q_5 flood) which mobilized sediments from the toe of the adjacent medial bar and deposited them into the side channel.

Measured scour

The net scour plots for the side channel, obtained by subtracting the post-flood bathymetry from the pre-flood bathymetry, are presented on Figure 12a, Figure 12b, and Figure 12c. Positive values indicate degradation depths, while hatched contoured areas represent aggradation. Only net degradation depths in excess of 0.2 m are shown. Thick black lines represent the channel bed boundary. Up to 0.43 m of scour was measured in the lower portion of the side channel (at the apex of Str11) while maximum scour in the middle portion was up to 0.7 m (adjacent to Str9).

Degradation zones, in Figure 12a through Figure 12c, are observed to extend up to 40 m downstream of their related structures (Str9 and Str11). The deepest scour holes are located adjacent the apex of the multiple-LWD triangular and rock-groin structures. This finding is consistent with Lisle (1986) who observed the deepest scour to occur just downstream of the farthest obstruction projection. Backwater and sheltering effects of the triangular structures led to the deposition of fine material directly downstream and upstream along the banks of the channel. Scour and deposition around the single-LWD rootwad structures (specifically Str10 and Str12) appears to be consistent with the alluvial bedforms described by Abbe and Montgomery (1996) – a crescent pool can be seen just upstream of the rootwad, a depositional bar formed further upstream and a second depositional bar formed downstream along the LWD trunk. Field observations indicated that sediments that deposited along the LWD trunks were of a finer calibre than the sediment composition of the upstream bar (or in the channel).

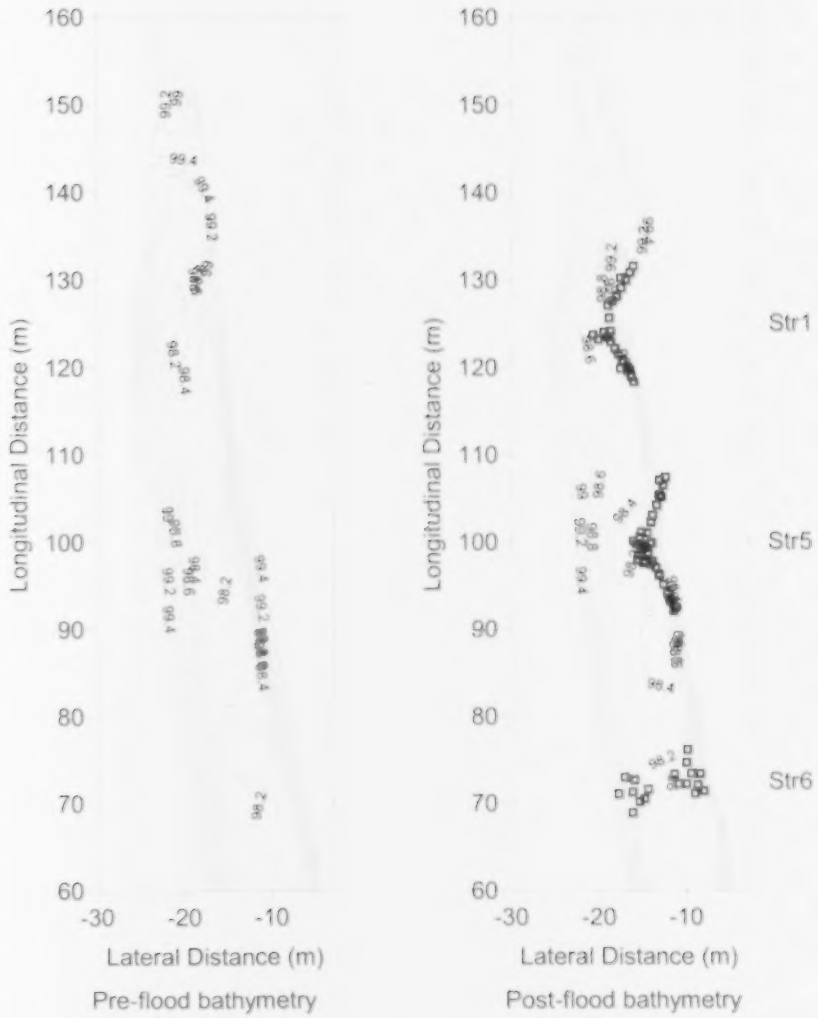

Figure 10a: Upper Tamihi side channel pre- and post-flood bathymetry. Contours represent elevation levels (m). Instream structures are represented by square symbols

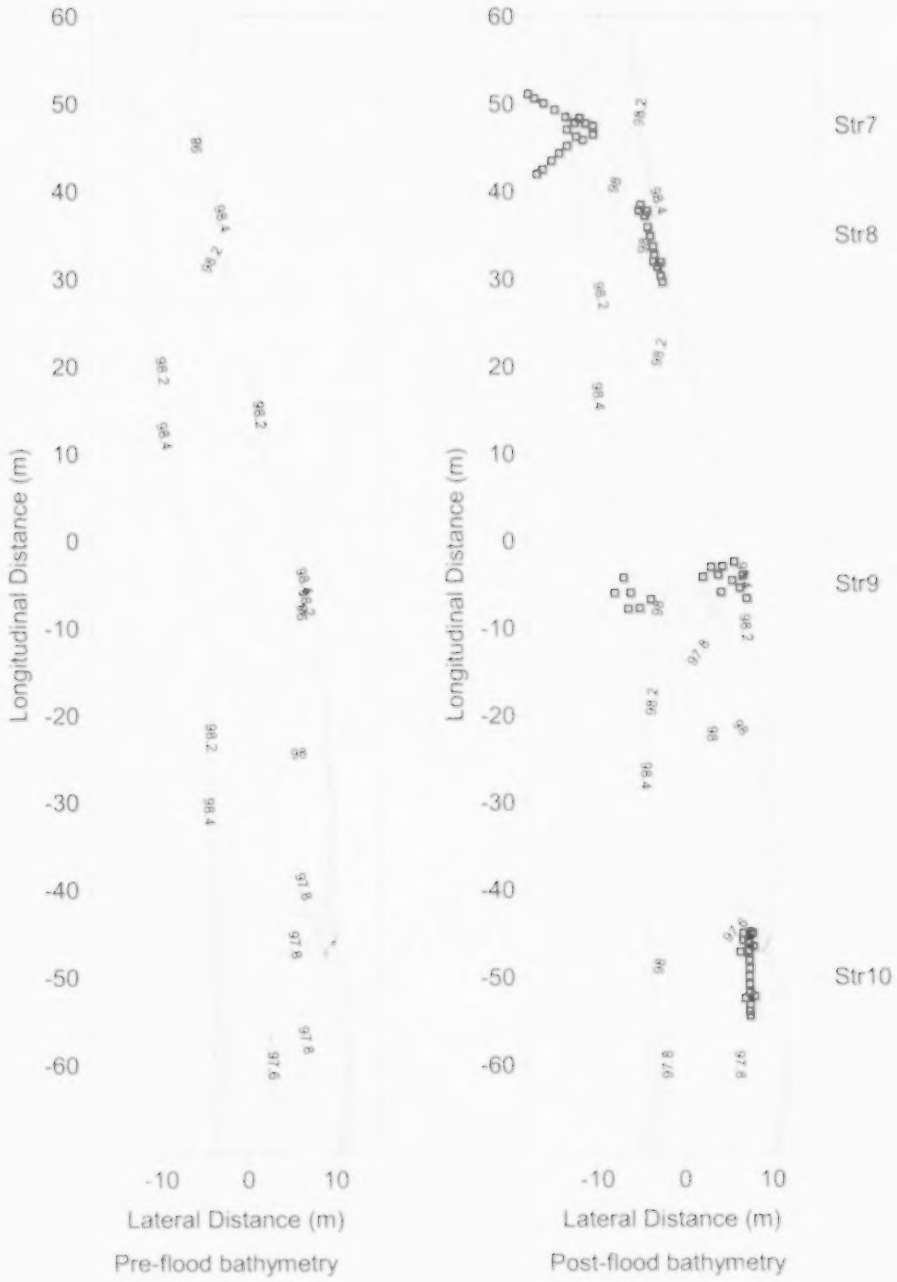

Figure 10b: Middle Tamihi side channel pre- and post-flood bathymetry. Contours represent elevation levels (m). Instream structures are represented by square symbols.

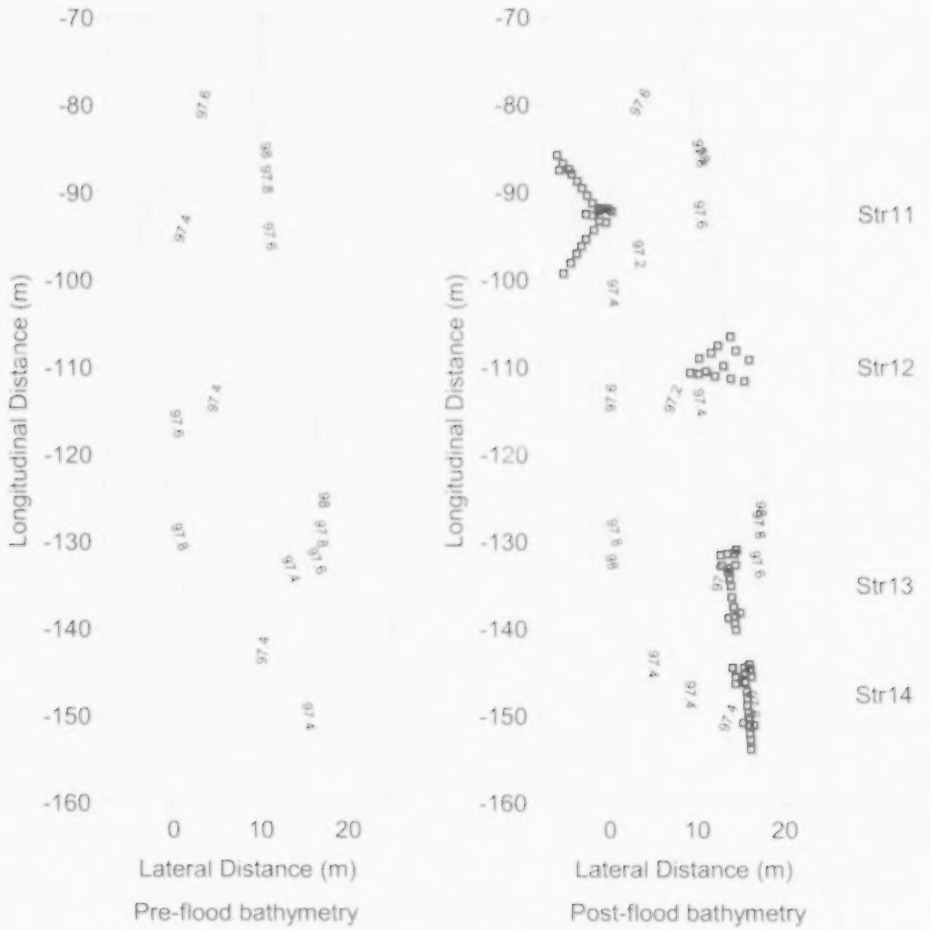

Figure 10c: Lower Tamihi side channel pre- and post-flood bathymetry. Contours represent elevation levels (m). Instream structures are represented by square symbols.

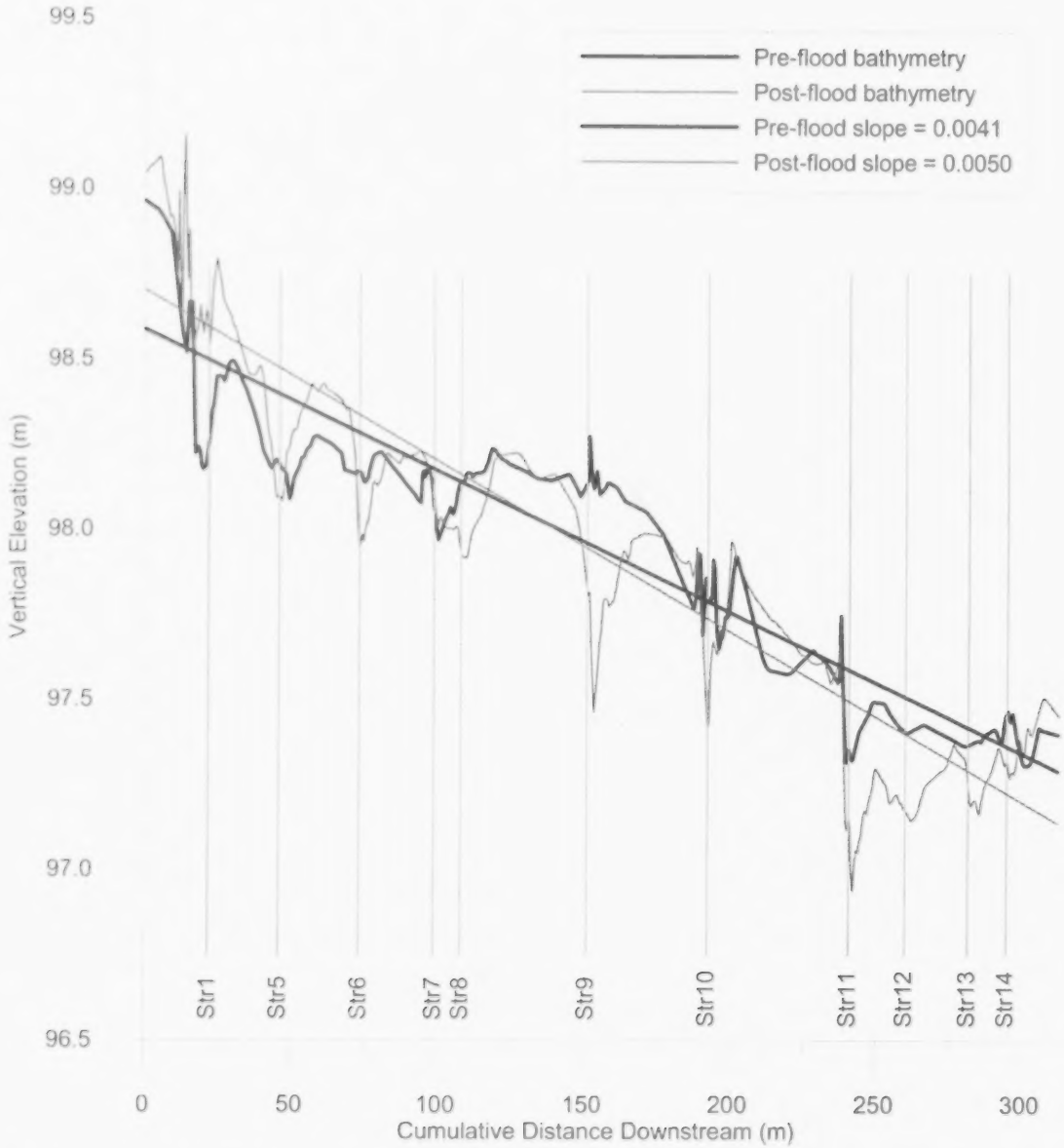

Figure 11: Tamihi side channel longitudinal thalweg pre- and post-flood profiles. The instream structure locations indicated represent the apex or furthest point projected into flow.

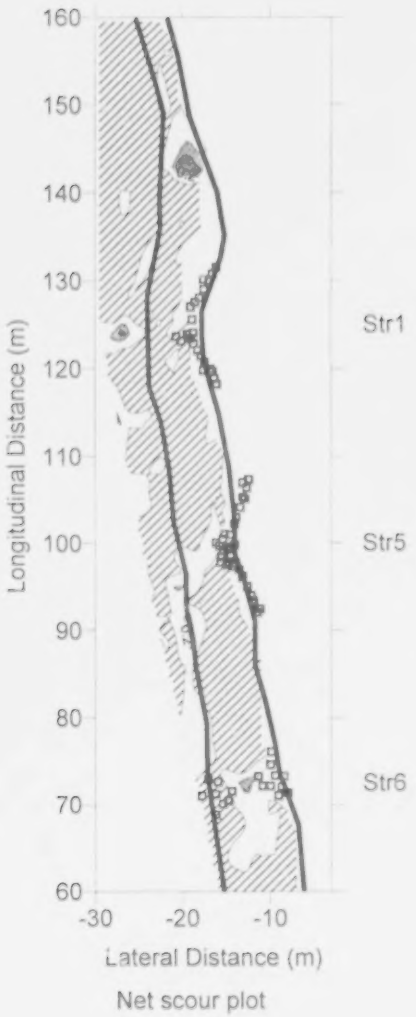

Figure 12a: Upper Tamihi side channel net scour plot. Positive contours represent degradation, while hatched contoured areas represent aggradation. Thick black lines represent the channel bed boundary. Instream structures are represented by square symbols.

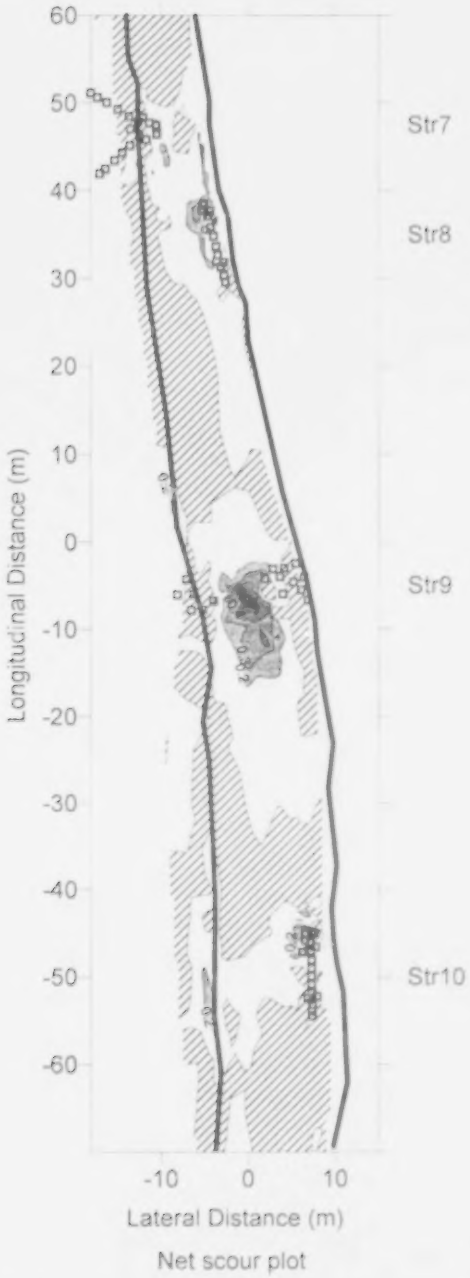

Figure 12b: Middle Tamihi side channel net scour plot. Positive contours represent degradation, while hatched contoured areas represent aggradation. Thick black lines represent the channel bed boundary. Instream structures are represented by square symbols.

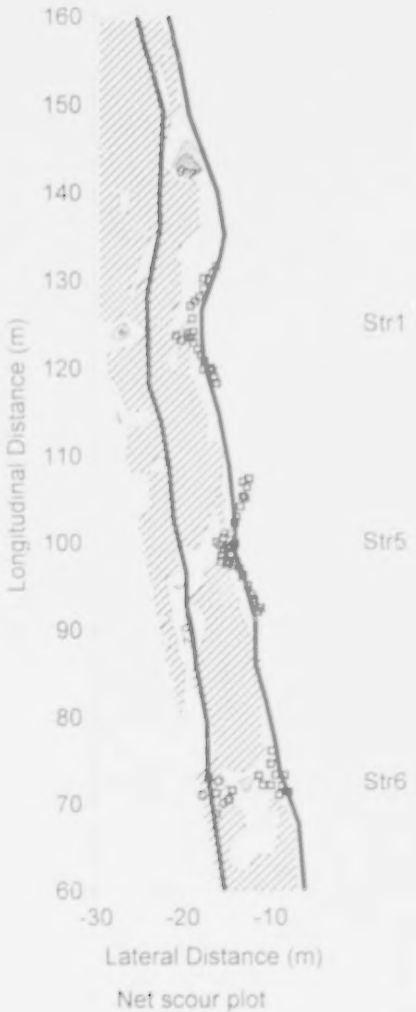

Figure 12a: Upper Tamihi side channel net scour plot. Positive contours represent degradation, while hatched contoured areas represent aggradation. Thick black lines represent the channel bed boundary. Instream structures are represented by square symbols.

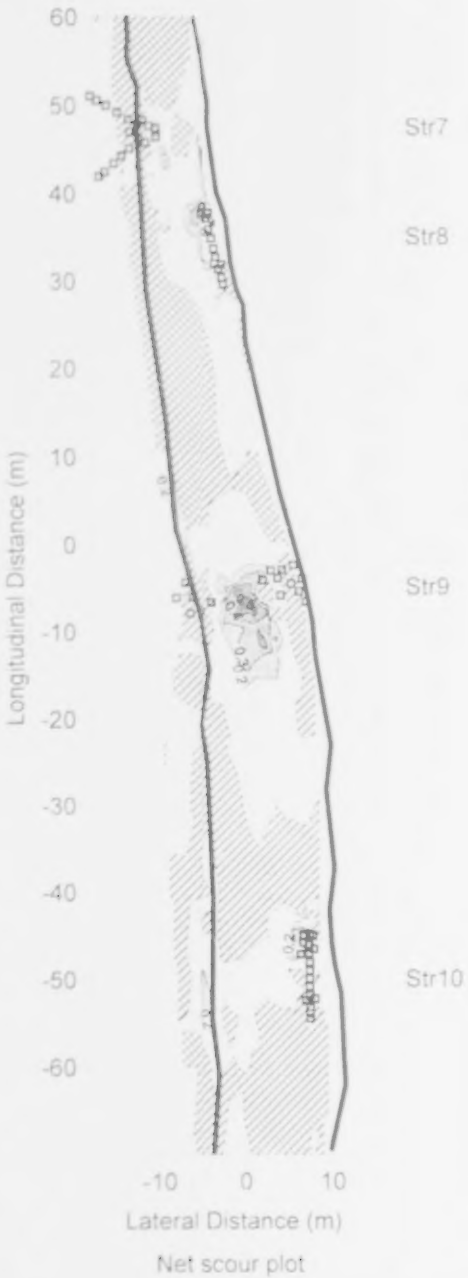

Figure 12b: Middle Tamihi side channel net scour plot. Positive contours represent degradation, while hatched contoured areas represent aggradation. Thick black lines represent the channel bed boundary. Instream structures are represented by square symbols.

Figure 12c: Lower Tamihi side channel net scour plot. Positive contours represent degradation, while hatched contoured areas represent aggradation. Thick black lines represent the channel bed boundary. Instream structures are represented by square symbols.

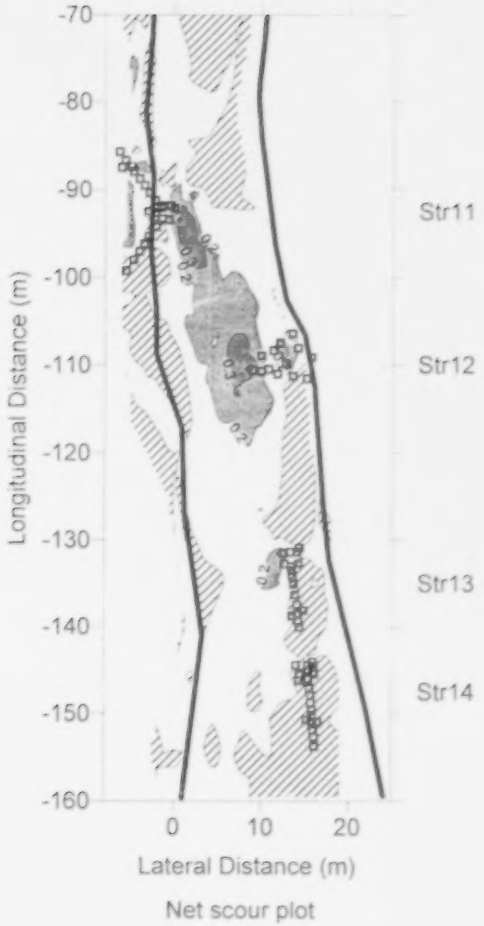

Figure 12c: Lower Tamihi side channel net scour plot. Positive contours represent degradation, while hatched contoured areas represent aggradation. Thick black lines represent the channel bed boundary. Instream structures are represented by square symbols.

Two-Dimensional Flow Model – River2D

Data manipulation

The pre- and post-flood DEM bathymetries produced by Surfer™ were converted into .CSV format with a 1.0 m spacing. A programme was written in Visual Basic to filter out the extraneous values outside the area of interest. Due to the computational restrictions of River2D the resulting .CSV files (representing the channel bathymetry) were subdivided into upper and lower reaches that were modeled in separate runs. Four different .CSV (bed) files representing pre- and post-flood bathymetries with and without instream structure representation (plain bed and bed with structures) were developed for River2D input. The instream structure representation was removed from the pre-flood bathymetry (plain bed) in order to give a representation of the channel prior to structure installation. Instream structures were assumed to be shelf like solid obstructions where water was restricted to flowing overtop and around – not through. Shields and Gippel (1995) used a similar assumption when considering natural LWD: field observations indicate that the interstitial spaces between branches and/or roots are often filled with leaves and sediment and serve as solid objects rather than permeable clusters. River2D was used to create finite element meshes for the four bed files and were then modeled at different discharge scenarios.

Model verification

Field velocity and water surface surveys were completed on 29/05/00 and 15/06/00 (velocity measurements on 15/06/00 were limited to a single cross-section) using flow metering and Leika 700 series total station equipment. Velocity, depth and water surface values were measured at 1.0 m spacing intervals along channel cross-sections from which specific discharge was calculated. Random velocity, depth and water surface values were also measured throughout the channel for model verification purposes. Flows determined from the cross-sectional velocity and area measurements were 4.7 m^3/s and 11.3 m^3/s for the first and second surveys, respectively. The 4.7 m^3/s flow scenario was modelled using post-flood bathymetry (with structures). Calculated water depth (y_{mod}) and velocity (u_{mod}) values from this scenario were compared to observed values. Comparison plots are presented on Figure 13 and Figure 14 (comparison plots for $Q = 11.3$ m^3/s were not prepared due to insufficient data points). A line representing a 1:1 relationship ($u_{mod} = u_{obs}$ or $y_{mod} = y_{obs}$) is presented on the two plots. The mean absolute error (MAE) and the mean error (ME) are presented in Table 4 and were calculated given the following equations (velocity forms presented):

$$\mathrm{MAE} = \frac{100}{n}\sum\left|\frac{u_{mod} - u_{obs}}{u_{obs}}\right| \tag{20}$$

$$\mathrm{ME} = \frac{100}{n}\sum\left(\frac{u_{mod} - u_{obs}}{u_{obs}}\right) \tag{21}$$

where u_{mod} is the modelled velocity, u_{obs} is the observed velocity and n is the number of samples.

Table 4: Model verification – mean absolute error (MAE) and mean error (ME).

Unit	Q (m^3/s)	MEA (%)	ME (%)
velocity verification	4.7	24	15
water depth	4.7	6.1	-0.65

Table 4 indicates that River2D predicts y_{mod} well, while more scatter is observed with the predicted u_{mod}. Yet u_{mod} values predicted by River2D are still within 24% of u_{obs}. The ME for both verifications is less than the MEA indicating that the spread tends to be centred on the $u_{mod} = u_{obs}$ (or $y_{mod} = y_{obs}$) line.

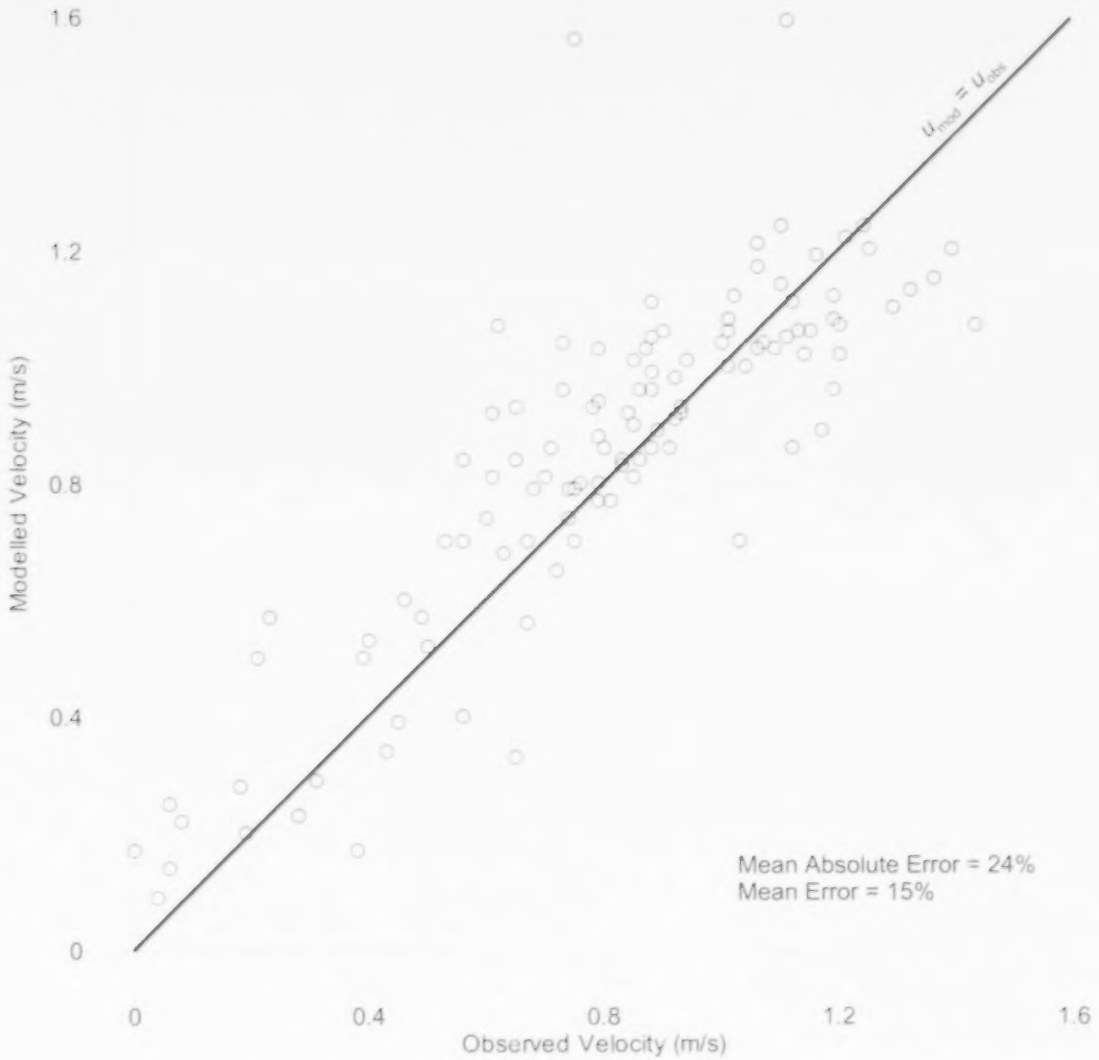

Figure 13: Tamihi side channel velocity verification plot (Q = 4.7 m^3/s).

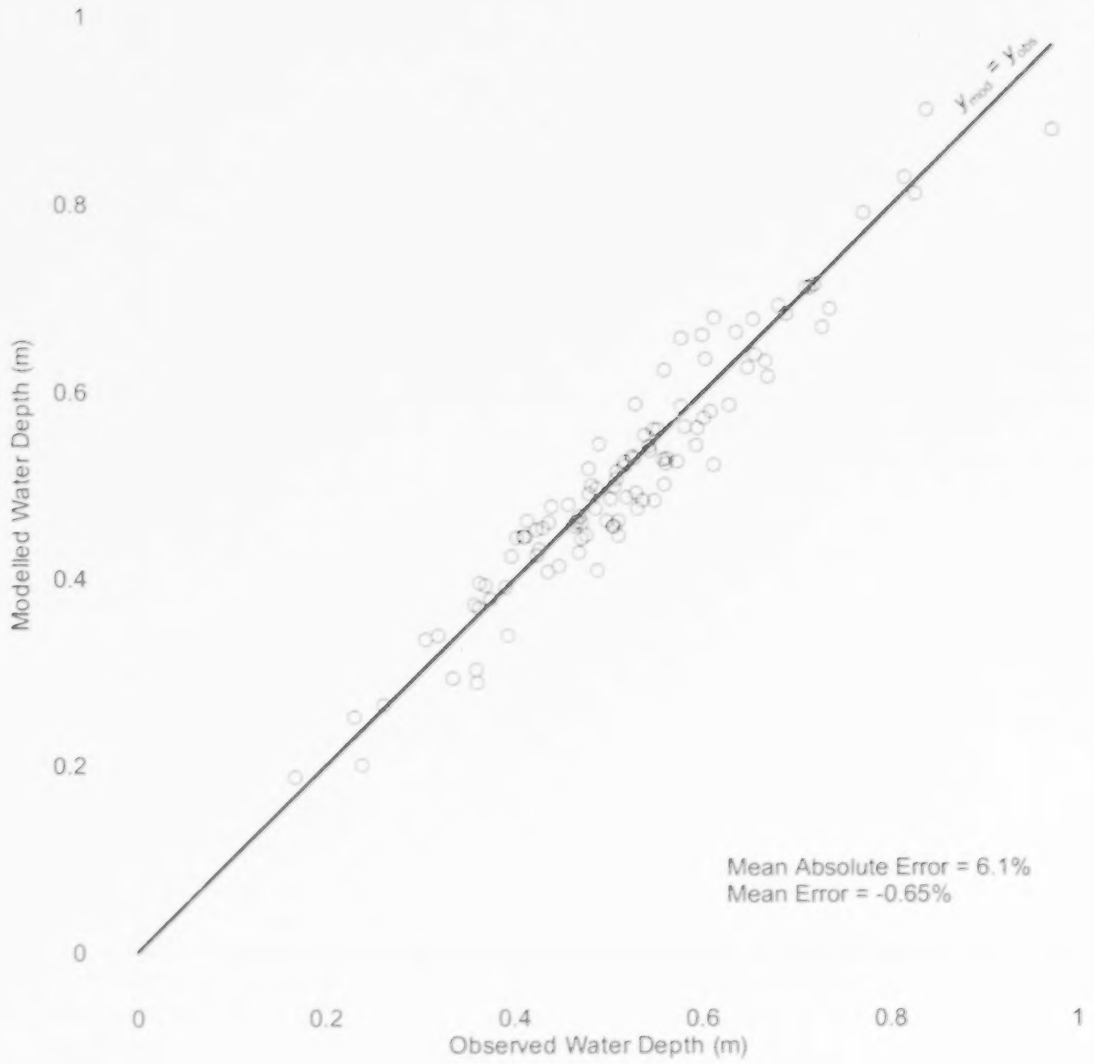

Figure 14: Tamihi side channel water depth verification plot (Q= 4.7 m^3/s).

Discharge scenarios

Four different discharge scenarios were modelled using River2D: 40 m^3/s (Q_b), 5.0 m^3/s, 0.5 m^3/s, and 0.05 m^3/s. The downstream boundary condition (water surface elevation) for each case was obtained through an iterative process: by changing downstream conditions until observed output water depths were approximately uniform. Modelled velocity contour plots of the 40 m^3/s discharge are presented on Figure 15a, Figure 15b, and Figure 15c.

Greater variations in local velocity magnitudes are observed when instream structures are included. Plain bed velocities, over the entire reach, tend to be uniform over long stretches (up to 110 m) with thalweg values ranging from 2.0 m/s to 3.0 m/s. With the inclusion of structures, the long stretches of constant velocity are reduced to distinct structure dependent zones (less then 35 m) with velocity values ranging from 1.5 m/s to 4.0 m/s. Maximum modelled velocities tend to occur close to the apex on the downstream side of the instream structures. Local flow hydraulics are affected by structure placement and spacing. The spacing between Str13 and Sr14 is small enough (approximately 4 m) so that Str14 is somewhat sheltered from flow and has less hydraulic significance. Lisle (1986) suggests that obstructions spaced less than 2 w_b from each other restrict pool formation. While this is true in the above case with Str13 and Str14, other structures that are within 2 w_b from each other still cause local flow variation (such as between Str7 and Str8 (see Figure 15b), and Str11and Str12 (see Figure 15c)). It may therefore be more appropriate to state that flow disturbance and variation would be maximized at a spacing greater than 2 w_b.

Modelled velocity vector plots are presented on Figure 16a, Figure 16b, and Figure 16c and demonstrate output velocities calculated by River2D. The thick black lines represent the channel bed boundary, which was subjectively determined by analysing the bathymetric contour plots. The vectors are scaled with velocity magnitude and greater variation can again be seen around structures, especially Str9, Str11 and Str12. The vector plots give a good indication of where flow acceleration and slack water occurs throughout the reach. Side currents and backwater eddies can be seen along the bank on the downstream side of Str7, Str11 and Str12 (similarly to those observed in Figure 1 and Figure 2).

Pool distributions

River2D was used to determine pre- and post-flood pool distributions for the Tamihi side channel by modelling a low discharge (0.5 m^3/s) and retrieving the water depth (y) from the output files. The retrieved depths were contoured and plotted using Surfer™ and are presented on Figure 17a, Figure 17b, and Figure 17c. A pool was defined as any area of the bed that has a calculated depth greater than 0.3 m at a low flow discharge of $Q = 0.5$ m^3/s. The pre-flood pool distributions indicate that pools were already in existence around Str1, Str5, Str6, Str7 and Str11. The formation of these initial pools is uncertain. The structures may have been installed in pre-existing pools or the pools may have been created at these locations during instream structure placement. The post-flood distributions indicate that pool formation and shape adjustment are a direct result of structure placement. Multiple-LWD triangular and rock-groyne structures appear to cause larger pools than single-LWD rootwad structures. This is most likely a reflection of constriction width (blockage ratio), which Lisle (1986) had found to be instrumental in causing channel-spanning pools. Likewise, Shields and Gippel (1995) found blockage ratio to be the most important parameter influencing flow resistance. With the exception of Str1, pool depth increased around all structures (up to a maximum of 0.6 m). In most cases, large increases in pool area were measured. Pool area deeper than 0.3 m increased from 320 m^2 to 470 m^2 in the pre- and post-bathymetric conditions, respectively. While pool area deeper than 0.4 m increased from 55 m^2 to 165 m^2, respectively. The changes in pool area correspond to a 50% and 150% increase (deeper than 0.3 m and 0.4 m cases, respectively).

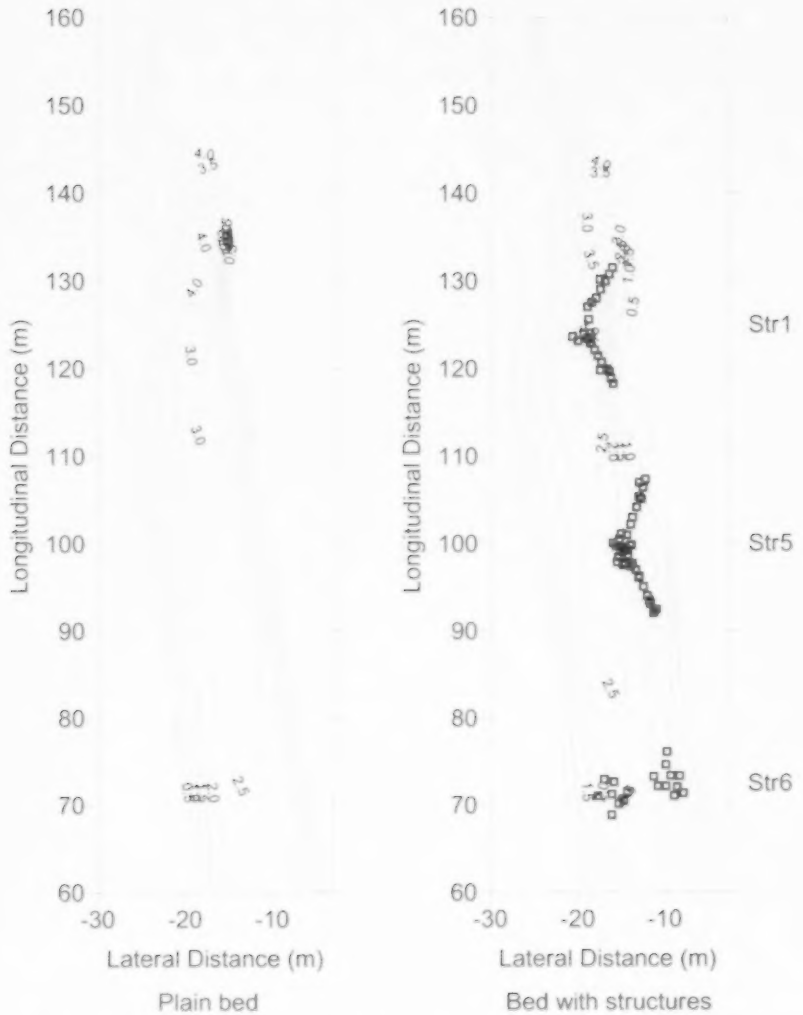

Figure 15a: Upper Tamihi side channel modelled velocity magnitude plots (m/s). Two pre-flood bathymetry modelling scenarios are presented (Q = 40 m3/s): plain bed and bed with structure representation. Instream structures are represented by brown square symbols.

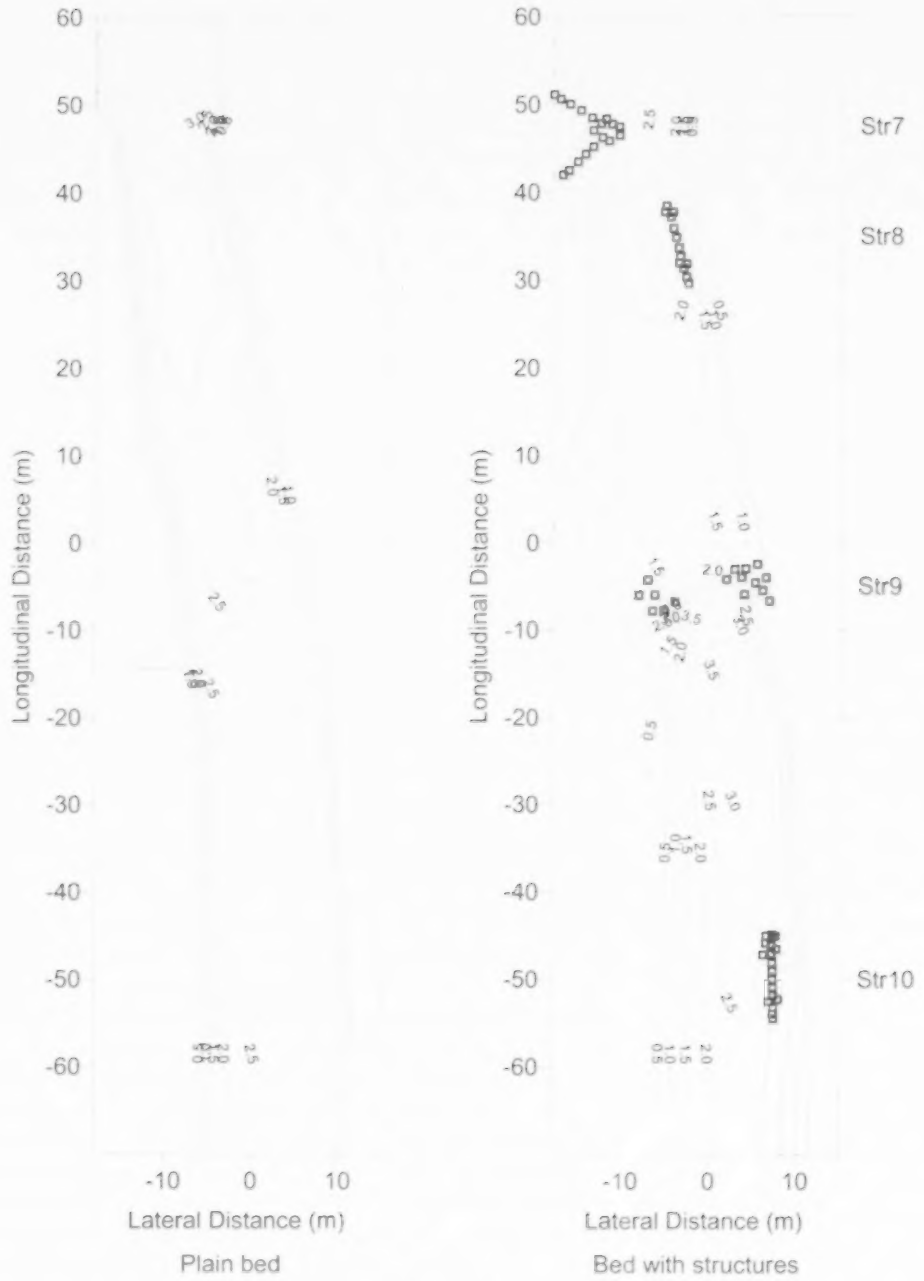

Figure 15b: Middle Tamihi side channel modelled velocity magnitude plots (m/s). Two pre-flood bathymetry modelling scenarios are presented (Q = 40 m3/s): plain bed and bed with structure representation. Instream structures are represented by brown square symbols.

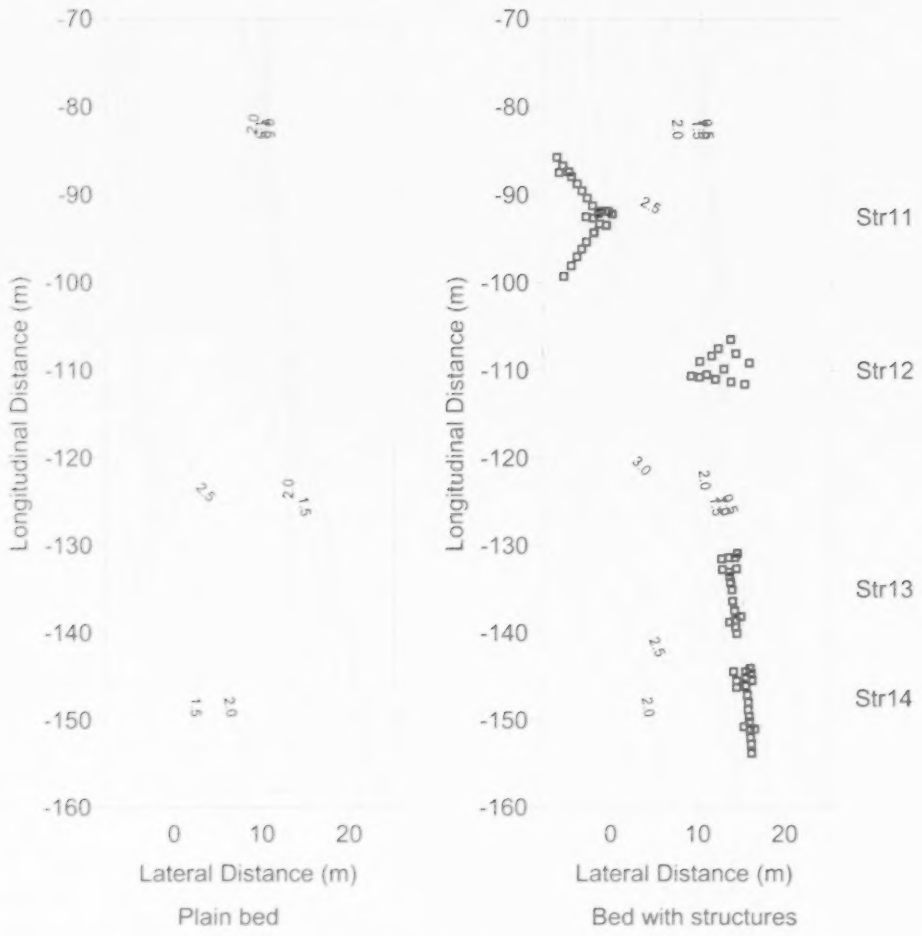

Figure 15c: Lower Tamihi side channel modelled velocity magnitude plots (m/s). Two pre-flood bathymetry modelling scenarios are presented (Q = 40 m3/s): plain bed and bed with structure representation. Instream structures are represented by brown square symbols.

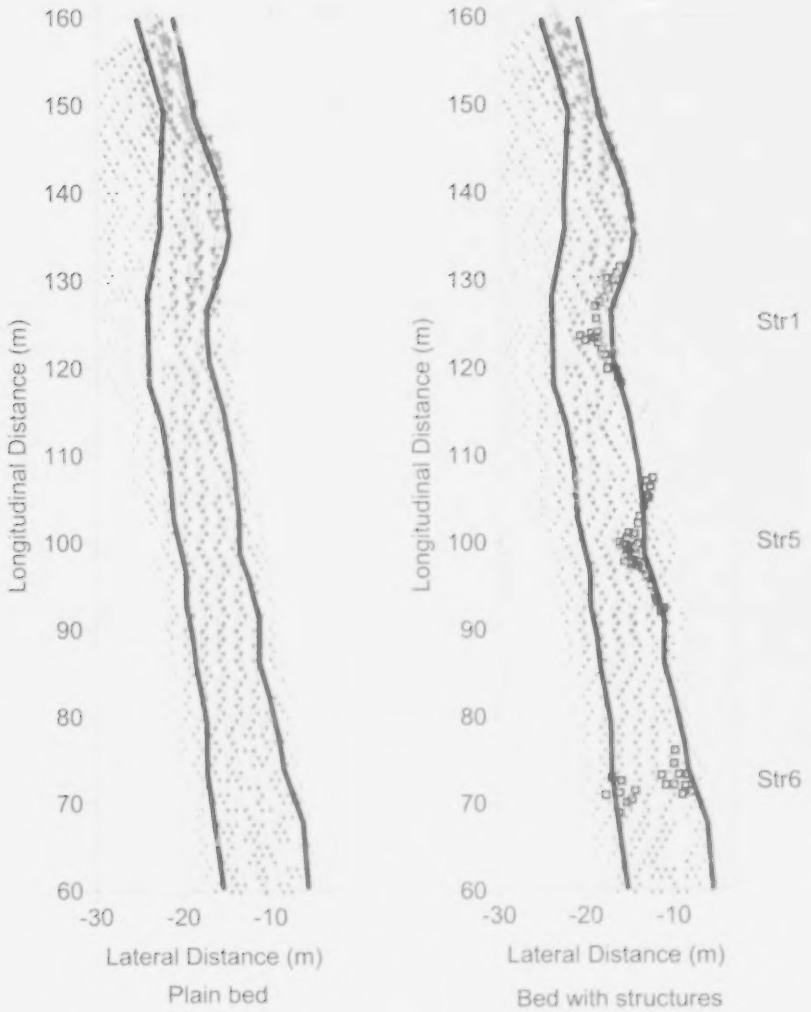

Figure 16a: Upper Tamihi side channel modelled velocity vector plots. Two pre-flood bathymetry modelling scenarios are presented (Q = 40 m3/s): plain bed and bed with structure representation. Plotted vectors are scaled to modelled velocity magnitudes. Thick black lines represent channel bed boundary. Instream structures are represented by square symbols.

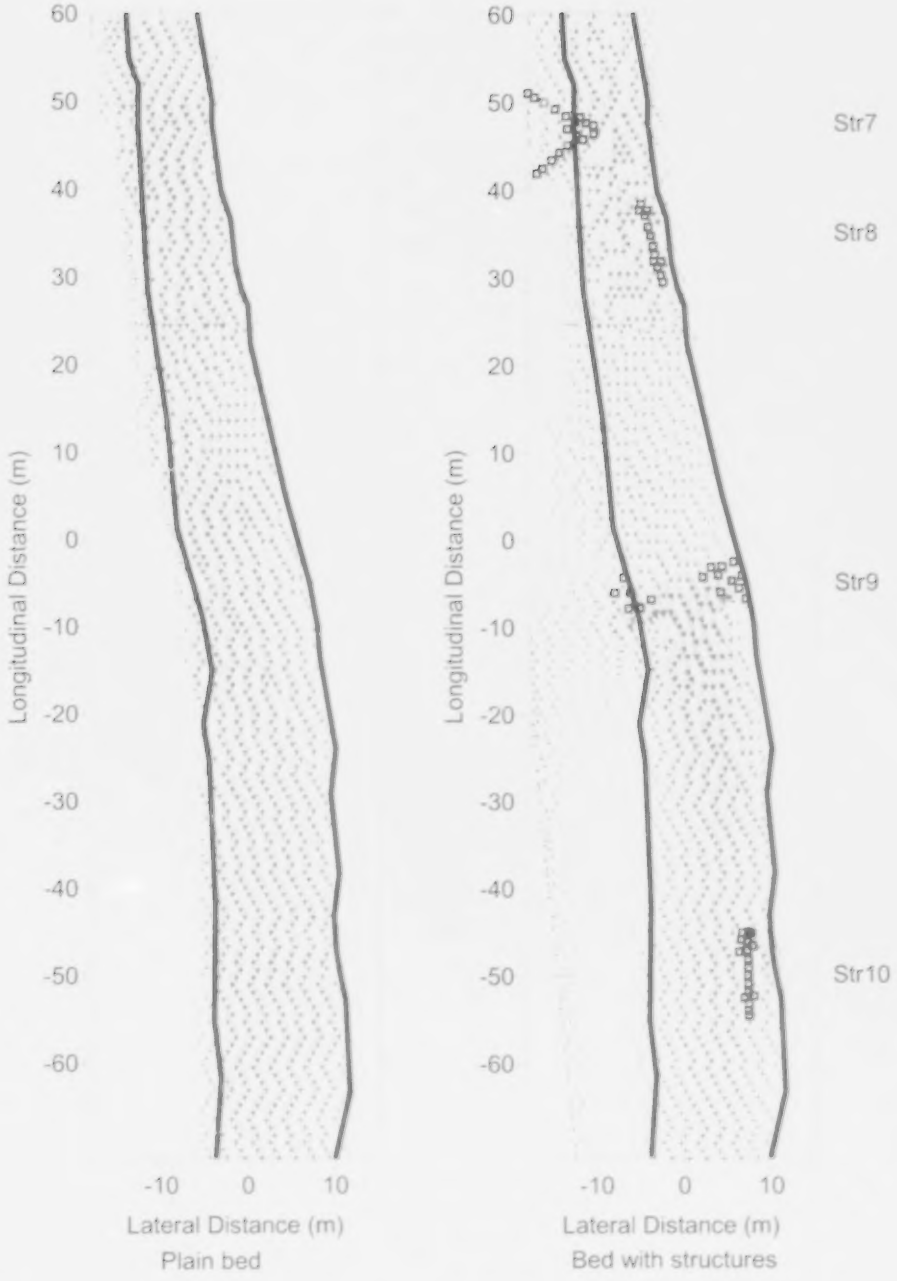

Figure 16b: Middle Tamihi side channel modelled velocity vector plots. Two pre-flood bathymetry modelling scenarios are presented (Q = 40 m3/s): plain bed and bed with structure representation. Plotted vectors are scaled to modelled velocity magnitudes. Thick black lines represent channel bed boundary. Instream structures are represented by square symbols.

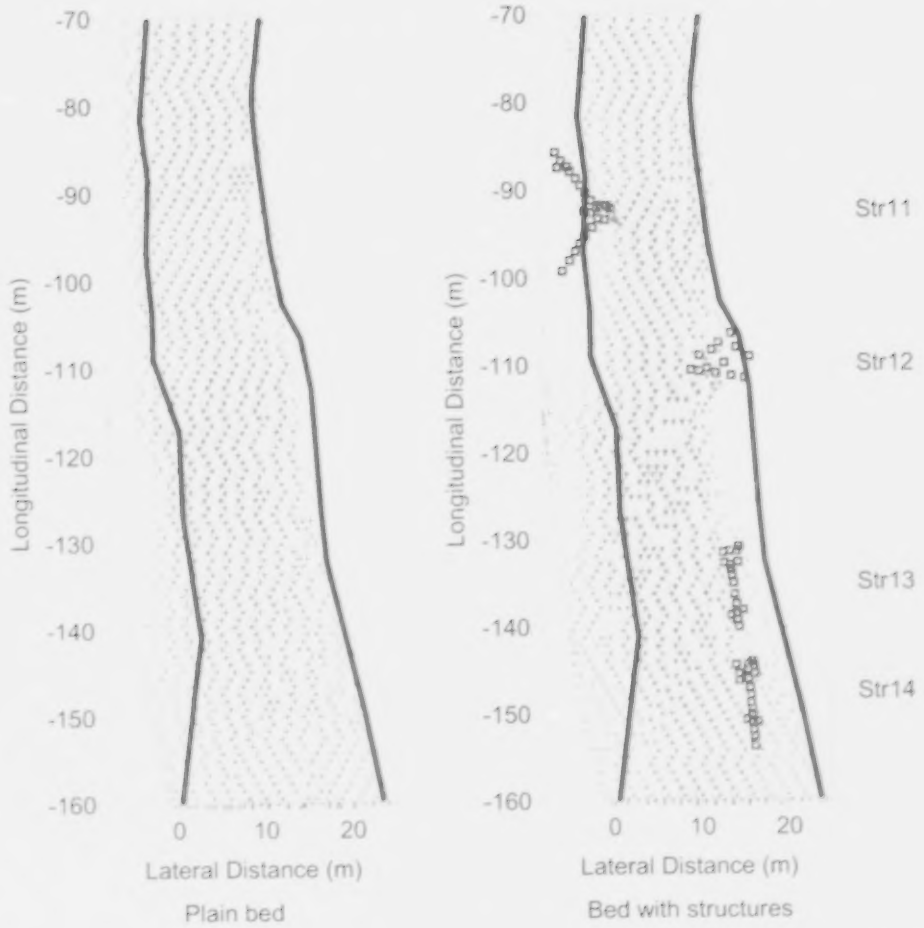

Figure 16c: Lower Tamihi side channel modelled velocity vector plots. Two pre-flood bathymetry modelling scenarios are presented (Q = 40 m3/s): plain bed and bed with structure representation. Plotted vectors are scaled to modelled velocity magnitudes. Thick black lines represent channel bed boundary. Instream structures are represented by square symbols.

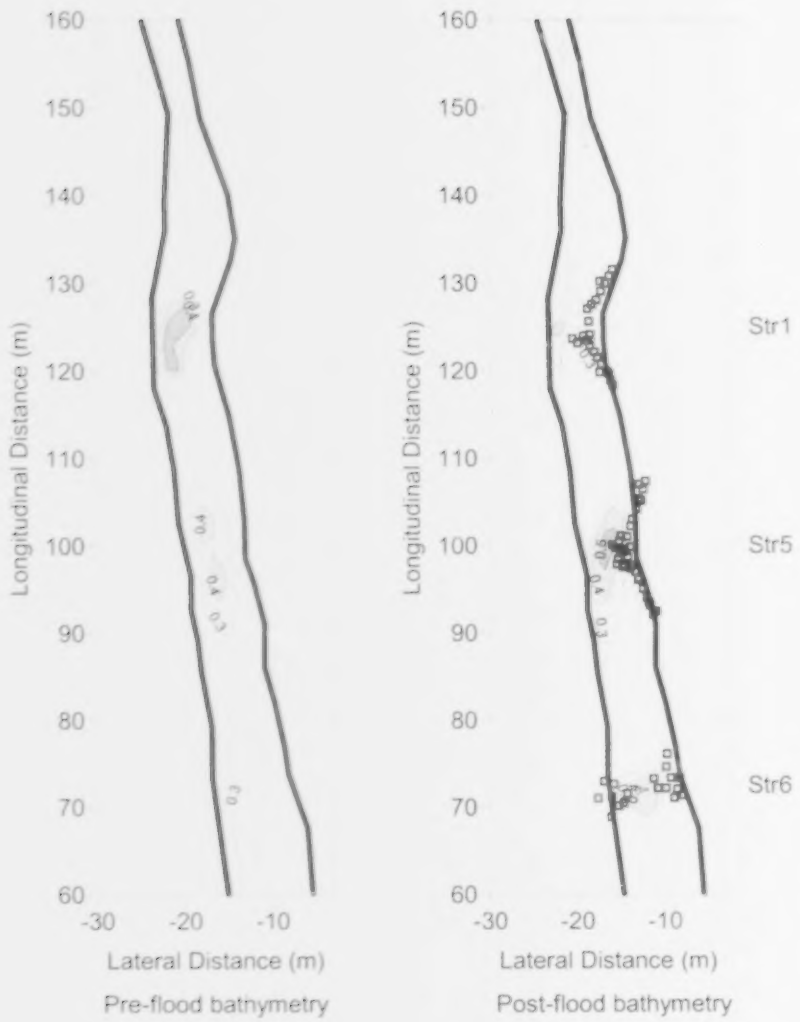

Figure 17a: Upper Tamihi side channel pre- and post-flood pool distributions. Contours represent pool depths (m). Thick black lines represent channel bed boundary. Instream structures are represented by square symbols.

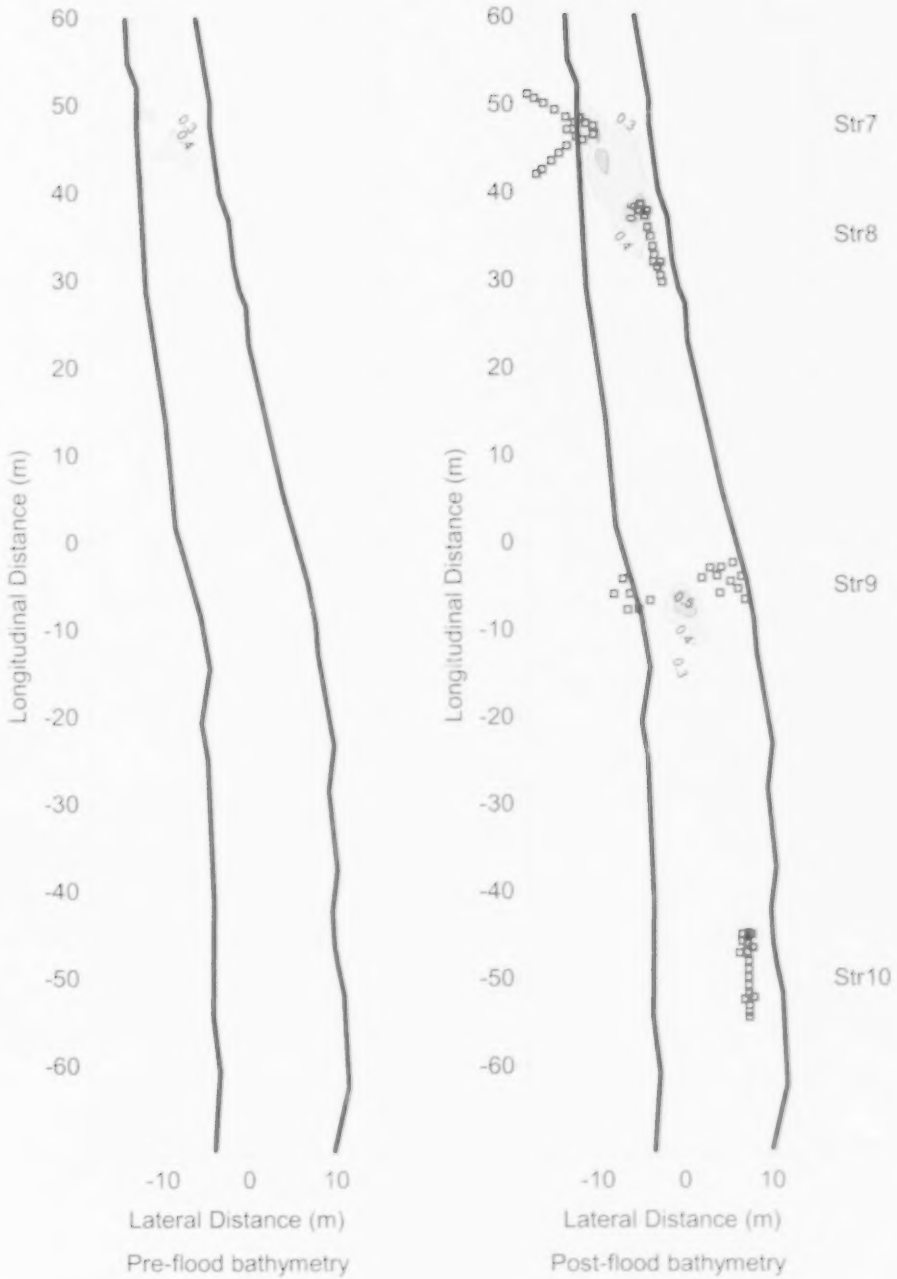

Figure 17b: Middle Tamihi side channel pre- and post-flood pool distributions. Contours represent pool depths (m). Thick black lines represent channel bed boundary. Instream structures are represented by square symbols.

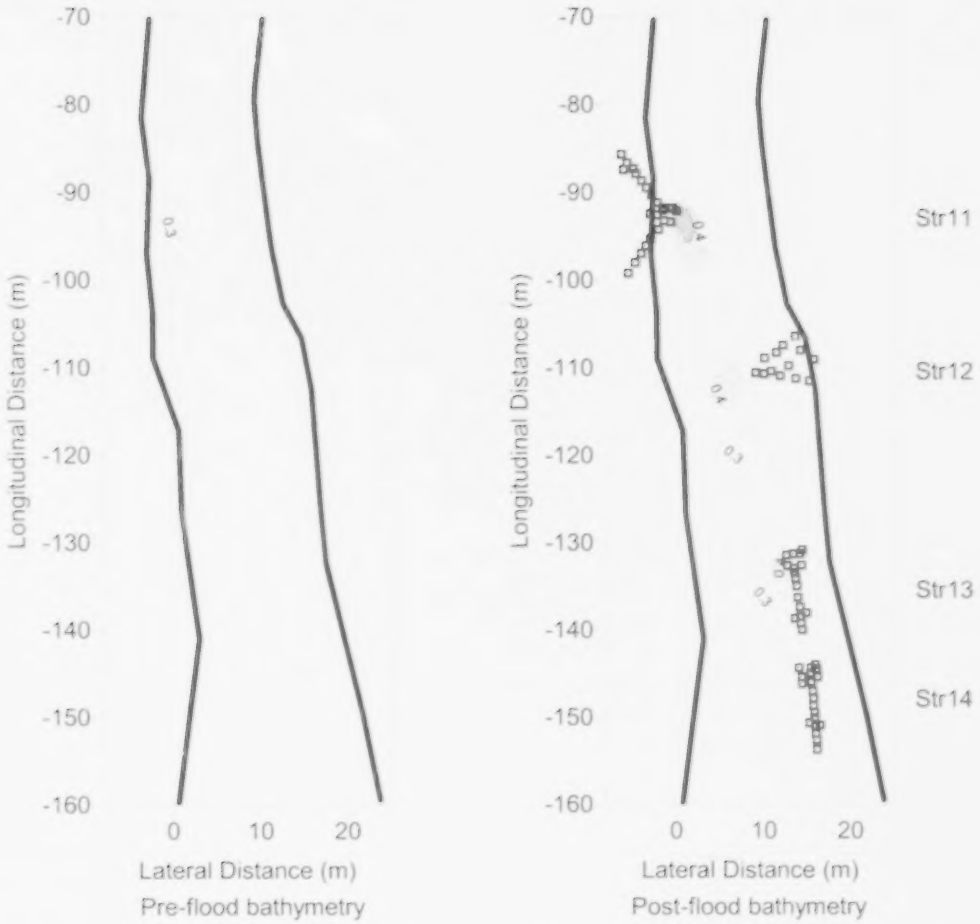

Figure 17c: Lower Tamihi side channel pre- and post-flood pool distributions. Contours represent pool depths (m). Thick black lines represent channel bed boundary. Instream structures are represented by square symbols.

Shear predictions

The $\bar{u}$ and y values produced by River2D using the pre-flood bathymetry (with structure representation) were used to calculate τ_o values given Equation 5. This bed scenario was used for the shear stress calculations since it represents the in situ conditions encountered by the flood (Q_b = 40 m^3/s). Shear stress intensity (τ_{*int}) is equal to the ratio of the calculated local shear stress over the dimensionalised critical shear stress (τ_o/τ_{crit}) where τ_{*crit} = 0.056 (from Shields) and was dimensionalised using Equation 6. The τ_{*int} plots are presented (along with the previously presented net scour plots) on Figure 18a, Figure 18b, and Figure 18c. The thick black lines represent the channel bed boundary.

It is difficult to draw any specific conclusions from Figure 18a, Figure 18b, and Figure 18c as they compare two separate parameters (scour depth (d_s) and τ_{*int}). Nevertheless, the locations of deep scour (in the middle and lower portions of the channel) appear to be in close proximity to the locations of predicted τ_{*int} greater than 1.0. The predicted τ_{*int} area is much more uniform than the measured extent of d_s, however the overall area between the two plots (in the middle and lower portions, Figure 18b and Figure 18c) is similar. Discrepancies occur due to small irregularities in the channel that may have been smoothed over in the process of transferring the bathymetric survey data to the DEM and bed files.

The predicted τ_{*int} values at Str5 through Str8 seem low considering the scour that that can be seen around these structures (see Figure 18a and Figure 18b). This may be a result of structure burial. The reach narrows and deepens in its upper portion, and, as a result, instream structures (such as Str6 and Str8) are likely to be buried during high flow events. As water depth increases overtop of the structures, the hydraulic influence (flow separation losses and local high velocities) would be reduced. This reduction in hydraulic influence was investigated by calculating τ_{*int} using a lower discharge (20 m^3/s). Under this scenario, the model predicted a larger area of high τ_{*int} values around Str7 and Str8 than was predicted using Q_b – indicating burial was an issue at high flows. Likewise, Shields and Gippel (1995) found pool-forming processes around LWD were reduced with increased discharges; furthermore, Smith and Beschta (1994) found scour and deposition occurred at discharges well below bankfull.

The model predicted very high shear stresses at the upper most region of the side channel (see Figure 18a). Contrarily, the net scour plot indicates that aggradation has taken place in this region. As discussed previously, aggradation occurred in the upper channel most likely because of large classed sediments, which were transported from the adjacent medial bar. River2D could not predict this occurrence. As well, model output close to the upper boundary may be erroneous and produce higher shear stress than realistic.

For completeness the selected Shields value of τ_{*crit} = 0.056 was compared to the value suggested by Church *et al* (1998) and τ_{*crit} = 0.079. The model results appear to be quite sensitive to the τ_{*crit} selected. With increased τ_{*crit} values from 0.056 to 0.079, the area of predicted shear is substantially reduced. The reduction in shear is even more apparent in the upper portion of the channel.

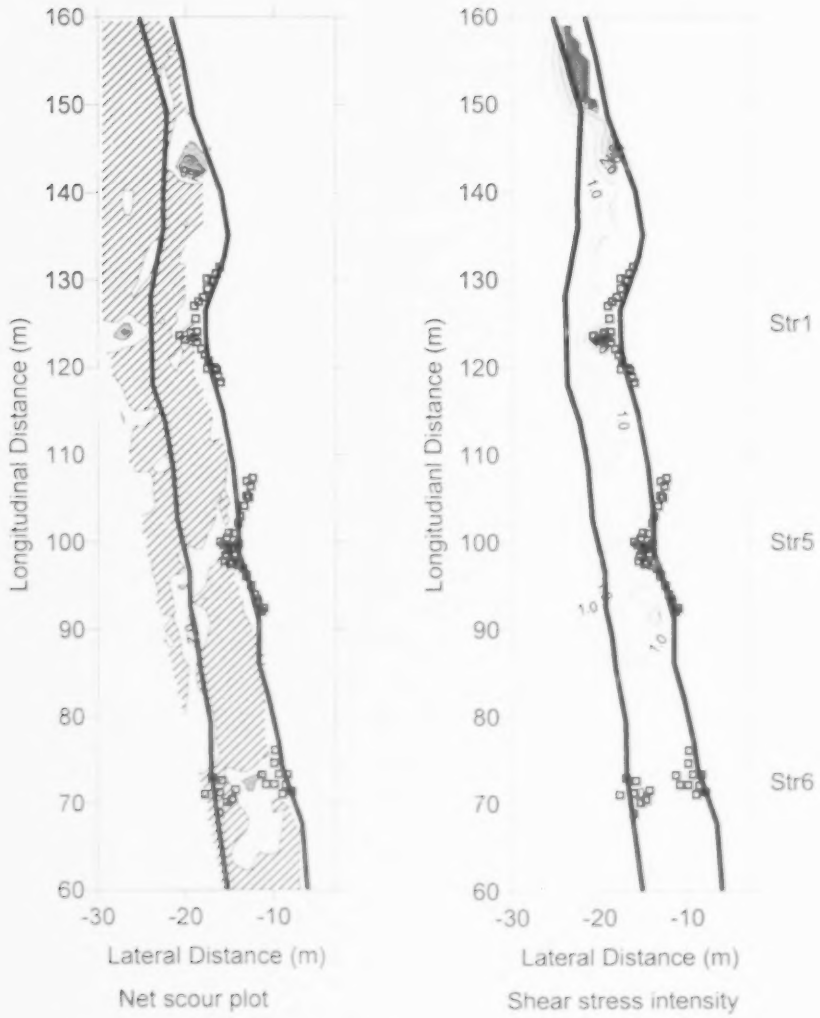

Figure 18a: Upper Tamihi side channel net scour and shear stress intensity plots. The net scour plot was previously presented as Figure 12a. Positive contours represent degradation, while hatched contoured areas represent aggradation. The shear stress intensity plot is based on the model results using the pre-flood bathymetry with structure representation. Plot contours represent the ratio of bed shear/critical shear. Shear stress intensity contours greater than 1.0 indicate areas of potential scour. Thick black lines represent the channel bed boundary. Instream structures are represented by square symbols.

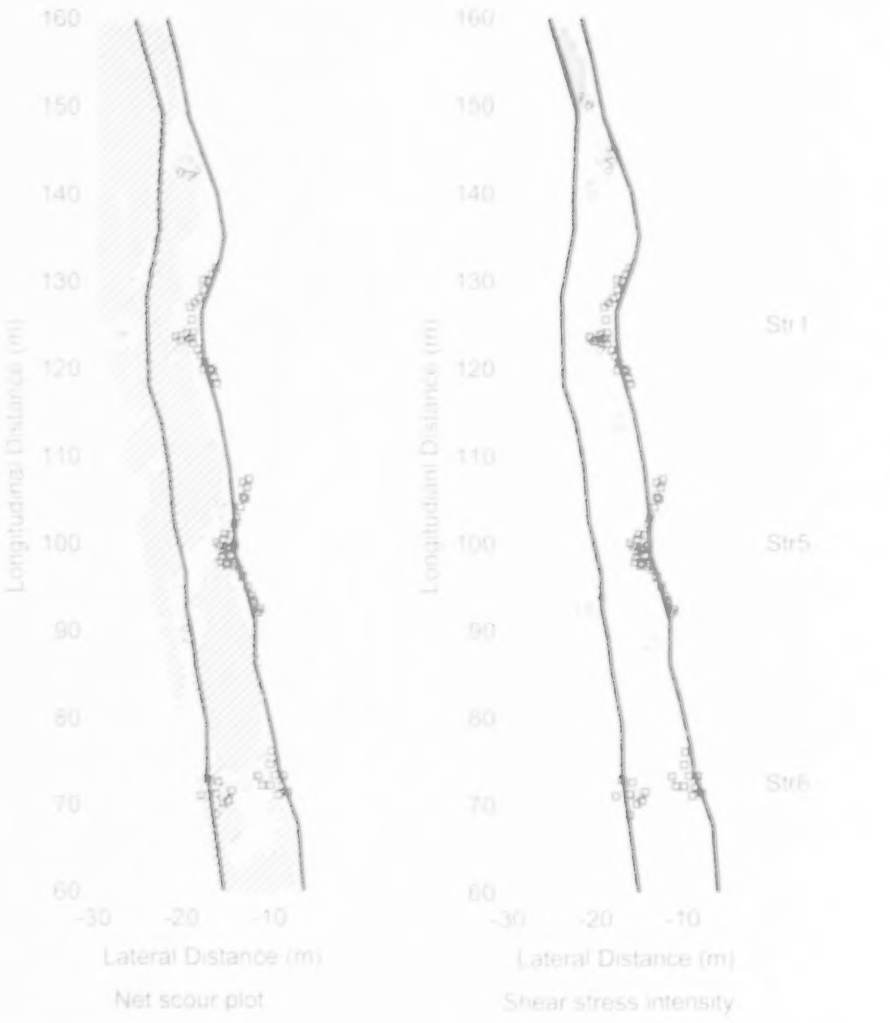

Figure 18a: Upper Tamihi side channel net scour and shear stress intensity plots. The net scour plot was previously presented as Figure 12a. Positive contours represent degradation, while hatched contoured areas represent aggradation. The shear stress intensity plot is based on the model results using the pre-flood bathymetry with structure representation. Plot contours represent the ratio of bed shear/critical shear. Shear stress intensity contours greater than 1.0 indicate areas of potential scour. Thick black lines represent the channel bed boundary. Instream structures are represented by square symbols.

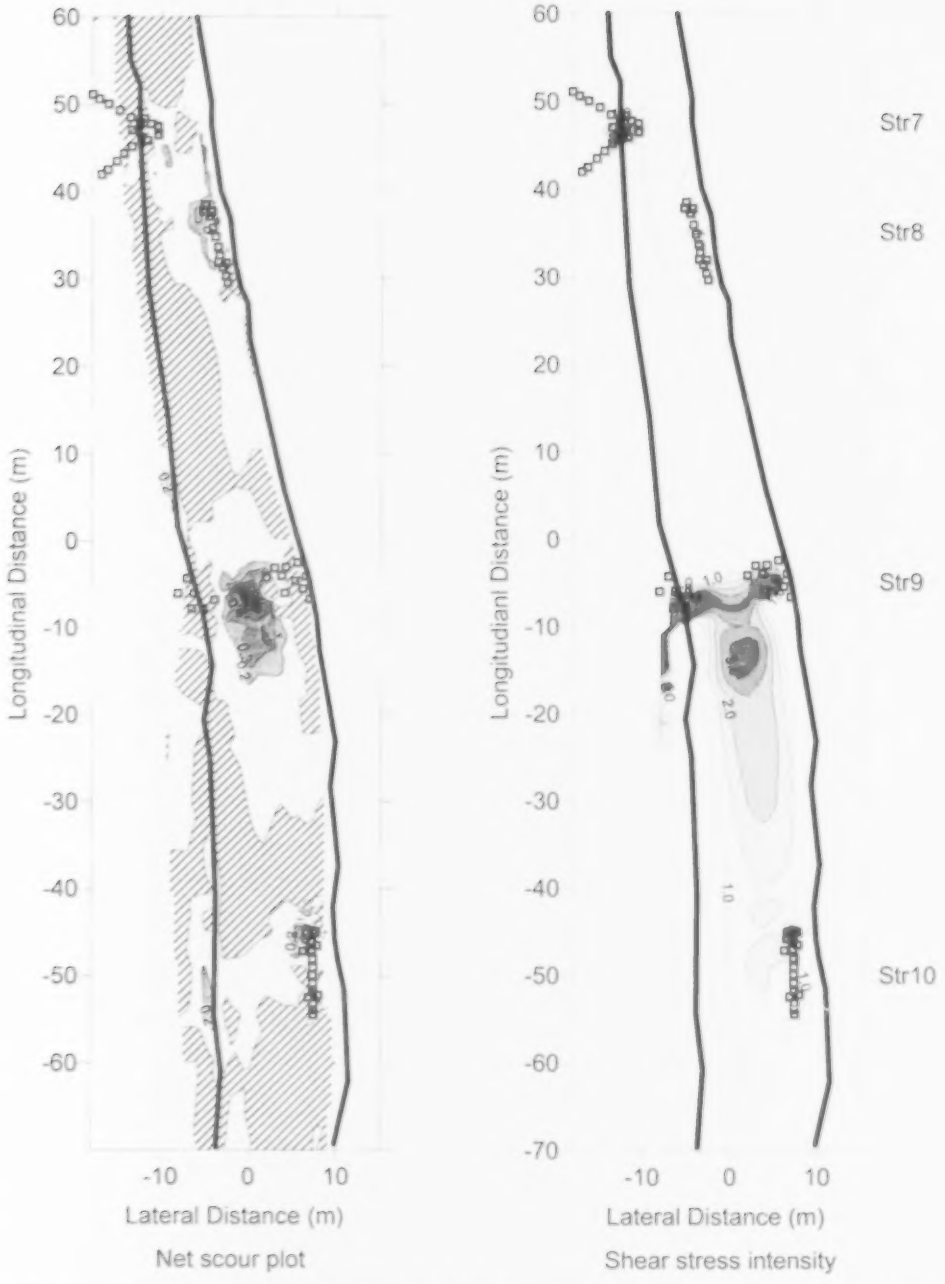

Figure 18b: Middle Tamihi side channel net scour and shear stress intensity plots. The net scour plot was previously presented as Figure 12b. Positive contours represent degradation, while hatched contoured areas represent aggradation. The shear stress intensity plot is based on the model results using the pre-flood bathymetry with structure representation. Plot contours represent the ratio of bed shear/critical shear. Shear stress intensity contours greater than 1.0 indicate areas of potential scour. Thick black lines represent the channel bed boundary. Instream structures are represented by square symbols.

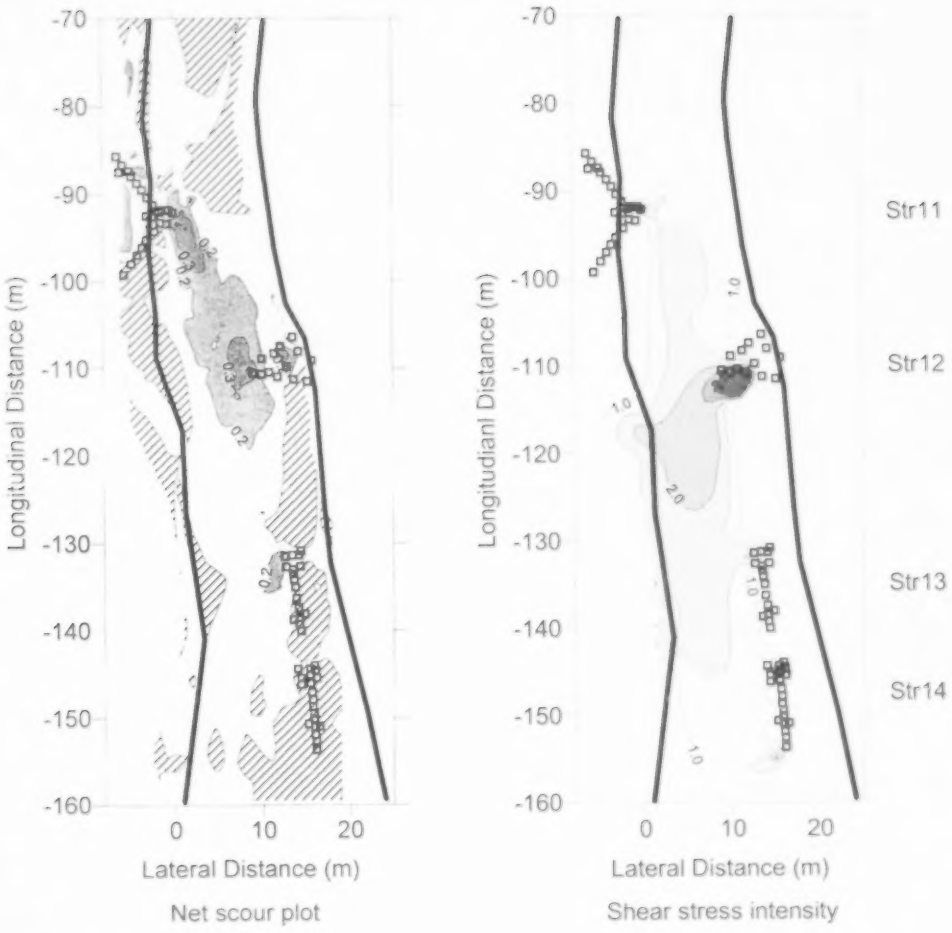

Figure 18c: Lower Tamihi side channel net scour and shear stress intensity plots. The net scour plot was previously presented as Figure 12c. Positive contours represent degradation, while hatched contoured areas represent aggradation. The shear stress intensity plot is based on the model results using the pre-flood bathymetry with structure representation. Plot contours represent the ratio of bed shear/critical shear. Shear stress intensity contours greater than 1.0 indicate areas of potential scour. Thick black lines represent the channel bed boundary. Instream structures are represented by square symbols.

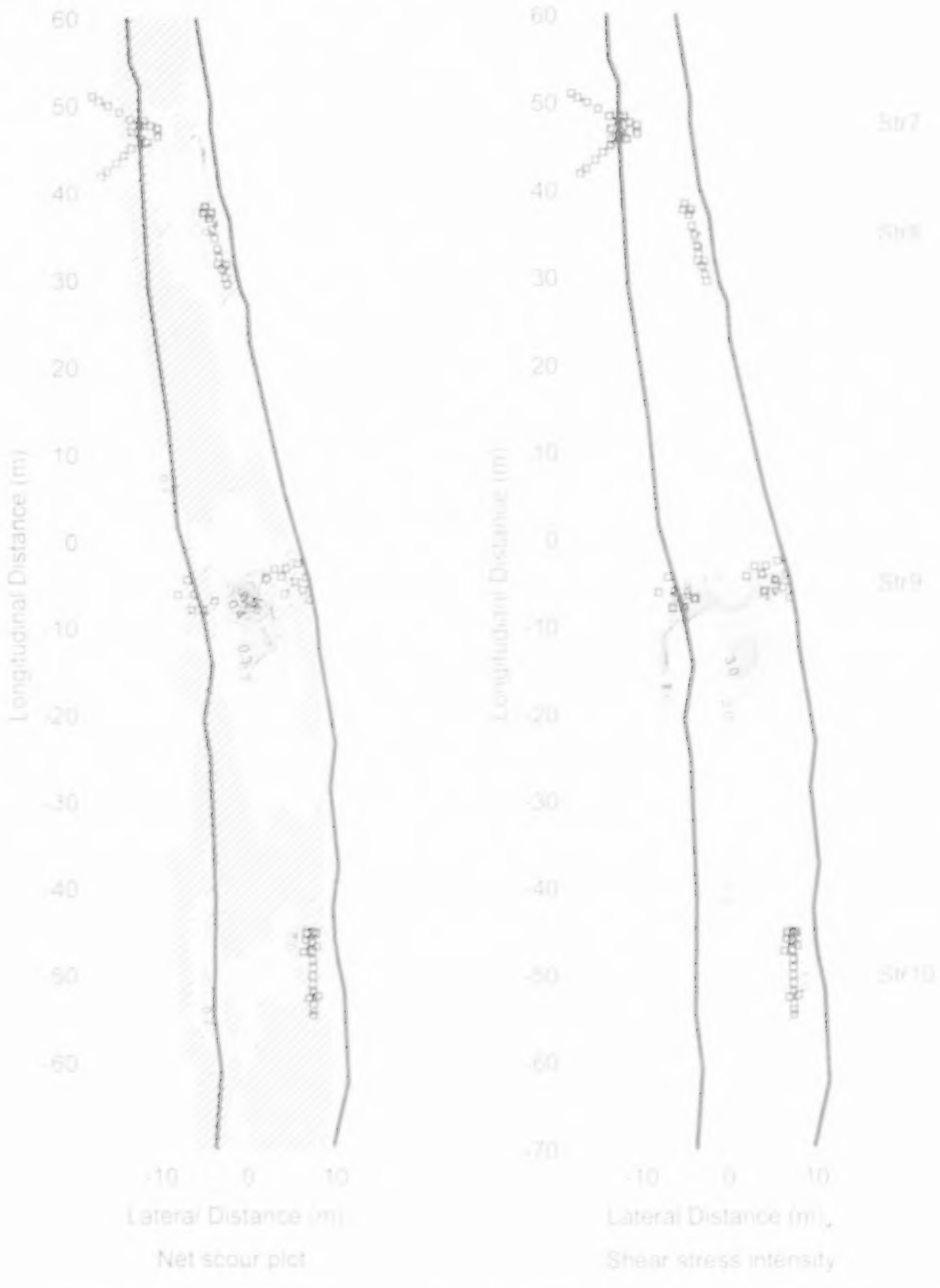

Figure 18b: Middle Tamihi side channel net scour and shear stress intensity plots. The net scour plot was previously presented as Figure 12b. Positive contours represent degradation, while hatched contoured areas represent aggradation. The shear stress intensity plot is based on the model results using the pre-flood bathymetry with structure representation. Plot contours represent the ratio of bed shear/critical shear. Shear stress intensity contours greater than 1.0 indicate areas of potential scour. Thick black lines represent the channel bed boundary. Instream structures are represented by square symbols.

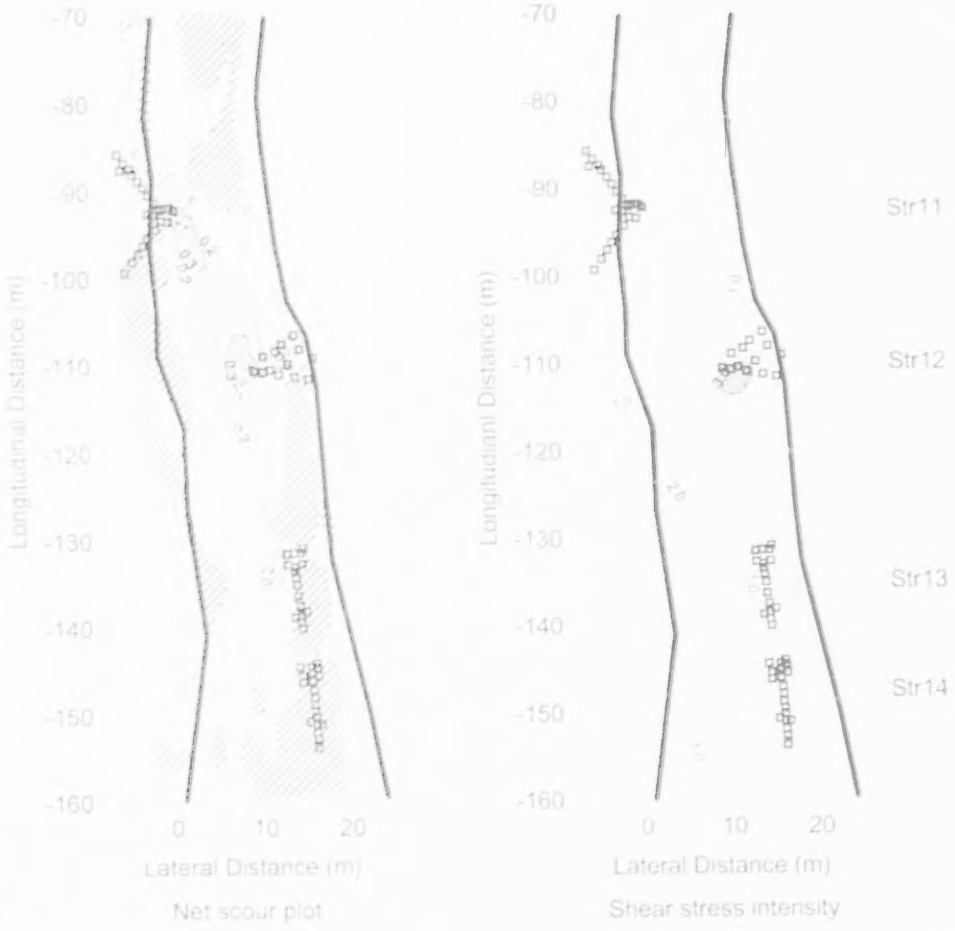

Figure 18c: Lower Tamihi side channel net scour and shear stress intensity plots. The net scour plot was previously presented as Figure 12c. Positive contours represent degradation, while hatched contoured areas represent aggradation. The shear stress intensity plot is based on the model results using the pre-flood bathymetry with structure representation. Plot contours represent the ratio of bed shear/critical shear. Shear stress intensity contours greater than 1.0 indicate areas of potential scour. Thick black lines represent the channel bed boundary. Instream structures are represented by square symbols.

Fish habitat

The Bovee (1978) preference curves, for the site's target species (coho and steelhead), were used to develop velocity and depth lookup tables required for the habitat component of River2D. The depth and velocity preference tables are used by River2D to determine the WUA for each flow scenario (40 m^3/s, 5.0 m^3/s, 0.5 m^3/s, 0.05 m^3/s). As with Mosley (1982), and Hogan and Church (1989), cover, temperature and substrate preferences were assumed to be optimum to simplify results. Table 5, Table 6, Figure 19 and Figure 20 summarize the WUA of the target species computed by River2D for the discharges investigated.

Table 5: Modelled %WUA for coho salmon at selected discharges.

Q (m^3/s)	fry			spawners		
	pre-	post-	% change	pre-	post-	% change
40	**0.9**	**2.5**	**180**	**2.0**	**5.5**	**175**
5.0	1.0	1.5	50	4.6	4.1	-10
0.5	1.3	2.5	90	11.9	8.9	-25
0.05	0.2	0.8	300	0.2	0.3	50

Table 6: Modelled %WUA for steelhead trout at selected discharges.

Q (m^3/s)	fry			juveniles		
	pre-	post-	% change	pre-	post-	% change
40	**4.3**	**13.4**	**210**	**4.9**	**12.1**	**150**
5.0	6.1	5.9	-5	10.8	10.1	-5
0.5	20.5	17.0	-15	15.3	13.6	-10
0.05	11.0	12.0	10	3.7	4.8	30

Under the bankfull flow modelling scenario, the affect of the instream structures was to substantially increase %WUA for both coho salmon and steelhead trout. The percent difference in %WUA is between 150% and 210% (see Table 5 and Table 6). The results also indicate that steelhead prefer the higher flows more than coho. The difference between the two species is not unexpected. Juvenile steelhead prefer fast flowing water, while coho being not as well adapted for high velocity zones prefer off-channel areas (such as ponds) with lower velocities and shallower depths (Swales and Levings 1989).

During low flow seasons in the Chilliwack River (late summer and late winter (before spring freshet)), flow into the Tamihi side channel is restricted to groundwater seepage due to the entrance sill. Table 5 and Table 6 indicate that the %WUA for Q = 0.05 m^3/s increases slightly from pre- to post-flood due to instream morphologic and hydraulic changes. The hydraulic effects of instream structures at low flows are minimal since flow is restricted to the centre portion of the channel, yet the increased pool area (created by the structures during high flows) results in more refuge areas being available. The large percent change for coho fry between pre- and post-structure placement at Q = 0.05 m^3/s is more a reflection of the very small %WUA calculated in the pre-structure scenario than representative of a large increase in %WUA after structures were installed.

The %WUAs obtained during the Q = 0.5 m^3/s flow scenarios decreased slightly post-flood for coho spawners, steelhead fry and steelhead juveniles, while coho fry incurred an increase. The decrease in coho spawners is understandable since the formation of pools would reduce available spawning area. The decrease in steelhead %WUA in the post-flood run may be a result of their preference for faster, shallower water (Bisson *et al* 1981).

Figure 19 and Figure 20 indicate that the most beneficial aspect of the instream structures is to offer refuge areas during high-flow events for steelhead and coho of both ages. As stage increases there is a trend towards faster moving water. Fish must find refuge areas behind boulders or in pools to avoid being swept downstream by the current. The instream structures create low velocity zones on their downstream sides where fish can hold and rest. At lower flows these refuge areas become less important. The results seem to indicate that the importance of the pools formed by the structures only become important when flows reach critically low levels. Yet as was discussed previously, deep pool areas (such as those created by the instream structures) are desirable for older salmonids (Bustard and Narver 1975) and may not be well represented by the Bovee (1978) preference curves.

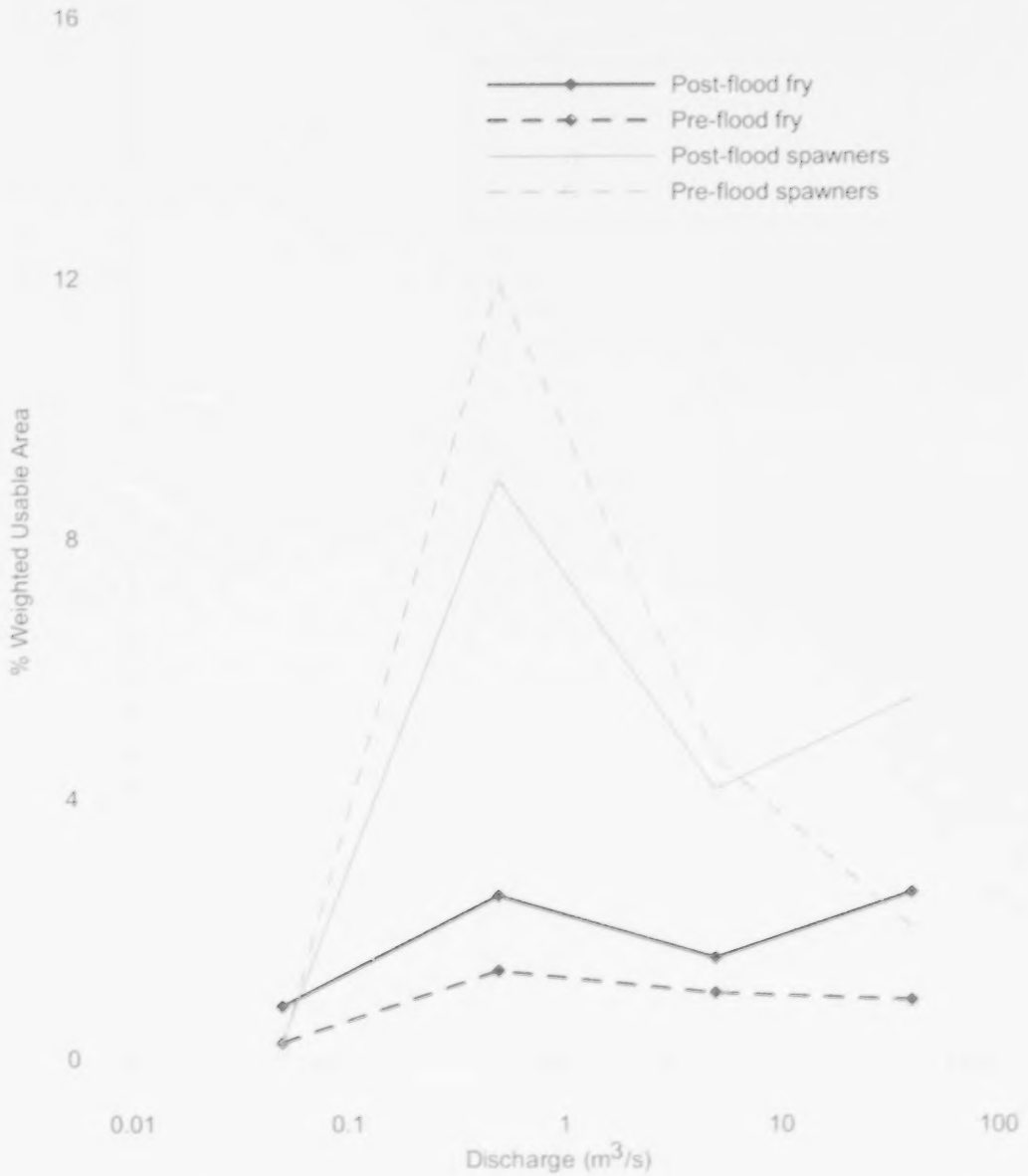

Figure 19: Tamihi side channel percent weighted usable area for coho salmon. Post-flood values were modelled using the bed with structure representation bathymetry, while the pre-flood values were modelled using the plain bed bathymetry.

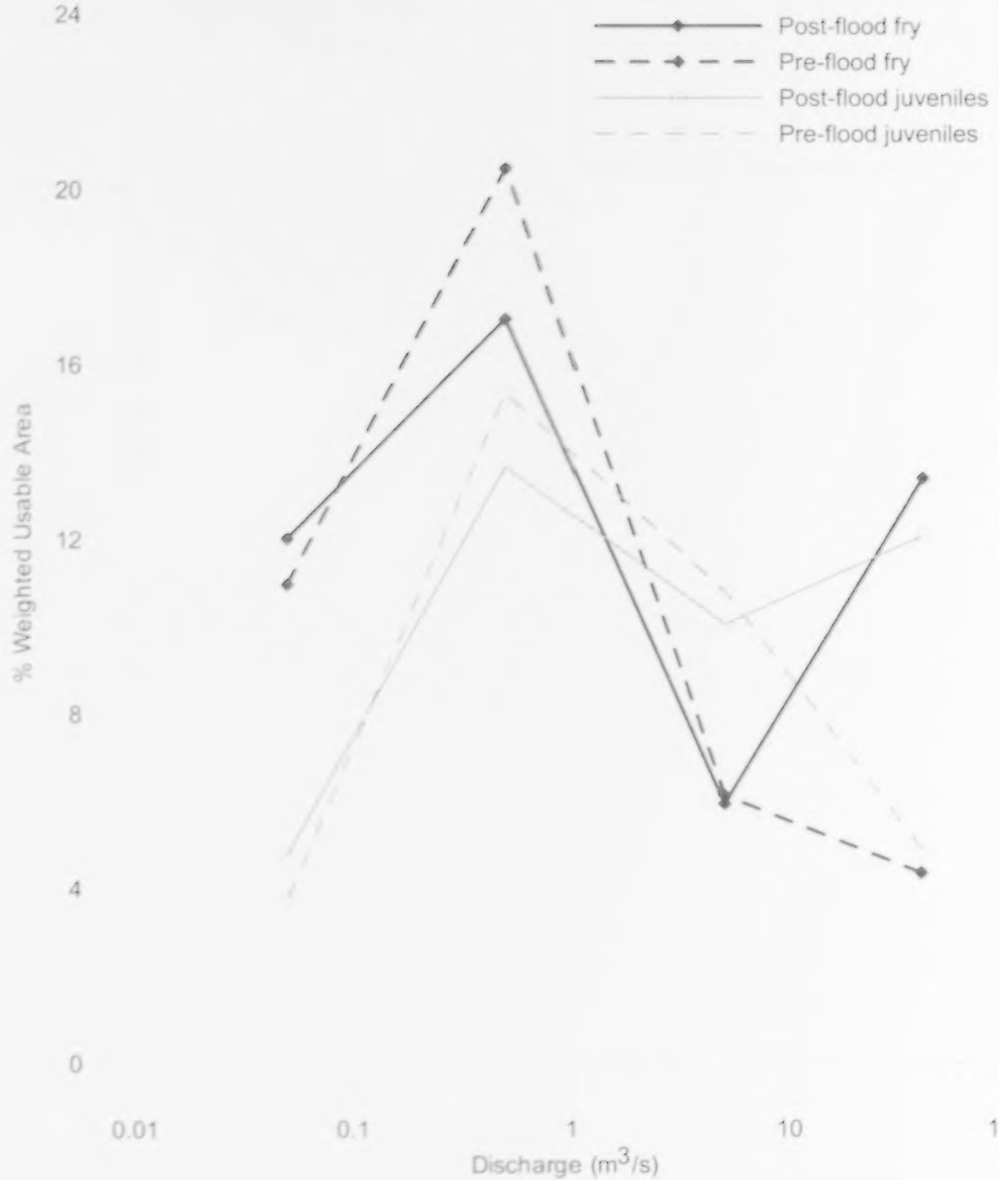

Figure 20: Tamihi side channel percent weighted usable area for steelhead trout. Post-flood values were modelled using the bed with structure representation bathymetry, while the pre-flood values were modelled using the plain bed bathymetry.

SUMMARY AND RECOMMENDATIONS

This study assesses the morphological and hydraulic effects, as well as, the habitat benefits of instream LWD and boulder structures using a two-dimensional hydrodynamic model (River2D). Eleven instream structures, installed on the Tamihi side channel in August 1999, were investigated. Pre- and post-flood bathymetric surveys revealed bed scour to have occurred, to a maximum of 0.7 m, adjacent to and downstream of instream structures. Bed variation and complexity was also seen to increase. The observed scour was qualitatively seen to be a result of structure placement. Shape and location of scour holes around instream structure types were consistent with the literature findings of Lisle (1986), and Abbe and Montgomery (1996). Instream structures had a direct effect on local thalweg slope, yet the overall channel slope increased only marginally and was not attributed to instream structures.

River2D was used to predict channel hydraulic variables (local velocities and depths) for both the pre- and post-structure scenarios. Comparison between pre- and post-structure velocities indicated a trend towards greater velocity variation and higher local velocity values resulting form instream structures. Comparisons between modelled and observed $\overline{u}$ and y indicate River2D's predictions of $\overline{u}$ to be satisfactory (MAE = 24%), while y is well predicted (MAE = 6.1%). The verification results lend confidence in the use of River2D in predicting local channel hydraulics.

River2D was used as a tool to assess pool changes resulting from instream structure placement. Pool formation and shape adjustment were directly related to instream structures. Blockage ratio appeared to be an important factor in determining pool size. Reach length pool area deeper than 0.3 m increased by 50%, while pool area deeper than 0.4 m increased by 150%.

The hydraulic variables predicted by River2D were used to calculate local shear stress throughout the reach. Areas of possible mobility were determined by dividing the predicted local bed shear stress by the critical shear stress suggested by Shields. Predicted bed mobility coincided with areas of scour in the middle and lower portions of the channel, while the upper portion of the channel, which underwent substantial aggradation during the November 12th 1999 flood, was poorly related. Structure position and spacing affected predicted shear. Reduced shear values were predicted when instream structures were positioned directly downstream from each other with less than 2 w_b spacing. This sheltering effect was also observed in the net scour plots.

Fish habitat analysis was performed on the pre- and post-flood bathymetry of the Tamihi side channel using River2D at various discharge scenarios. The results for the bankfull condition (Q_b) indicated that the %WUA of coho salmon and steelhead trout have a percent difference greater than 150% with the addition of instream structures. The effect of instream structures was reduced at lower discharges and in some cases resulted in a decrease in available %WUA. The WUA method was used to rate the potential habitat benefits of instream structures in the Tamihi side channel. The Bovee (1978) preference curves offer a simple indices for determining site specific fish habitat preference; yet the analysis is dependent on the correctness and applicability of transferring the preference curves from the regions and specific conditions under which they were developed to other regions.

The methods used in this study for scour and habitat analysis can be followed and used for other systems where instream works are planned. Planned instream works could be optimized to produce greater hydraulic variation and fish habitat. Furthermore, optimization would target specific species. The following steps, derived from this study, provide an iterative methodology for the optimization of instream works:

1. Conduct a bathymetric survey of the reach under investigation. Spacing between sample points can be variable but should be sufficient to pick up bed and bank elevation changes.

2. Conduct pebble counts and grain size analyses to characterize channel roughness.

3. Investigate watershed hydrology to determine the bankfull flow (Q_b) (the event which would likely induce the most scour and hydraulic variance). Calculate the bankfull depth (y_b) for the downstream boundary using Equation 1.

4. Convert survey data into a digital elevation model (DEM) and add in preferred instream structure design representation. Spacing between nodes should be around 1.0 m or less.

5. Convert DEM to mesh files (with equivalent roughness height k_s values) for input into River2D

6. Run River2D under the bankfull boundary conditions and adjust downstream condition to delineate for backwater or draw-down effects.

7. Input target species preference curves and run the habitat component River2D to determine the WUA for the particular species of interest. Cover information can also be added if desired.

8. Using River2D's output file produce a velocity contour plot and a shear stress intensity plot using Equation 5 and Equation 6. The plots can be used to determine areas of influence, and optimal positioning and spacing of instream structures.

9. Adjust the design of the instream structures (given the information learned in the above steps) and then repeat steps 5 through 8, until an optimum design is reached.

Fish habitat assessment is site, discharge and species specific and is related to local hydraulic and morphologic conditions. The habitat component River2D uses the predicted local hydraulic characteristics for evaluating the WUA and as such offers a powerful tool for assessing instream structure designs before they are installed. The methodology described above could also be used as a post-installation assessment to verify the value of previous restoration works. Without the use of River2D (or other 2D flow models), detailed local high-flow hydraulic information could only otherwise be gained through rigorous field sampling during high discharges (which is in many cases not possible).

The current study offers a methodology for standardising instream restoration practices such that some of the subjectivity and randomness of structure placement is removed. Unfortunately, the lack of a direct relationship between measured scour and predicted shear stress intensity, and the simplification of fish preferences into two hydraulic parameters ($\overline{u}$ and y) make it difficult to obtain a truly optimal design. But given the lack of methodologies currently available, the above technique, although not optimal, is a few steps closer towards that goal. Furthermore the information gleaned on structure spacing and size, through the use of local hydraulic analyses, is valuable and has previously been unavailable. As the study's methodology is highly field data dependent, the practical application of this method should be reserved for sites where bathymetric information is already available or where the most optimal solution is a design requirement.

Further areas of interest and possible research would be in investigating the relationship between observed scour and the shear stress intensity predicted by 2D hydrodynamic models. Much work in the past has been spent on trying to predict scour through the use of general or averaged channel hydraulic parameters and perhaps advances could be gained by investigating local hydraulics with the aid of 2D models. The fish preference curves are a simple method of identifying stream habitat availability, but

research needs to be carried out to verify that the curves are indeed representative of fish preference and that the curves are applicable to river systems deferent from those they were originally developed from. Furthermore, in this study, as with Mosley (1982) and Hogan and Church (1989), the Bovee (1978) preference curves for streamside cover, substrate size and water temperature were assumed to be optimum. This assumption should be tested through the use of a 2D model and biological fish numeration.

On a much more general level, it is important to remember that instream structure restoration activities should be viewed as interim management tools to improve habitat until restoration of riparian zones or upslope conditions occurs (House 1996; Roper *et al* 1998). River restoration projects should use instream structures to hasten ecological recovery, yet it may take up to 200 years before the rehabilitated riparian vegetation makes a significant contribution of LWD to rivers (Gippel *et al* 1992). Two-dimensional modelling offers the opportunity to improve interim habitat restoration practices, but watershed wide restoration must be addressed or instabilities caused by upstream and/or upslope effects will prematurely affect the durability and life of instream restoration works.

REFERENCES

Abbe, T.B., and D.R. Mongomery. 1996. Large woody debris jams, channel hydraulics and habitat formation in large rivers. Regulated Rivers Research and Management 12: 201-221.

Allan, J.H., and S. Lowe. 1997. Chapter 11: Rehabilitating mainstem holding and rearing habitat. *In* Slaney, P.A., and D. Zaldokas. [ed.] Fish Habitat Rehabilitation Procedures. Province of British Columbia, Ministry of Environment, Lands and Parks, and Ministry of Forests. Watershed Restoration Technical Circular No. 9: 341p.

Beschta, R.L. 1984. River channel responses to accelerated mass soil erosion. Presented at Symposium on the Effects of Forest Land Use on Erosion and Slope Stability, May 7-11, Honolulu, Hawaii, pp.155-163.

Bilby, R.E., and J.W. Ward. 1989. Changes in characteristics and function of woody debris with increasing size of streams in western Washington. Transactions of the American Fisheries Society 118: 368-378.

Bisson P.A., J.L. Nielsen, R.A. Palmason, and L.E. Grove. 1981. A system of naming habitat types in small streams, with examples of habitat utilization by salmonids during low streamflow. *In* N.B. Armantrout [ed.] Acquisition and utilization of aquatic habitat inventory information, American Fisheries Society Western Division, pp. 62-73.

Blackwell, C.N., C.R. Picard, and M. Foy. 1999. Smolt productivity of off-channel habitat in the Chilliwack River watershed. Province of British Columbia, Ministry of Environment, Lands and Parks, and Ministry of Forests. Watershed Restoration Project Report No. 14: 42 p.

Bovee, K.D. 1978. Probability of use criteria for the family *salmonidae*. U.S.D.I., Fish and Wildlife Service, Office of Biological Services. Instream Flow Information Paper No. 4: 80p.

Bovee, K.D. 1982. A guide to stream habitat analysis using the Instream Flow Incremental Methodology. U.S.D.I., Fish and Wildlife Service, Office of Biological Services. Instream Flow Information Paper No: 12: 248p.

Bray, D.I. 1980. Evaluation of effective boundary roughness for gravel-bed rivers. Canadian Journal of Civil Engineering 7: 392-397.

Bustard, D.R., and D.W. Narver. 1975. Aspects of the winter ecology of juvenile coho salmon (*Oncohynchus kisutch*) and steelhead trout (*Salmo gairdneri*). Journal of the Fisheries Research Board of Canada 32: 667-680.

Carling, P.A. 1996. In-stream hydraulics and sediment transport. *In* Petts, G.E., and P. Calow [ed.] River flows and channel forms. Oxford, Blackwell Science, pp. 160-184.

Cherry, J., and R.L. Beschta. 1989 Course woody debris and channel morphology: a flume study. Water Resources Bulletin 25 (5): 1031-1036.

Christner, W.T.Jr., and S.G. Custer. 1998. In-stream obstructions and the formation of pools and scour holes. Presented at Wetlands Engineering and River Restoration Conference, ASCE, March 22-27, Denver, Colorado.

Chow, V.T. 1959. Open–Channel Hydraulics, McGraw-Hill Book Company, Inc., Boston, Massachusetts, 680 pp.

Church, M. 1992. Channel morphology and typology. *In* Calow, P. and Petts, G.E., [ed.] The Rivers handbook. Oxford, Blackwell, 1: 126-143.

Church, M., M.A. Hassan, and J.F. Wolcott. 1998. Stabilizing self-organized structures in gravel-bed stream channels: Field and experimental observations. Water Resources Research 34(11): 3169-1379.

Coulson, C.H., and W. Obedkoff. 1998. British Columbia Streamflow Inventory. Province of B.C., Ministry of Environment, Lands and Parks, Resources Inventory Branch, 49 pp.

D'Aoust, S.G., and R.G. Millar. 1999 Large woody debris fish habitat structure performance and ballasting requirements. Province of B.C., Ministry of Environment, Lands and Parks, and Ministry of Forests. Watershed Restoration Management Report No. 8: 119 p.

Enggrob, H.G., and P.H. von Lany. 1994. An application of 2-D mathematical modelling on the Brahmaputra River. p. 1-14. Proceedings of the 2nd International Conference on River Flood Hydraulics 22-25 March, York, England.

Frissell, C.A., and R.K. Nawa. 1992. Incidence and causes of physical failure of artificial structures in streams of western Oregon and Washington. North American Journal of Fisheries Management 12: 182-197.

Galay, V.J., E.K. Yaremko, and M.E. Quazi. 1987. River bed scour and construction of stone riprap protection. *In* Thorne, C.R., J.C.Bathurst, and R.D. Hey [ed.] Sediment transport in gravel-bed rivers. John Wiley and Sons Ltd., New York, USA, pp. 353-379.

Garde, R.J., K. Subramanya, and K.D. Nambudripad. 1961. Study of scour around spur-dikes. Journal of the Hydraulics Division, ASCE 87(HY6): 23-37.

Gippel, C.J., I.C. O'Neill, and B.L. Finlayson. 1992. The hydraulic basis of snag management. Report, Centre for Environmental Applied Hydrology, Department of Civil and Agricultural Engineering, University of Melbourne, Australia, 116 pp.

Hartman, G.G., and J.C. Scrivener. 1990. Impacts of forestry practices on a coastal stream ecosystem, Carnation Creek. Department of Fisheries and Oceans, Ottawa, ON. Canadian Bulletin of Fisheries and Aquatic Sciences 223: 148p.

Hartman, G.F. 1965. The role of behaviour in the ecology and interaction of underyearling coho salmon and steelhead trout. Journal of the Fisheries Research Board of Canada 22: 1035-1081.

Hay and Company Consultants Limited. 1992. Chilliwack River hazard management study interim report. Fraser Cheam Regional District, Volume 1.

Heede, B.H. 1972 Influences of a forest on the hydraulic geometry of two mountain streams. Water Resources Bulletin 8(3): 523-530.

Hogan, D.L., and M. Church. 1989. Hydraulic geometry in small, coastal streams: progress toward quantification of salmonid habitat. Canadian Journal of Fisheries and Aquatic Science 46: 844-852.

Hogan, D.L., S.A. Bird, and M.A. Hassan. 1998. Spatial and temporal evolution of small coastal gravel-bed streams: influenced of forest management on channel morphology and fish habitats. *In* P.C. Klingeman, R.L. Beschta, P.D. Komar, and J.B. Bradley [ed.] Gravel-bed rivers in the environment. Highlands Ranch, CO., Water Resources Publications: 365-392.

House, R. 1996. An evaluation of stream restoration structures in a coastal Oregon stream, 1984-1993. North American Journal of Fisheries Management 16: 272-281.

Jia, Y., and C.V. Alonso. 1994. One- and two-dimensional analysis of flow in Hotophia Creek, MS. Proceeding of the A.S.C.E Hydraulic Engineering '94 conference, August 1-5, Buffalo, New York (1): 589-594.

Keller, E.A., and T. Tally. 1979. Effects of large organic debris on channel form and fluvial processes in the coastal redwood environment. *In* D.D. Rhodes, and G.P. Williams [ed.] Adjustments of the fluvial system. Dubuque, Iowa, Kendall-Hunt, pp. 169-197.

Kellerhals, R., and M. Church. 1989. The morphology of large rivers: characterization and management, p. 31-48. In D.P. Dodge [ed.] Proceedings of the International Large River Symposium. Canadian Special Publication of Fisheries and Aquatic Sciences 106.

Klein, R.D. 1984. Channel adjustments following logging road removal in small steep land drainages. Presented at Symposium on the Effects of Forest Land Use on Erosion and Slope Stability, 7-11 May, Honolulu, Hawaii, pp. 187-195.

Laursen, E.M. 1963. An analysis of relief bridge scour. Journal of the Hydraulics Division, ASCE 89(HY3), pp. 93-118.

Lisle, T.E. 1986. Stabilization of a gravel channel by large streamside obstructions and bedrock bends, Jacoby Creek, northwestern California. Geological Society of America Bulletin 97: 999-1011.

Lisle, T.E., J.M. Nelson, J. Pitlick, M.A. Madej, and B.L. Barkett. 2000. Variability of bed mobility in natural, gravel-bed channels and adjustments to sediment load at local and reach scales. Water Resources Research 36(12): 3743-3755.

Madej, M.A. 1978. Sediment transport and channel changes in an aggrading stream in the Puget Lowland, Washington. U.S.D.A. Forest Service. General Technical Report PNW-141: 97-108.

McMahon T.E., and G.F. Hartman. 1989. Influence of cover complexity and current velocity on winter habitat use by juvenile coho salmon (*Oncorhynchus kisutch*). Canadian Journal of Fisheries and Aquatic Science 46:1551-1557.

Melville, B.W., and S.E. Coleman. 2000. Bridge Scour. Water Resources Publications, LLC. Colorado, USA, 550 pp.

Millar, R.G. 2000. Influence of bank vegetation on alluvial channel patterns. Water Resources Research 36(4): 1109-1118.

Montgomery, D.R., J.M. Buffington, R.D. Smith, K.M. Schmidt, and G. Pess. 1995. Pool spacing in forest channels. Water Resources Research 31(4): 1097-1105.

Mosley, M.P. 1981. The influence of organic debris on channel morphology and bedload transport in a New Zealand forest stream. Earth Surface Processes and Landforms 6: 571-579.

Mosley, M.P. 1982. Analysis of the effect of changing discharge on channel morphology and instream uses in a braided river, Ohau River, New Zealand. Water Resources Research 18(4): 800-812

Nakamura, F., and F.J. Swanson. 1993. Effects of coarse woody debris on morphology and sediment storage of a mountain stream system in western Oregon. Earth surface Processes and Landforms 18: 43-61.

Nickelson, T.E, M.F. Solazzi, S.L. Johnson, and J.D. Rodgers. 1991. Effectiveness of selected stream improvement techniques to create suitable summer and winter rearing habitat for juvenile coho salmon (*Oncorhynchus kisutch*) in Oregon coastal streams. Canadian Journal of Fisheries and Aquatic Science 49: 790-794.

Robison, E.G., and R.L. Beschta. 1990. Coarse woody debris and channel morphology interactions for undisturbed streams in southeast Alaska, U.S.A. Earth Surface Processes and Landforms 15: 149-156.

Ralph, S.C., G.C. Poole, L.L. Conquest, and R.J. Naiman. 1994. Stream channel morphology and woody debris in logged and unlogged basins of western Washington. Canadian Journal of Fisheries and Aquatic Science 51: 37-51.

Roper, B.B., D. Konnoff, D. Heller, and K. Wieman. 1998. Durability of pacific northwest in stream structures following floods of a five-year or greater return interval. North American Journal of Fisheries Management. 18: 686-693.

Rutherfurd, I.D., K. Jerie, and N. Marsh. 1999. A Rehabilitation Manual for Australian Streams Volume 2. LWRRDC and CRCCH, World Wide Web, 400 pp.

Shields, F.D.Jr., and C.J. Gippel. 1995. Prediction of effects of woody debris removal on flow resistance. Journal of Hydraulic Engineering121(4): 341-354.

Shvidchenko, A.B., and G. Pender. 2000. Flume study of the effect of relative depth on the incipient motion of coarse uniform sediments. Water Resources Research 36(2): 619-628.

Slaney, T.L., K.D. Hyatt, T.G. Northcote, and R.J. Fielden. 1996. Status of anadromous salmon and trout in British Columbia and Yukon. Fisheries 21(10): 20-35.

Slaney, P.A., and D. Zaldokas. 1997. Fish Habitat Rehabilitation Procedures. Province of B.C., Ministry of Environment, Lands and Parks, and Ministry of Forests. Watershed Restoration Technical Circular No. 9: 341p.

Slaney, P.A., and A.D. Martin. 1997. Chapter 1, Planning fish habitat rehabilitation: linking to habitat protection. In Slaney, P.A., and D. Zaldokas. [ed.] Fish Habitat Rehabilitation Procedures. Province of B.C., Ministry of Environment, Lands and Parks, and Ministry of Forests. Watershed Restoration Technical Circular No. 9: 341p.

Smith, R.D., and R.L. Beschta. 1994. A mechanism of pool formation and maintenance in forest streams. Proceeding of the A.S.C.E Hydraulic Engineering '94 conference, August 1-5, Buffalo, New York (2): 824-828.

Steffler, P. 1999. River2D two-dimensional depth average model of river hydrodynamics and fish habitat. Unpublished user's manual, University of Alberta, 45pp.

Swales, S., and C.D. Levings. 1989. Role of off-channel ponds in the life cycle of coho salmon and other juvenile salmonids in the Coldwater River, British Columbia. Canadian Journal of Fisheries and Aquatic Sciences 46: 232-242.

Tripp, D. 1996. Using large organic debris to restore fish habitat in debris-torrented streams. Province of B.C., Ministry of Forests and Lands, Land management report no. 47, ISSN 0702-9861, 26 p.

Wolman, M.G. 1954. A method of sampling coarse river-bed material. Transactions, American Geophysical Union 35 (6): 951-956.

Zaldokas, D.O. [editor] 1999. Annual compendium of aquatic rehabilitation projects for the Watershed Restoration Program 1998-1999. Province of B.C., Ministry of Environment, Lands and Parks, and Ministry of Forests. Watershed Restoration Project Report No. 13: 378p.

APPENDIX A: GRAIN SIZE DISTRIBUTION CURVES

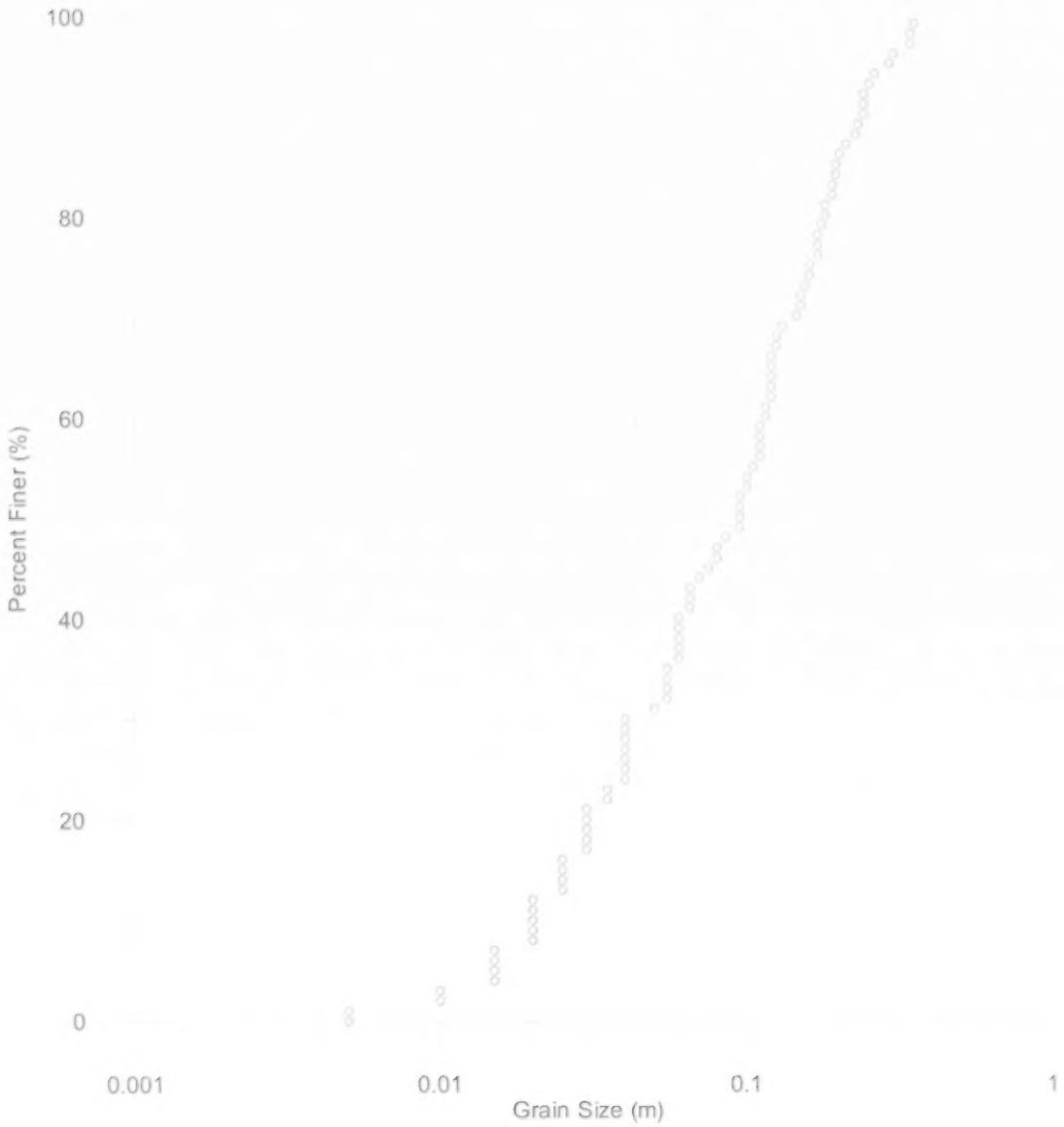

Figure A.1a: Upper Tamihi side channel grain size distribution.

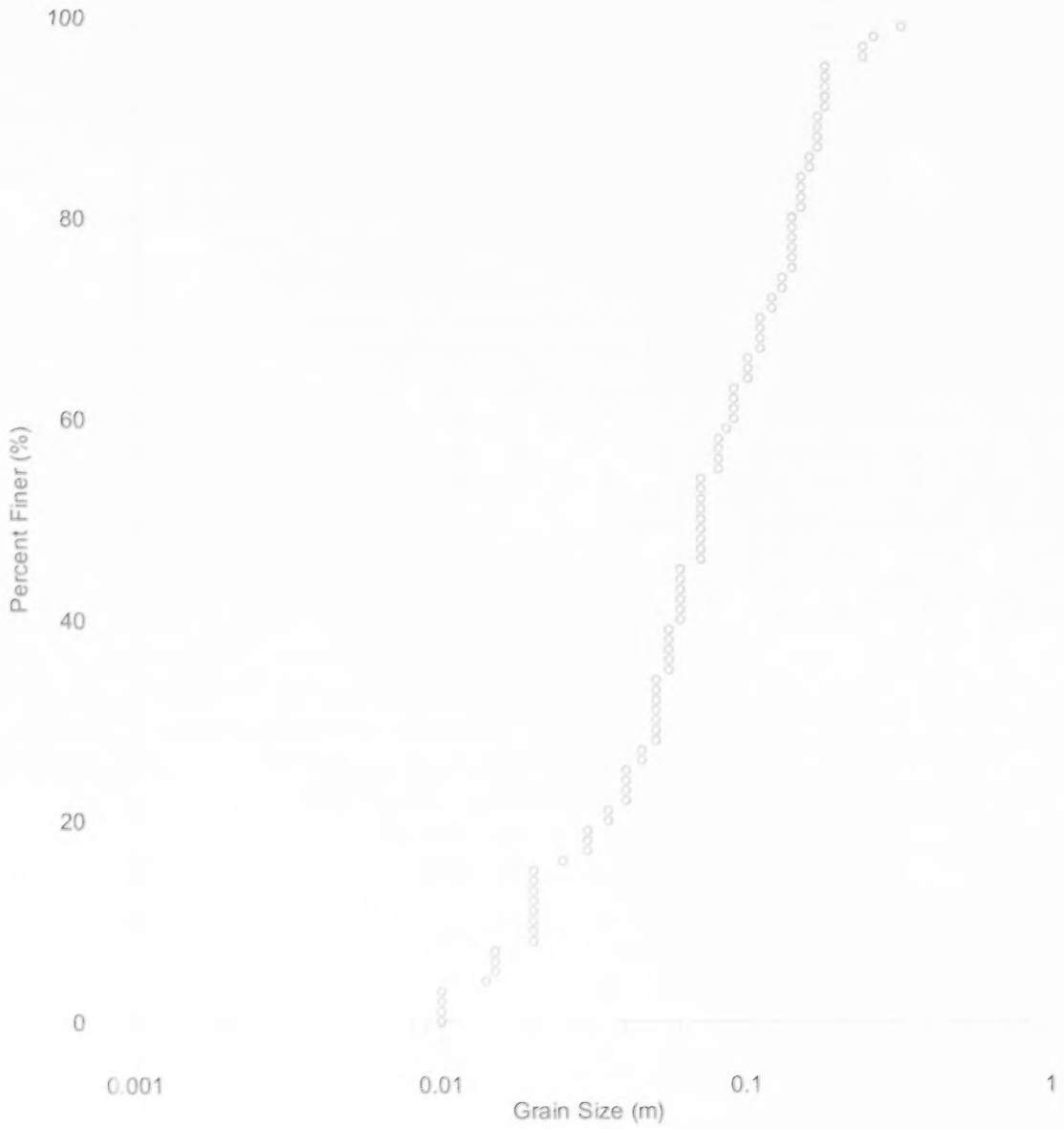

Figure A.1b: Middle Tamihi side channel grain size distribution.

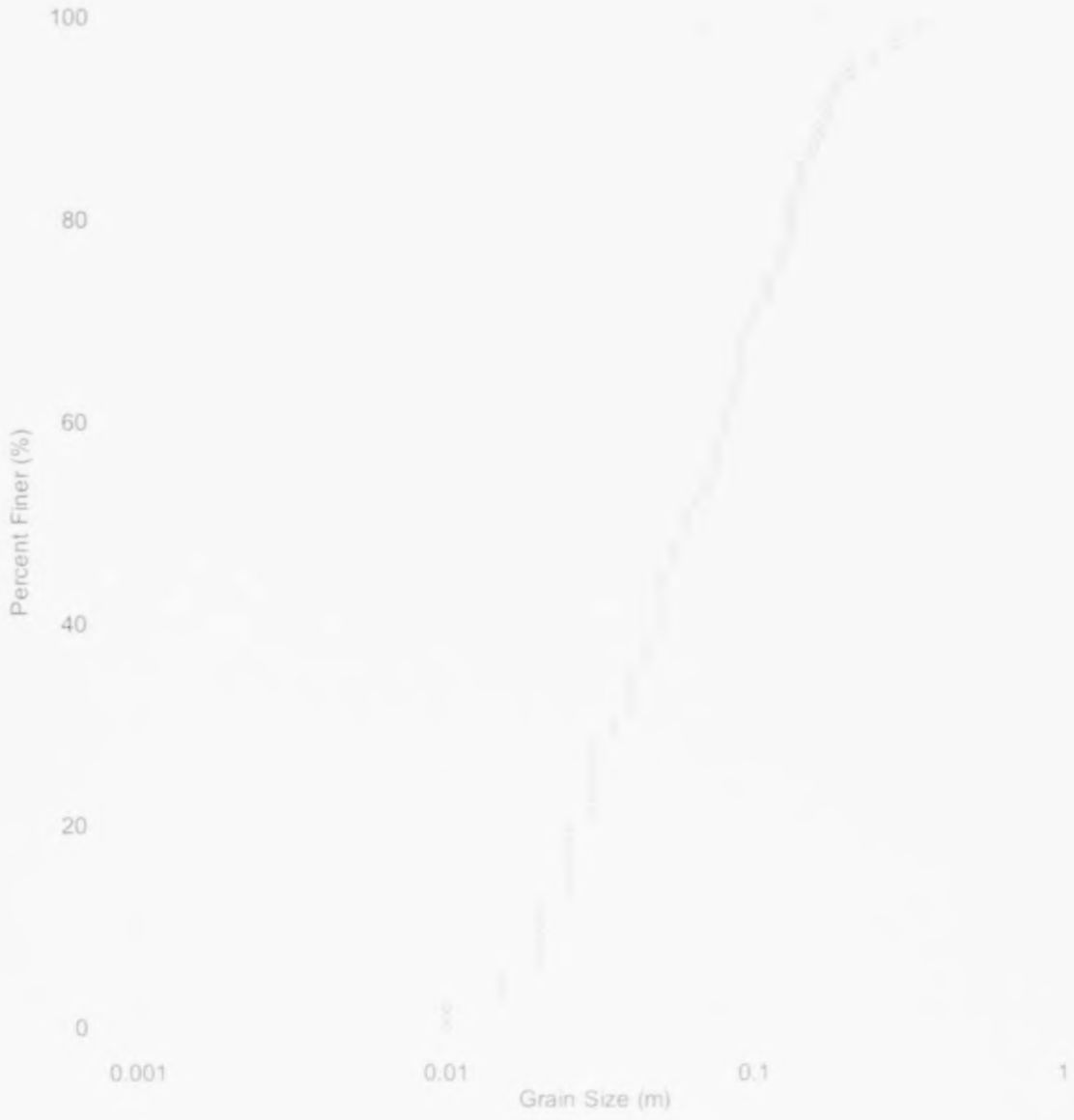

Figure A.1c: Lower Tamihi side channel grain size distribution.